Fluorescent Aptasensors: Design Strategies and Applications in Analyzing Chemical Contamination of Food

Niko Hildebrandt, Ying Li, Ruifang Su, Hongxia Li, Jiajia Guo, Chunyan Sun

Fluorescent Aptasensors: Design Strategies and Applications in Analyzing Chemical Contamination of Food

Ying Li,[a] Ruifang Su,[b] Hongxia Li,[a] Jiajia Guo,[c] Niko Hildebrandt,[b,d,e*] Chunyan Sun [a*]

[a] *Department of Food Quality and Safety, College of Food Science and Engineering, Jilin University, Changchun 130062, China*

[b] *nanoFRET.com, Laboratoire COBRA (Chimie Organique, Bioorganique : Réactivité et Analyse), UMR 6014, CNRS, Université de Rouen Normandie, INSA, 76821 Mont-Saint-Aignan cedex, France.*

[c] *Bionic Sensing and Intelligence Center, Institute of Biomedical and Health Engineering, Shenzhen Institutes of Advanced Technology, Chinese Academy of Sciences, 518055 Shenzhen, China*

[d] *Université Paris-Saclay, 91190 Saint-Aubin, France*

[e] *Department of Chemistry, Seoul National University, Seoul 08826, South Korea*

* *e-mail: niko.hildebrandt@univ-rouen.fr; sunchuny@jlu.edu.cn*

CONTENTS

1 Introduction

Caused by various factors, including planting, breeding, production, processing, packaging, and environmental pollution, most food is inevitably contaminated at a certain degree by common chemical substances, such as pesticides, veterinary drugs, toxins, or heavy metals. These substances can have negative effects on human health depending on their levels within the food and the amount of food we consume. Therefore, food chemical contaminants have been recognized as food safety issue worldwide. For example, the National Health Commission of the People's Republic of China (http://www.nhc.gov.cn/) and the EU (http://ec.europa.eu/food/safety) have set regulations on the residue limits concerning food chemical contaminants, and only low levels of contamination are permitted after those legal requirements. To reliably and easily quantify food contamination for controlling food safety and protecting human health, the development of accurate, sensitive, simple, and rapid detection methods is of paramount importance. Traditional analytical methods[1,2] include chromatography, mass spectrometry, atomic absorption spectroscopy, and biological detection techniques,[3] such as enzyme-linked immunosorbent assays (ELISAs) and other antibody-related methods. Although significant progress has been made in terms of sensitivity and reproducibility, those common approaches are often limited by drawbacks concerning complex instrumental operation, cumbersome sample pretreatments, high costs, and poor adaptability for on-site screening. Biosensors, which can convert target recognition into a physically detectable signal, mainly include two functional elements, namely molecular recognition and signal transduction. The excellent selectivity, high sensitivity, and broad applicability have made biosensors an increasingly applied tool to accomplish simple, rapid, and sensitive quantification of specific food chemical pollutants.

The key to high-performance biosensors is the selection of molecular recognition elements with good affinity and specificity,[4] which include enzymes, nucleic acids, molecularly imprinted polymers, antibodies, and aptamers.[5] Although aptamers can be composed of oligonucleotides or peptides, they are most often referred to as oligonucleotide sequences that were obtained by means of *in vitro* systematic evolution of ligands by exponential enrichment (SELEX)[6,7] and can

recognize a variety of targets with high affinity and strong specificity, including small molecules, proteins and even cells.[8] Due to their availability against many different targets, production by chemical synthesis, moderate price, good stability, and easy chemical modification, aptamers have found broad application, *e.g.*, in biomolecular research, disease diagnostics, biosensing, bioimaging, or chromatographic purification.[9-13] Molecular recognition in aptamer-based biosensors (aptasensors) is mainly based on DNA/DNA or DNA/RNA hybridization and aptamer/target binding.[14,15]

Depending on the different signal transduction elements, aptasensors can be classified by their physical signals, *i.e.*, electrochemistry, fluorescence, colorimetry, chemiluminescence, thermometry, surface-enhanced Raman spectroscopy (SERS), *etc*. Fluorescent aptasensors have attracted much attention due to their simple signal transduction, high sensitivity, easy operation, and fast response. Because the fluorescent probe is another key factor concerning the performance of fluorescent aptasensors, several considerations are necessary for its selection: *i)* it should be easily excitable (convenient wavelength and high absorptivity); *ii)* its fluorescence should not be affected by other components in the matrix; *iii)* it should be able to produce a clear and detectable signal (convenient wavelength and high quantum yield); *iv)* it should possess good stability and water solubility; *v)* it should be modifiable with specific functional groups.[16] Currently used fluorescent probes include fluorescent dyes, quantum dots (QDs), carbon dots (CDs), metal nanoclusters (MNCs), upconverting (or upconversion) nanoparticles (UCNPs), fluorescent biomolecules, and luminescent lanthanide complexes.[17,18] In aptasensors, the fluorescent probe can be applied as a single signal transduction element, for which the aptamer-target recognition induces a specific fluorescence change (*e.g.*, intensity or wavelength). It can also be composed of two elements (*e.g.*, fluorophore and quencher), and the aptamer-target binding can regulate the interaction between the two elements, *e.g.*, via Förster resonance energy transfer (FRET), inner filter effect (IFE), or aggregation-induced emission (AIE). Generally, the design of a fluorescent aptasensor is based on an efficient conversion of the conformational change of the aptamer before and after binding to the target into a fluorescent signal for a direct analysis of the target. In cases

for which the sensitivity of one fluorescent probe per one target is not sufficient, the oligonucleotide nature of aptamers can be adapted to different nucleic acid signal amplification strategies for further decreasing the limits of detection (LODs).

The increasing popularity of aptasensors has been witnessed by several recent reviews that discuss their progress and applications from different perspectives.[9,19-25] In this review, we focus on design strategies of fluorescent aptasensors and their recent applications in the detection of common food chemical contaminants since 2019 (**Scheme 1**). First, food chemical contaminants, aptasensors, molecular recognition, and fluorescence signal transduction approaches are introduced. Then, different design strategies for fluorescence aptasensors using various fluorescent molecules and nanomaterials are discussed, including the strategies based on various nucleic acid signal amplification techniques. Then, the application status and development of fluorescent aptasensors in the detection of common food chemical contaminants are elaborated and illustrated via selected examples. Finally, recent applications (including pros and cons) of fluorescent aptasensors in the quantification of food chemical pollutants such as toxins, veterinary drug residues, pesticides, and heavy metal ions are reviewed, and potential research orientations and future challenges are discussed.

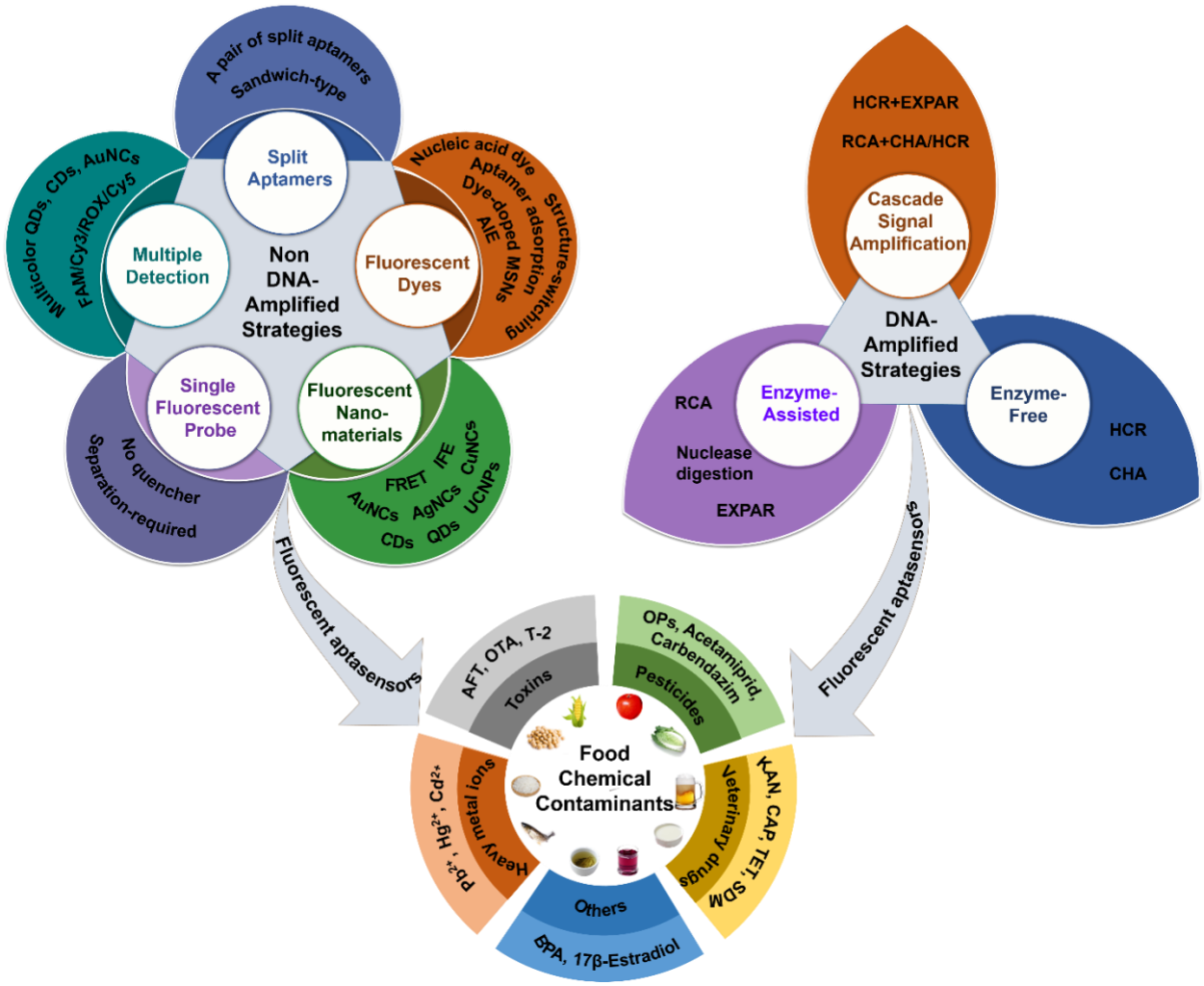

Scheme 1. Schematic overview of design strategies of fluorescent aptasensors and their recent applications in the detection of common food chemical contaminants.

2 Fluorescent aptasensors without signal amplification

According to the types of fluorescent probes and the transduction mechanism of fluorescence signal, we divide the discussion of traditional (non-amplified) fluorescent aptasensors into the following five subsections: *i)* fluorescent dye-based aptasensors; *ii)* fluorescent nanomaterial-based aptasensors; *iii)* aptasensors with a single fluorescent probe; *iv)* aptasensors with multiple fluorescent probes; *v)* aptasensors based on sandwich-type split aptamers.

2.1 Aptasensors using fluorescent dyes as probes

Concerning fluorescent dye-based aptasensors, we mainly focus on five types of design strategies, namely, *i)* dye displacement aptasensors, *ii)* structure-switching aptasensors, *iii)* nanosurface-adsorption aptasensors, *iv)* dye-doped mesoporous silica nanoparticle (NP) aptasensors, and *v)* aggregation-induced emission (AIE) aptasensors.

2.1.1 Dye displacement aptasensors

Nucleic acid-specific dye displacement aptasensors mainly rely on the aptamer-target interaction and the structure change of nucleic acid. Fluorescent dyes play a key role as the signal reporter in the design of this type of aptasensor. Typically used dyes are Thioflavin T (ThT) and N-methylmorpholine (NMM), which are specifically sensitive to the G-quadruplex (G4) DNA structure. Some aptamers spontaneously form stable G4 structures by themselves and can be disassembled by binding to specific targets, thus establishing fluorescence "turn-off" assays (**Figure1A(a)**). In the absence of targets, the G4-specific dyes are highly fluorescent because they bind with the aptamer-containing G4 structure. In the presence of the target, the G4-specific dyes are displaced, leading to a fluorescence intensity decrease.[26] For aptamers that cannot form G4 structures on their own, other displacement aptasensor strategies can be deployed. For example, a "turn-on" strategy using aptamer chimera is shown in **Figure 1A(b)**. In case the aptamer chimera is designed with a locked-G4-forming stem sequence, G4-specific dyes are weakly fluorescent in the absence of the target and highly fluorescent in the presence of the target, thus forming "turn-on" aptasensors.[27] The performance of the dye-displacement assay is dependent on the sensitivity of the G4-specific dye. Since no modification of the aptamer with the dye is required, the displacement design can be regarded as a label-free method and the target detection can be achieved in a single step. The design from **Figure 1A(a)** is only applicable to the detection of targets with aptamers containing G4 structures and exhibiting significant structural change upon target binding, while the method from **Figure 1A(b)** is relatively universal without specific requirements concerning conformation and structural changes of the aptamers.

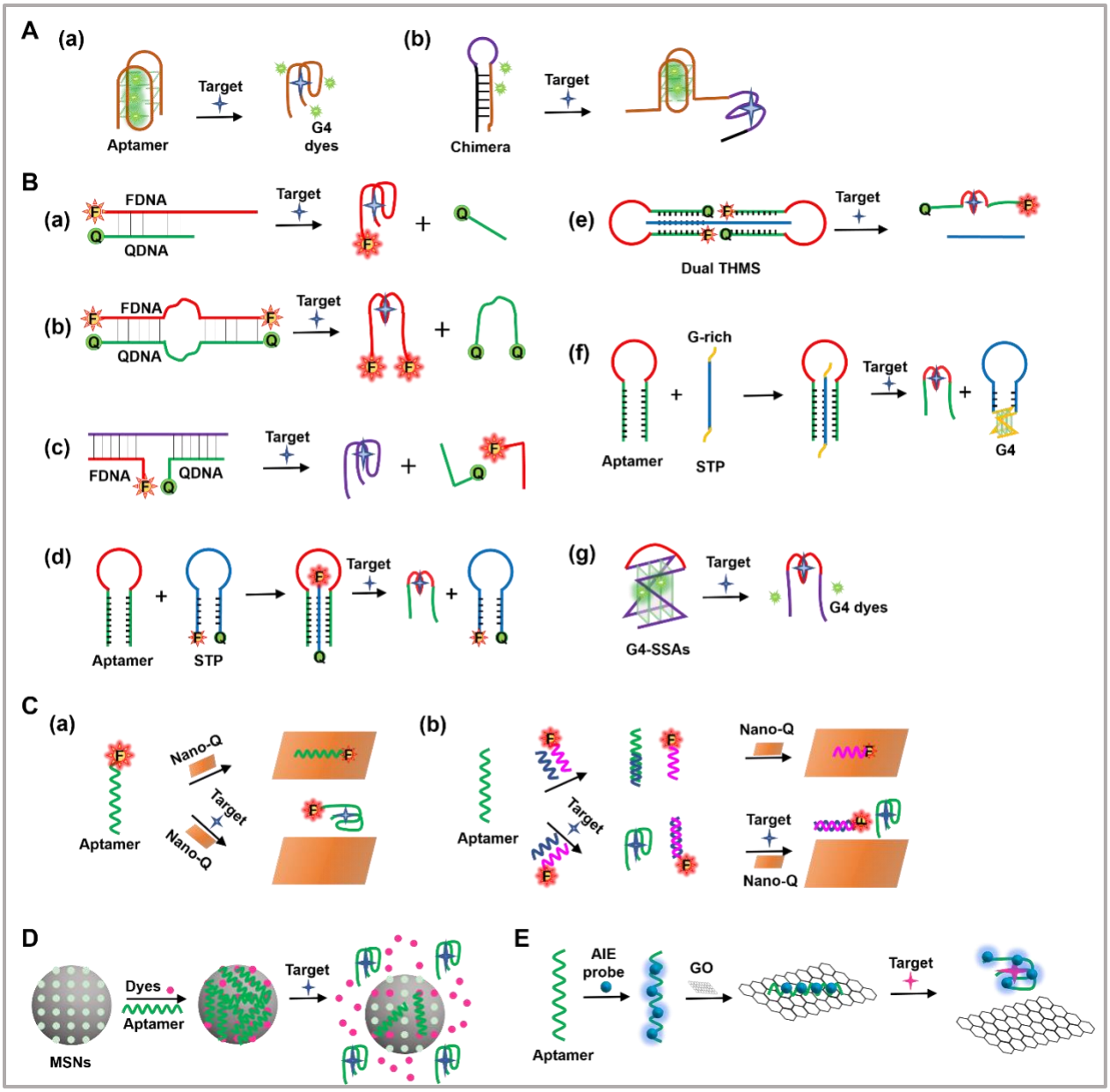

Figure 1. Design strategies of aptasensors using organic dyes as fluorescent probes. **A:** Nucleic acid-specific dye-based displacement aptasensors: (a) In the aptamers that form G4 structure, the fluorescence intensity is decreased upon target binding (disassembly of G4); (b) An aptamer chimera containing a G-rich stem sequence activates the fluorescence switch upon binding to the target. **B:** Fluorescent dye-based biosensors using structure-switching aptamers: (a) In a single F-Q pair-labeled dual-strand structure switch, the fluorescence is switched on upon aptamer-target binding; (b) For higher sensitivity, the same principle can be adapted to a SSA with a double F-Q pair; (c) In a triple-DNA SSA, FDNA and QDNA hybridize to the aptamer DNA and aptamer-target recognition results in fluorescence intensity increase; (d) A THMS consisting of an unlabeled aptamer and a F-Q pair labeled STP is opened upon target binding, which results in fluorescence quenching; (e) A dual THMS composed of dually F-Q pair-labeled aptamers and unlabeled

STP is disassembled upon target binding, which leads to fluorescence enhancement; (f) In a label-free THMS format, target-dependent formation of a G4 structure can combine with hemin to catalyze the redox reaction for signal readout; (g) In a typical G4-SSA design, a fluorescent G4 structure is disassembled upon target binding, leading to decreased fluorescence intensity. **C:** Nanosurface-adsorption aptasensors: (a) A F-labeled aptamer is adsorbed on the nanomaterial-based fluorescence quencher (Nano-Q) and the target-dependent formation of target-aptamer complexes results in surface detachment and fluorescence recovery; (b) The same fluorescence turn-on strategy can be applied with unlabeled aptamers and two cDNAs, one of which is labeled with F. **D:** The pores of MSNs can be filled with fluorescent dyes and sealed by aptamers. Upon target-dependent aptamer release, the dyes can be released from the pores, leading to a fluorescence intensity increase. **E:** Binding of AIE probes to an aptamer results in strong fluorescence, which is quenched upon binding to a nanosurface quencher, such as GO. Target-aptamer binding results in detachment from GO and a strong increase of fluorescence intensity.

2.1.2 Structure-switching aptasensors

Aptamers not only can bind to targets to form aptamer-target complexes but also can hybridize with their complementary sequences to form double-stranded (ds) DNA. Such aptamers can be engineered to convert structures between dsDNA and aptamer-target complexes, thus converting target binding events into detectable signals.[13] Inspired by this principle, structure-switching aptamers (SSAs) have been applied to develop aptasensors for various targets.[28,29] The design strategies of dye-based fluorescent biosensors using SSAs can be classified into four types: *i)* structure switches using two DNA strands, *ii)* structure switches using three DNA strands, *iii)* triple-helix DNA molecular switch (THMS), and *iv)* G-quadruplex structure-switching aptamers (G4-SSAs).

Dual-strand structure switches are usually formed between a fluorophore-labeled single-stranded DNA (ssDNA) aptamer and a quencher-modified complementary DNA (cDNA) by switching structures from the aptamer-cDNA duplex to an aptamer-target complex. A typical example is shown in **Figure 1B(a)**, where a fluorophore-labeled aptamer (FDNA) and a quencher-labeled cDNA (QDNA) form a duplex structure through DNA hybridization, resulting in F-Q proximity and concomitant fluorescence quenching of the fluorophore. When the target specifically binds to FDNA, QDNA is released and the fluorescence intensity increases.[30] The

same target-dependent unquenching principle can also be applied to the dual-strand switch with F and Q labeled on both termini of FDNA and QDNA (**Figure 1B(b)**).[31] The two F-Q pairs in the dual-terminal proximity structure are applied to transduce the molecular recognition, which is usually more sensitive than a single pair transduction. Different F-Q pairs are available, such as carboxyfluorescein (FAM) and black hole quencher 1 (FAM-BHQ1) or FAM and carboxytetramethylrhodamine (FAM/TAMRA).[30,31] Triple-DNA strand structure switches comprise one aptamer DNA, one FDNA, and one QDNA to accomplish F-Q proximity. Upon aptamer-target binding, the triple-DNA is disassembled, resulting in free diffusion of FDNA and QDNA in the solution (long distance between F and Q), and the fluorescence is restored (**Figure 1B(c)**).[32] For both dual and triple DNA strand structure switches, it is critical to optimize the complementary length and complementary position of the aptamer and the cDNA. If the dsDNA formed by aptamer and cDNA possesses high structural stability, it is difficult to accomplish effective structural transformation by target-aptamer recognition. Unstable dsDNA structures, in turn, can result in high background signal. Thus, to achieve high sensing performance, it is necessary to reasonably adjust the number of mismatched base pairs[33] and optimize the complementary length and position.[32]

THMS contain a third ssDNA strand that is inserted into the major groove of a Watson–Crick duplex via Hoogsteen hydrogen bonding.[34] Typical aptamer-based THMS consist of two distinct DNA constructs: a target specific aptamer sequence flanked by two arm segments, and a signal transduction probe (STP). Depending on the different signal probes in STP, both labeled and label-free designs are available for target sensing. As an example for the labeled design (**Figure 1B(d)**),[35] the STP contains a fluorophore and a quencher labeled at the 3' and 5' ends, respectively. In the absence of the target, an aptamer-STP complex forms the THMS, exhibiting strong fluorescence. Upon target-aptamer binding, the THMS is disassembled and releases the STP, which results in fluorescence quenching due to F-Q proximity. Whereas this example represents a turn-off fluorescence approach, the same principle can be used to design a turn-on assay when F and Q in the STP are replaced by two pyrenes, which are strongly fluorescent only when the dimer is formed

at close proximity.[36] Another turn-on approach can be designed using dual THMS.[37] As shown in **Figure 1B(e)**, two aptamer probes contain fluorophores and quenchers at the terminals, and they can combine with STP to form dumbbell-shaped dual THMS structures, with the close proximity of two pairs of F and Q. In the form of dual THMS structures, dual quenching will lead to a very low fluorescence background. Target-aptamer binding will induce the disassembly of dual THMS and the separation of F and Q, thus lighting up the fluorophores and resulting in fluorescence enhancement. A label-free THMS approach (**Figure 1B(f)**) used a STP extended with two split guanine-rich (G-rich) DNA sequences at its two ends. In the absence of the target, STP and aptamer are assembled into a THMS with low fluorescence. Upon target-dependent disassembly of the THMS, the released STP forms a G4 structure, which combines with hemin to form G4-hemin DNAzyme with peroxidase-mimicking catalytic activity, and acts as a platform for fluorescence signal output by combining with appropriate substrates, *e.g.* o-phenylenediamine (OPD).[38] The DNAzyme catalyzes the oxidation of OPD by H_2O_2 to produce a yellow fluorescent product 2,3-diaminophenazine (DAP) with excitation/emission maxima at 420/560 nm, and turn-on detection was achieved in the G4-based label-free THMS assay. When designing THMS, the sequence length of the two arms extended at the two ends of the aptamer must be optimized to maintain the aptamer affinity and ensure the formation of stable THMS. In addition, parameters (*e.g.*, temperature, pH, and Mg^{2+} concentration) that affect the formation of THMS must be carefully optimized for each aptasensor.

A typical G4-SSAs design comprises a variable aptamer domain for target recognition and a constant split DNAzyme G4 domain for signal transduction (**Figure 1B(g)**).[39] The variable domain is inserted between two DNAzyme fragments and can theoretically be any target-specific aptamer. Without target, the G4-SSAs folds into a stable parallel G4 structure, showing strong fluorescence of the specific G4-binding dye. Upon target binding, the G4 structure is disrupted and shows low fluorescence, thus forming a turn-off fluorescent aptasensor. It has been demonstrated that aptamers with diverse target specificities (*e.g.*, metal ions, small molecules, and proteins), binding affinities (from pico- to micromolar K_d), lengths (11 to 35 nt), and secondary structures (*e.g.*,

duplex, G4, stem-loop, and three-way-junctions) can be engineered into G4-SSA constructs.[39] The G4-SSA design exhibits an excellent universal approach for the fabrication and application of aptasensors. Although there is no need for the assistance of cDNA, the chimera that contains aptamer and G4 sequence need to be rationally designed to maintain a stable structure in the absence of the target.

2.1.3 Nanosurface-adsorption aptasensors

SsDNA can adsorb on the surface of certain nanomaterials (NMs) that can also be applied as fluorescence quenchers for fluorophores. The strategy for designing aptasensors using nanosurface adsorption takes advantage of the fact that folded DNA (*i.e.*, G4 complexes) and dsDNA do not adsorb to these NMs. NMs commonly used to adsorb nucleic acids and as fluorescence quenchers involve five types: *i)* carbon nanomaterials (CNMs), such as graphene oxide (GO), single-walled carbon nanotubes (SWCNTs), multi-walled carbon nanotubes (MWCNTs), and single-walled carbon nanohorns (SWCNHs); *ii)* transition-metal chalcogenides and oxides nanosheets (TMDNSs), such as MoS_2, WS_2 and MnO_2; *iii)* transition-metal carbides and carbonitrides (MXenes), such as Ti_3C_2; *iv)* metal nanomaterials (MNMs), such as gold NPs (AuNPs) and gold nanorods (AuNRs); and *v)* metal-organic frameworks (MOFs), such as Cu-MOFs.[17,18,40,41] The adsorption and quenching properties of these nanomaterials toward dye-labeled aptamers have been frequently exploited for the development of aptasensors. Although these NMs exhibit different adsorption approaches and fluorescence quenching mechanisms, the design strategies of the fluorescent aptasensors using nanosurface-adsorption are similar. Usually, these aptasensors are designed as turn-on assays, in which the adsorbed and quenched F-DNA on the nanosurface is released by the target due to the formation of target-aptamer complexes or dsDNA, which results in fluorescence recovery. This approach can be applied with F-labeled aptamers that form target-aptamer complexes upon target binding (**Figure 1C(a)**) or with unlabeled aptamers and F-labeled cDNAs that form dsDNA with another aptamer-complementary cDNA upon target-aptamer binding (**Figure 1C(b)**). Various nanosurface-adsorption aptasensors have been designed with different analytical performances that usually rely on the different adsorption and quenching

efficiencies of the distinct NM.[17,18,40-42]

2.1.4 Dye-doped mesoporous silica nanoparticle aptasensors

Owing to their adjustable pore volume and the capability to bind to biomacromolecules, such as DNA, RNA, and proteins, mesoporous silica nanoparticles (MSNs) have attracted great attention in the fabrication of fluorescent aptasensors for detecting a broad range of targets with advantages of simple operation, high sensitivity, rapid detection, and good selectivity.[43] The common strategy of MSNs-based fluorescent aptasensors is based on the target-aptamer binding-modulated leakage of dyes enclosed in the pores of MSNs. One example is illustrated in **Figure 1D**, where rhodamine 6G (Rh6G) dyes are filled in the pores of amino-modified MSNs (MSN-NH_2) and then blocked with aptamers.[44] Upon target binding, the aptamers are separated from MSN-NH_2, such that the pores of the MSN-NH_2 are opened and Rh6G can leak out, resulting in a target-dependent fluorescence intensity increase due to the improved environment for Rh6G fluorescence. To ensure the stability and analytical performance of MSNs-based aptasensors, various types of MSNs (*e.g.*, MCM-41, SBA-15, MCF, FSM-16)[43] and different blocking methods (*e.g.*, click chemistry) can also be adopted.[45]

2.1.5 Aggregation induced emission aptasensors

Although the phenomenon has been discovered and investigated since the 20th century, the term aggregation-induced emission (AIE) was coined in 2001 by Tang and co-workers.[46,47] AIE refers to the phenomenon that a class of non-planar molecules do not luminesce when dissolved but exhibit enhanced fluorescence upon aggregation. The AIE effect is mainly attributed to restricted intramolecular rotation of its phenyl peripheries against the central double bond in the aggregate state.[48] Based on the AIE mechanism, fluorescent aptasensors have been established for the detection of various targets, such as toxin[49,50] and foodborne pathogens.[51] The common AIE probes contain 1,2-diphenyl-1,2-di(p-tolyl)ethene (TPE), 9,10-distyrylanthracene (DSA), and their derivatives. AIE-based fluorescent aptasensors have been designed relying on the phenomenon that the positively charged AIE probes bind with negatively charged aptamers in an aggregated state with strong emission. For example, in the absence of the target, the strong emission produced

by the interaction of positively charged AIE probe and negatively charged aptamer is quenched by GO. Upon target binding, the formed aptamer-target complex is released from GO, restoring fluorescence and thus establishing a turn-on sensor (**Figure 1E**).[49] Another design for label-free and turn-on analysis can be accomplished using only one aptamer sequence through the synergy of AIE dye and exonuclease I (Exo I).[52] Exo I can digest the aptamer and interfere with its interaction with the AIE probes, while the target-aptamer complex is resistant to digestion, thus modulating the AIE effect and fluorescence change.

2.1.6 Pros and cons

Dye displacement aptasensors provide a facile mode for one-pot, label-free, rapid, and low-cost detection. However, these methods exhibit limited sensitivity and cannot be easily combined with DNA amplification technology. Structure-switching aptasensors can be versatilely applied to detect various targets and have great potential in conjunction with DNA signal amplification technologies. However, the incomplete F quenching in single-ended F-Q labeling assays can result in high fluorescence background and thus reduce the sensitivity towards the targets. Dual-terminal F-Q labeling can improve the fluorescence quenching efficiency and reduce the background but the labeling cost increases in this design. The label-free G4-SSAs strategy adopts a turn-off signal output mode, which may be interfered by the sample matrix, undermining the sensitivity and selectivity of the method. The label-free THMS assays in turn-on format has demonstrated favorable sensitivity and selectivity, however, they are mainly applicable in the detection of targets with short-sequence aptamers, and their applications in long-sequence aptamers remain to be explored. For the design of structure-switching aptasensors, some key factors including the sequence length of the aptamer, the affinity of the aptamer towards the target, the competition between the stability of DNA structures (duplex, triplex, G4) and the structure-switching induced by target-aptamer binding, are important to be carefully considered and investigated for high sensing performance.

Nanosurface-adsorption aptasensors avoid the unsatisfactory fluorescence quenching when nucleic acids are labeled with F and Q and can usually ensure a low fluorescence background.

Moreover, it is convenient to use multi-color fluorescent probes to realize multiplexed detection. Also, these designs can be flexibly combined with nuclease-assisted recycling amplification to further improve sensitivity. However, different quenching materials demonstrate discrepant adsorption mechanism to DNA and concentration-dependent fluorescence quenching ability. Therefore, strong adsorption assembly of aptamers on the nanosurface and the limited fluorescence recovery would affect the analytical performance. Dye-doped MSNs aptasensors result in low background signal by enclosing the fluorescent probes in MSNs, displaying the advantages of easy operation and low cost but the disadvantages of long detection time and limited sensitivity. AIE aptasensors avoid the problems of fluorescence quenching caused by concentration or aggregation of traditional dyes, and can achieve simple, sensitive, and rapid detection through label-free and low-cost methods. The positively charged AIE dyes usually need to be synthesized by organic methods. The design strategies of AIE aptasensors are limited to Exo I digestion or GO adsorption, and more approaches need to be developed for broad application.

In general, dye-based fluorescent aptasensors are superior in terms of easy acquisition of the fluorescent probes and simple operation and inferior in terms of chemical, physical, and photo stability.

2.2 Aptasensors using fluorescent nanomaterials as probes

Most aptasensors based on fluorescent NMs use the following three design strategies, which we shortly discuss below: *i)* FRET-based nano-aptasensors, *ii)* IFE-based nano-aptasensors, and *iii)* DNA-templated metal nanocluster-based aptasensors.

2.2.1 Aptasensors based on fluorescent nanomaterials and FRET

FRET refers to a non-radiative energy transfer (ET) process from a luminescent donor (D) to an acceptor (A), accompanied by the disappearance or attenuation of the donor fluorescence and sensitization of acceptor fluorescence in case the acceptor is fluorescent. Two important requirements for FRET to occur are a close distance between D and A (typically between *circa* 1 and 10 nm) and a spectral overlap (resonance) of the emission of D and the absorption of A.[53] The

strong distance-dependence (~R^{-6}) of FRET has been frequently exploited for the design of aptasensors with different fluorescent NMs. Commonly utilized donors in FRET pairs comprise QDs, CDs, MNCs, and UCNPs, and corresponding FRET acceptors can be fluorophores, such as dyes (*e.g.*, Cy5.5) or QDs, or quenchers, such as AuNPs, GO, BHQ1, or MoS_2.[18,54] Although most biosensing studies assign ET with fluorescence quenching to FRET, the exact ET mechanisms have not been derived for all materials.[53] For example, AuNPs most probably quench fluorescence via the NSET (nanosurface ET) mechanism and not via FRET.[55] Therefore, many studies may claim FRET although the ET mechanism is actually of another type. Because the exact mechanism is most often not important for the aptasensing application, we usually refer to the specific ET term that was used in the original publication or use the general term ET. Due to the extraordinary sensitivity, FRET is popularly applied in the construction of aptasensors based on the distance-dependent FRET efficiency and associated fluorescence quenching during the process of molecular recognition.[18] Fluorescent NM-based FRET aptasensors (FRET nano-aptasensors) can be divided into two types: *i)* DNA-functionalized FRET nano-aptasensors through DNA hybridization, *ii)* DNA-functionalized FRET nano-aptasensors through aptamer adsorption.

The common design of DNA-functionalized FRET nano-aptasensors through DNA hybridization is illustrated in **Figure 2A(a)**.[56] The hybridization of D-functionalized aptamer and A-functionalized cDNA results in FRET quenching of D fluorescence. Target-aptamer binding separates D and A, thus resulting in fluorescence recovery (FRET off, fluorescence on). In this strategy, both D and A need to be efficiently functionalized, as commonly achieved by the amide reaction of 1-ethyl-3-(3-dimethyllaminopropyl) carbodiimide hydrochloride (EDC) and N-hydroxysuccinimide (NHS).

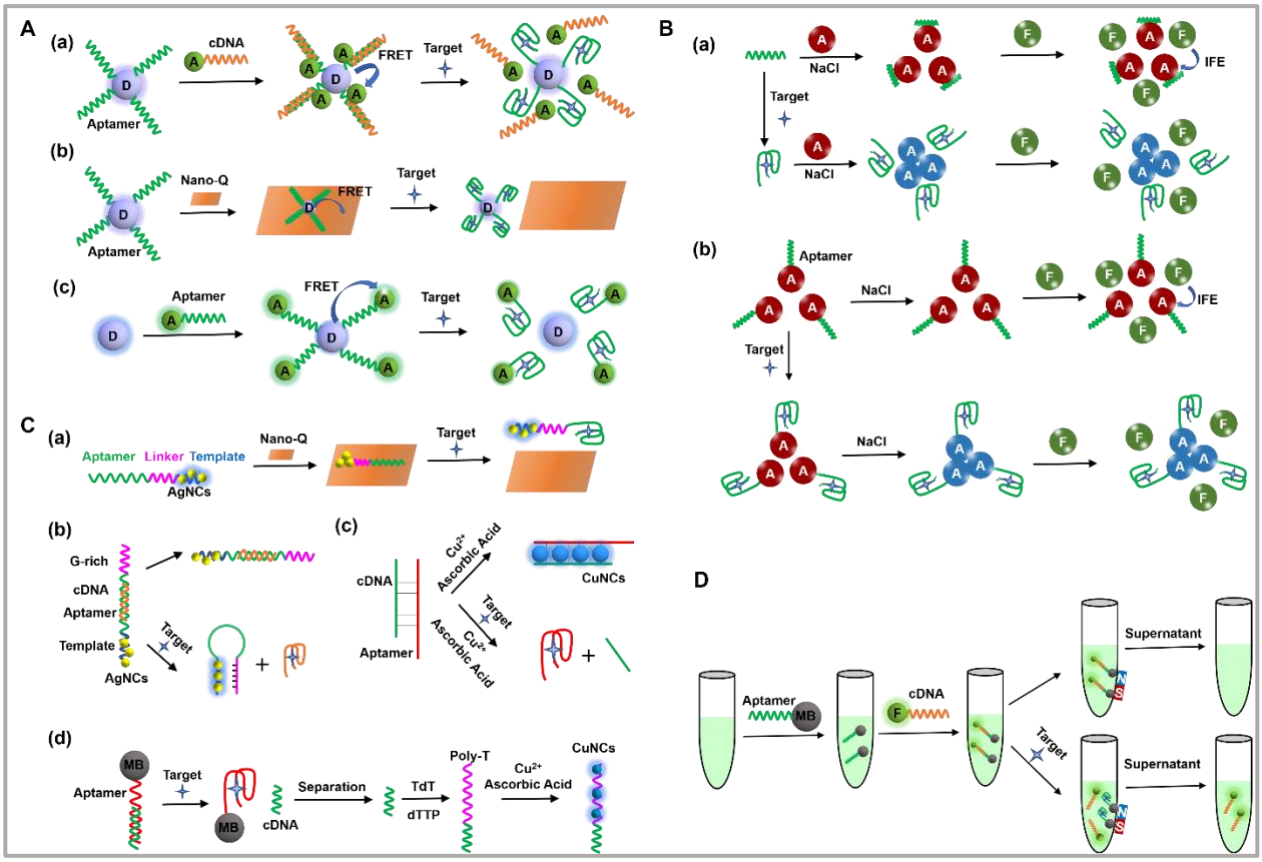

Figure 2. Design strategies of aptasensors using fluorescent NMs as probes. **A:** FRET nano-aptasensors: (a) Hybridization of A-cDNA to the aptamer on a NM D results in FRET and quenched D fluorescence, which is recovered upon target-aptamer binding and separation of D and A (FRET off); (b) Aptamer-labeled fluorescent D NMs adsorb to nanomaterials-based quenchers (Nano-Q) and get quenched via FRET. Aptamer-target binding releases D from the Nano-Q, resulting in fluorescence recovery (FRET off); (c) Interaction of aptamer modified on a NM A with π -rich CNP D leads to FRET (FRET on), which is disrupted by aptamer-target binding, resulting in a decreased FRET efficiency (FRET off). **B:** IFE nano-aptasensors: The aptamer (a: adsorbed on AuNPs, b: functionalized to AuNPs) prevents AuNPs from NaCl-mediated aggregation, which results in well dispersed AuNPs that function as absorbers for IFE of F-NP fluorescence. In the presence of the target, the folded aptamer-target structures fail to protect AuNPs, which aggregate and absorb less light (IFE off), resulting in fluorescence recovery. **C:** DNA-templated metal nanoclusters for fluorescent aptasensors: (a) Release of DNA-AgNCs from Nano-Q via aptamer-target binding results in fluorescence recovery; (b) Formation of dsDNA-AgNCs structure via aptamer-target binding results in fluorescence enhancement through the proximity of the G-rich DNA sequence to the AgNCs; (c) CuNCs synthesis within a dsDNA template results in strong fluorescence, which is interrupted upon aptamer-target binding ("no dsDNA" means "no CuNCs synthesis"); (d) Upon target-aptamer binding, the released cDNA after MB separation is extended with poly-T via TdT, which enables the synthesis of fluorescent CuNCs. **D:** Simple aptasensors with single fluorescent probes: disassembly of MB-aptamer-cDNA-F assemblies upon

aptamer-target binding releases the F-cDNA, and the fluorescence can be measured in the supernatant after magnetic separation of the MB-aptamer-target assemblies.

Adsorption-based FRET nano-aptasensors are very similar to their dye-based homologs (*vide supra*). The aptamer-functionalized fluorescent D nanoprobe is adsorbed on the surface of a NM-based quencher as A, leading to fluorescence quenching of D and fluorescence recovery upon target-aptamer binding (**Figure 2A(b)**).[57] Another approach employs the fact that ssDNA can bind to the surface of the π-rich electronic structure of carbon nanoparticles (CNPs) due to π–π stacking interactions.[58] Aptamer-functionalized fluorescent A nanoprobe can bind to the surface of fluorescent π-rich CNPs as D, and the close proximity of D-A triggers the FRET process, leading to fluorescence quenching of D and fluorescence enhancement of A. Target-aptamer binding reduces the π–π stacking interactions and disrupts FRET, which leads to enhanced fluorescence emission of D and attenuated fluorescence emission of A, achieving ratiometric fluorescence detection of targets.[59]

2.2.2 Aptasensors based on fluorescent nanomaterials and IFE

IFE refers to the absorption of the excitation or emission light of fluorophores by absorbers. It is a vital factor that the absorption spectrum of the absorber overlaps with the fluorescence excitation or emission spectrum of the fluorophore. In contrast to FRET, IFE is a radiative ET that can occur over much longer distances with an R^{-2} distance dependence, *e.g.*, within the solution of a cuvette with light path lengths of millimeters or centimeters.[60] Popular absorbers in IFE pairs are AuNPs[61] and AgNPs[62], and frequently-used fluorophores in IFE pairs include QDs,[61] CDs,[63] lanthanide complexes,[64] and UCNPs.[65] The higher the absorbance changes of the absorber, the stronger the fluorescence quenching of the fluorophore, which can be used to tune the sensitivity for target detection.[66] Various IFE nano-aptasensors have been developed and design strategies often rely on modulating the salt-induced aggregation of AuNPs.

One example is the IFE nano-aptasensor based on salt-induced aggregation of bare negatively charged AuNPs (**Figure 2B(a)**).[61] Fluorophores are quenched by well-dispersed AuNPs via IFE. A certain concentration of NaCl can cause aggregation of the AuNPs, weakening the efficiency of

IFE and recovering the fluorescence. Aptamers can adsorb on the surface of the AuNPs, thereby increasing the electrostatic repulsion and enhancing the stability of AuNPs, which are protected from salt-induced aggregation.[67] When combined with the target, the folded aptamers lose their ability to protect the AuNPs against salt-induced aggregation, which reduces the efficiency of IFE and restores the fluorescence. Another example uses DNA-functionalized AuNPs to modulate the stability of AuNPs against salt-induced aggregation (**Figure 2B(b)**).[68] Aptamers covalently attached to the surface of AuNPs can protect AuNPs through steric hindrance against aggregation, resulting in the quenching of fluorescence via IFE. Upon aptamer-target binding, folded DNA structures are formed and the AuNPs aggregate, accompanied by reduced IEF and fluorescence recovery. While direct aptamer functionalization is an additional step, this method is usually more stable to resist the influence of high salt concentrations.

2.2.3 Aptasensors based on DNA-templated fluorescent metal nanoclusters

Fluorescent metal nanoclusters (MNCs) are water-soluble molecular-level aggregates composed of several to dozens of atoms, which have been widely used in optical sensing, biomarkers detection, environmental monitoring, and other fields, owing to their advantageous properties, such as quantum size effect, good biocompatibility, and strong anti-polymerization ability.[69,70] The most commonly used templates for the preparation of MNCs include DNA, peptides, proteins, small molecule ligands, and polymers.[71] DNA templated MNCs (DNA-MNCs) have been frequently used in biosensors for the detection of various targets, such as nucleic acids, metal ions, small biomolecules, and proteins.[69] DNA-MNCs allow for *in-situ* synthesis under relatively mild preparation conditions, controllable operation process, adjustable fluorescence emission, and feasible coupling of DNA templates with aptamers, which are beneficial for their application as aptasensors. The key to efficient aptasensors is the design of the DNA probe, incorporating the template and the aptamer sequences. Currently, DNA-templated silver nanoclusters (DNA-AgNCs)[72] and DNA-templated copper nanoclusters (DNA-CuNCs)[73] are mainly applied.

Since the synthesis of DNA-AgNCs is based on the strong affinity between silver ions (Ag^+) and cytosine,[74] DNA templates of AgNCs are usually designed as cytosine-containing sequences,

e.g., CCCCCCGGGGGCCCCCC ($C_6G_5C_6$) or ACCCCAACCCC ($AC_4A_2C_4$).[75,76] In one representative approach, the DNA template is composed of the sequence for AgNCs synthesis, a linker, and the aptamer sequence (**Figure 2C(a)**).[76] In the absence of target, DNA-AgNCs are adsorbed on the surface of a quenching NM and target-aptamer binding results in the release of DNA-AgNCs and fluorescence recovery. Because the fluorescence of DNA-AgNCs can be significantly enhanced when they are close to G-rich DNA sequences,[77,78] they can be designed as fluorescence enhanced aptasensors. In one example (**Figure 2C(b)**), aptamers hybridize with the cDNA, containing template and G-rich sequences, such that DNA-AgNCs are well separated from the G-rich sequence and can exhibit only weak fluorescence. Upon aptamer-target binding, the cDNA is released and folded due to complementary bases at the terminals, which brings DNA-AgNCs in close proximity to the G-rich sequence and results in fluorescence enhancement.[75]

The application of DNA-CuNCs as fluorescent probes in aptasensors is primarily based on regulating the generation or disassembly of the specific DNA sequence to accomplish specific CuNC-fluorescence turn-on or turn-off. DNA templates for the synthesis of DNA-CuNCs include dsDNA templates[79] and poly-thymine (poly-T) templates.[80] A typical aptasensor using a dsDNA template is shown in **Figure 2C(c)**.[81] In the absence of targets, aptamers hybridize with the cDNA to form dsDNA as a template for CuNCs synthesis, which leads to intense fluorescence. The specific aptamer-target interaction disassembles the dsDNA, resulting in reduced fluorescence due to the inability of forming CuNCs. In a typical aptasensor using poly-T templates for CuNCs synthesis (**Figure 2C(d)**), structure-switching aptamers, terminal deoxynucleotidyl transferase (TdT), and magnetic separation are incorporated. The target-aptamer binding can lead to the release of cDNA after separation, and the generation of long poly-T as template for CuNPs with the assistance of TdT, bringing about high fluorescence signals.[73]

2.2.4 Pros and cons

Compared with organic dyes, aptasensors using fluorescent NMs as probes have specific advantages, such as good photostability and long shelf life. FRET nano-aptasensors, in which the effective performance depends on the quantum yield of the fluorescent probe and/or FRET

efficiencies, display good selectivity, high sensitivity, and strong anti-interference ability. However, most FRET nano-aptasensors require time-consuming and complicated covalent coupling of fluorescent probes and nucleic acids, and demand key experimental skills and nanotechnology knowledge to make them reproducible by others. The influence of modification on the affinity of the aptamers should also be considered and investigated. IFE nano-aptasensors do not require functionalization and labeling of the fluorescent NMs, which improves the simplicity of the method. However, these IFE nano-aptasensors rely on the salt-mediated aggregation of AuNPs, introducing some complications, such as unsatisfactory performance and stability in high-salt solutions, and the measurement should be completed in a short time to avoid excessive agglomeration, such that they are suitable for matrix analysis with lower salt concentrations within limited detection time. The most prominent feature of DNA-MNCs-based aptasensors is that they do not require expensive labels and complex functionalization, which contributes to low-cost and simple signal output for detection. In particular, sequence-dependent multicolor DNA-AgNCs can be used for multiplexed detection. However, the stability and anti-interference ability of the method is challenged by the photostability, batch differences, and photobleaching of DNA-MNCs. The key points of DNA-MNCs concerning the controllable synthesis and the mechanisms of fluorescence enhancement or quenching also lack clear theoretical guidance.

2.3 Aptasensors using a single fluorescent probe

Single fluorescent probes (SFP) can be used to fabricate relatively simple aptasensors for target detection through magnetic separation without the assistance of fluorescence quenchers. For SFP aptasensors, magnetic beads (MBs) can be used for the separation of the fluorescence signal. As illustrated in **Figure 2D**, assemblies between aptamer-MBs and cDNA-F (F: dye or fluorescent NM) are disassembled via aptamer-target binding and the fluorescent cDNA-F can be magnetically separated from the target-aptamer-MBs, such that the fluorescence intensity in the supernatant can be used for target quantification.[82] The design of magnetic separation in SFP aptasensors avoids the direct binding of the target with fluorescent probes, effectively eliminating the interferences of

target and probe. These methods do not need additional introduction of quenchers, and the detection can be achieved through a one-step mixing reaction. Magnetic separation contributes to reduce the interference of the sample matrix and enhance the anti-interference ability. However, complex functionalization or expensive labeling of fluorescent probes may be required.

2.4 Aptasensors using multiple fluorescent probes

More sophisticated fluorescent aptasensors for the use of multiple signals (*e.g.*, ratiometric detection) or the detection of multiple targets (multiplexing) can be accomplished through the application of multiple fluorescent probes. The commonly reported methods use fluorescent dyes with different emission colors, such as the green (*e.g.*, FAM), yellow (*e.g.*, carboxy-X-rhodamine, ROX), and red (*e.g.*, Cy5) dyes,[83] multicolor fluorescent NMs such as QDs,[84] CDs,[85] AuNCs,[86] AgNCs[87] and multicolor lanthanide complexes.[88] In order to accomplish multiplexed detection, the adsorption of ssDNA to fluorescence-quenching nanosurfaces (**Figures 1C**, **1E**, **2A**, and **2C**) and the target-dependent release and fluorescence recovery can be combined with aptamers that are labeled with different fluorophores (*e.g.*, Apt1-F1 and Apt2-F2).[84,86,88] Non-functionalized aptasensors for multiplexed detection can be designed using multicolor DNA-AgNCs and by modulating the DNA templates with different sequences.[87,89] Also, structure-switching aptamers (**Figure 1B**) can be adapted to multiple detection when different F-Q pairs with significant spectral differences of F (e.g., FAM-BHQ1 and Cy5-BHQ2 FRET pairs) are applied.[90]

Dye-based multiplexed detection methods have competitive advantages, including easy acquisition of fluorescent probes, simplicity, and versatility. However, FAM/ROX/Cy5 labeled on nucleic acids requires multi-wavelength excitation to obtain distinguishable fluorescence emission signals, leading to cumbersome operation. Aptasensors based on multicolor fluorescent NPs can obtain non-interfering fluorescence emission under a single excitation to realize simultaneous detection. However, in the establishment of the detection systems, the covalent coupling of aptamers to the surface of fluorescent probes is a prerequisite, which increases the difficulty and complexity of the assays. The method based on multicolor DNA-MNCs has the advantages of a

label-free format, non-functionalization, and low cost. However, it is necessary to change different excitations to determine multiple targets. In addition, the insufficiencies of DNA-MNCs, such as low quantum yield, poor photostability, and photobleaching can significantly affect the stability and accuracy of fluorescence detection methods.

2.5 Aptasensors based on sandwich-type split aptamers

In order to yield higher target specificities, sandwich-type aptasensors employ two (or more) recognition elements, such as aptamers and antibodies, or dual aptamers, which has been widely used in the detection of macromolecules (*e.g.*, thrombin).[91] However, this strategy is not feasible or efficient for small molecules (only with single binding sites or binding sites in too close proximity). Split aptamers, first introduced by Stojanovic and co-workers in 2000, derive from dividing the aptamer sequence into two fragments without affecting the affinity to its target.[92] They can be used to construct sandwich-type aptasensors for the determination of targets with low molecular weight by means of conjugating with different functional moieties and different signal transduction techniques.[93] Sensing of small organic molecules, *e.g.*, adenosine, has been realized with split aptamers, specifically, the development of a dual-emission ratiometric assay using F-labeled aptamers and quenching materials,[94] or fluorescent indicator displacement assays by incorporating G-rich sequences and G4-specific dyes[95].

Compared to full-length aptamers, fluorescent aptasensors using split aptamers show better specificity and higher sensitivity due to the improved affinity of split aptamers with the target. However, at present, only few split aptamers are available. In the successful design of split aptamers, 3D structure of the parent aptamer must be defined, which can be highly perturbed if the division is performed at the wrong site. Therefore, split aptamers are at the initial stage of design and biosensing application and remain a challenging topic.

3 Fluorescent aptasensors with DNA-based signal amplification

Whereas many analytes may be adequately quantifiable by non-amplified fluorescence detection, others require lower LODs that are not accessible by ordinary fluorescence sensing approaches. By combining DNA amplification techniques with aptamer-based assays for molecular recognition, the sensitivity of aptasensors can be greatly improved to meet the needs of trace detection. Here, we discuss the most frequently used enzyme-assisted and enzyme-free amplification techniques in aptasensors. Enzyme-assisted amplification techniques include rolling circle amplification (RCA), nuclease-assisted recycling amplification, and exponential amplification reaction (EXPAR). The enzyme-free amplification techniques involve hybridization chain reaction (HCR) and catalytic hairpin assembly (CHA). Both enzyme-assisted and enzyme-free methods can also be sequentially combined to so-called cascade signal amplification.

3.1 Enzyme assisted DNA amplification strategies

3.1.1 Rolling circle amplification (RCA)

RCA is an isothermal DNA amplification technique based on the rolling circle replication of circular DNA, and it mainly includes linear RCA (LRCA), hyperbranched RCA (HRCA) and multi-primed RCA.[96] In the process of a typical LRCA, the single-stranded DNA or RNA primer binds to the circular DNA template (*e.g.*, pre-circularized DNA or formed by target-specific ligation of a padlock probe), and under the action of DNA polymerase extends along the circular template to form a long ssDNA concatemer with hundreds to thousands of tandem repeats.[96] Since the RCA product is complementary to the circular DNA template, it can be controllably designed by adjusting the sequence of the template.[97] By modulating the template sequence, a series of fluorescent probes can be incorporated in the RCA products (RCPs) to amplify the target-specific detection signal. RCA-based aptasensors are expected to amplify a single molecular recognition event over a thousand-fold in a linear (LRCA) or exponential (HRCA or multi-primed RCA) manner. cDNA from a structure switch is commonly applied as the primer to hybridize to the

template for starting the RCA process (**Figure 3A**).[98] Aptamer-target binding releases the cDNA (from the aptamer-cDNA complex), which can then hybridize to the DNA padlock probe to be circularized by T4 DNA ligase, triggering the RCA process to produce a long ssDNA concatemer with the assistance of dNTPs and DNA polymerase. Depending on the functional moieties that hybridize to the RCP, RCA-based fluorescence aptasensors can be divided into five types: *i)* Molecular beacon probes that hybridize to the RCP (**Figure 3B(a)**);[99] *ii)* Label-free methods using dsDNA-specific dyes such as SYBR Green I, in response to the long dsDNA concatemers triggered by adding a second primer (**Figure 3B(b)**);[100,101] *iii)* Label-free methods using G4-specific dyes and G4-sequence containing RCPs (**Figure 3B(c)**);[102] *iv)* F-DNA probes that are adsorbed to a NM-based fluorescence quencher and released upon hybridization to the RCP (**Figure 3B(d)**);[103] *v)* F-labeled dNTPs that are directly incorporated in the RCP during RCA, which requires separation of fluorescent RCP and F-labeled dNTPs, *e.g.*, via DNA hydrogel formation of the RCP (**Figure 3B(e)**).[98]

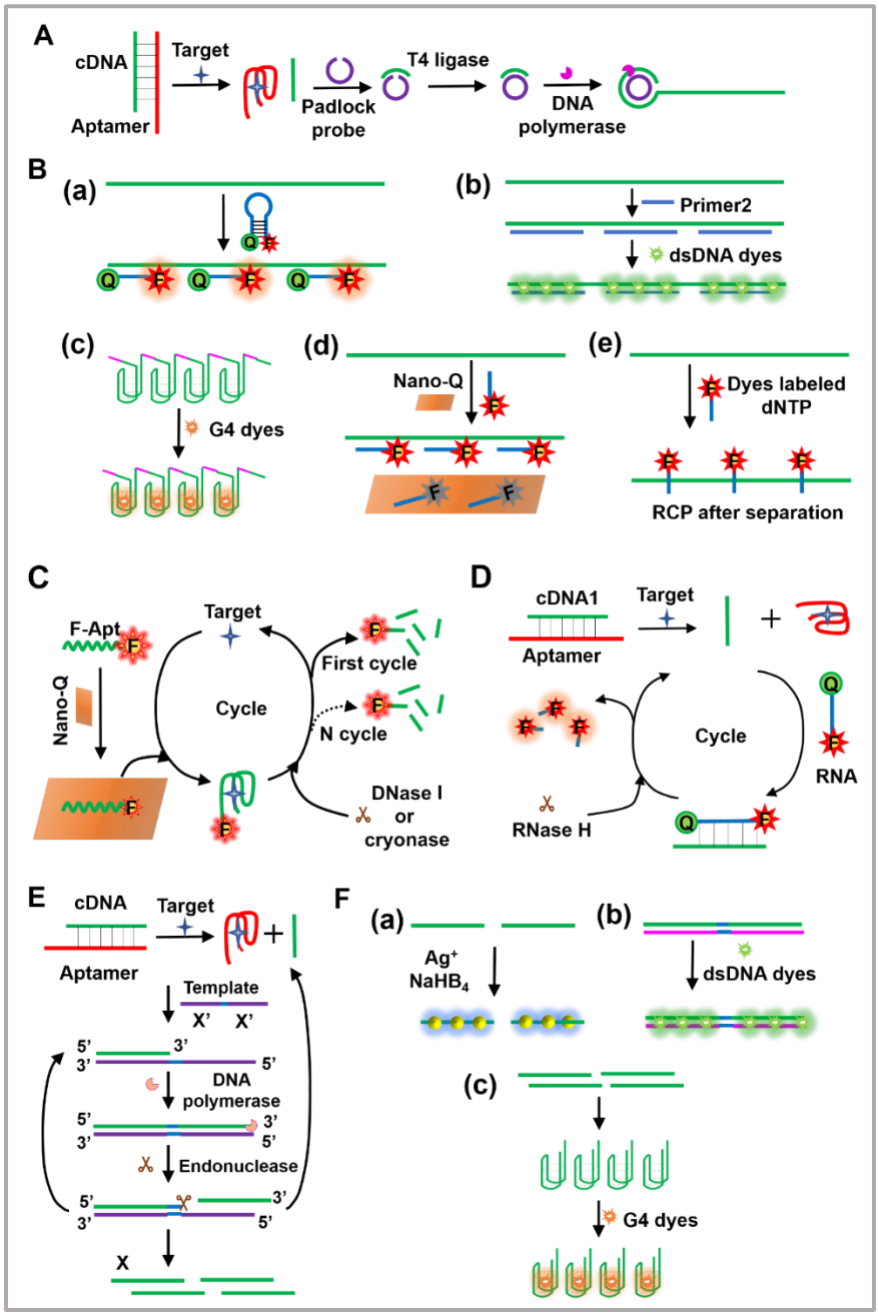

Figure 3. Enzyme-assisted DNA amplification techniques. **A:** In a typical RCA-based aptasensor, a cDNA is released from a cDNA-aptamer dsDNA through aptamer-target binding. The released cDNA is then hybridizing to a padlock DNA that is circularized (closed) via ligation (using T4 ligase) and the cDNA is used as a primer to start RCA (using a DNA polymerase and dNTPs) to produce a long ssDNA concatemer (RCP). **B:** Approaches of exploiting the RCP for amplified fluorescence signal generation: (a) Molecular beacon (F-Q) probes open when hybridizing to the RCP, which results in a target-specific RCP-amplified increase of fluorescence intensity; (b) When a second primer is used to transfer the ssDNA RCP into dsDNA, dsDNA-specific dyes (*e.g.*, SYBR Green) can be used to generate a target-specific RCP-amplified fluorescence

intensity increase; (c) When the RCP contains sequences to form G4 structures, G4-specific dyes can be used to generate a target-specific RCP-amplified fluorescence intensity increase; (d) F-DNA probes adsorbed to a Nano-Q can hybridize to the RCP and result in target-specific RCP-amplified fluorescence recovery; (e) When dye-labeled dNTPs are incorporated in the RCP during RCA, the highly fluorescent RCP must be separated from free dye-labeled dNTPs. **C:** A quenched F-aptamer (adsorbed to a Nano-Q) is released via aptamer-target binding resulting in fluorescence recovery. DNase I or cryonase can digest the aptamer-target complex and release the target, which can be used again to release a second F-aptamer. This recycling principle can be repeated over many cycles to amplify the fluorescence signal. **D:** Recycling of cDNA, released from an aptamer upon target binding, via hybridization to F-RNA-Q and subsequent digestion by RNase H. After cycling, the fluorescence intensity of liberated F is used as target quantification signal. **E:** Principle of EXPAR-based aptasensors using the target-induced release of cDNA as a trigger (X) to induce production of new X on the X'-X' template (via polymerase) and recycle X via cleavage of the produced dsDNA (via endonuclease). **F:** Formats of fluorescence signal generation using the EXPAR DNA products: (a) ssDNA products with a cytosine-rich sequence can be used as a template for the synthesis of DNA-AgNCs; (b) dsDNA products can activate dsDNA-specific dyes; (c) ssDNA products that form G4 complexes can activate G4-specific dyes.

3.1.2 Nuclease-assisted recycling amplification

Another possibility of signal amplification in aptasensors is the recycling of the same target or cDNA molecule for cyclic signal generation (one target activates many fluorophores). This strategy commonly applies nucleases for DNA digestion and has been used in electrochemical, fluorescent, chemiluminescence, and colorimetric aptasensors.[104] The appropriate design of DNA strands for efficient cleavage by the nucleases, and the target or the cDNA release is paramount for such aptasensors. Often used nucleases for target recycling are deoxyribonuclease I (DNase I) and cryonase cold active nuclease. In one aptasensor example (**Figure 3C**), the F-aptamer is absorbed on a Nano-Q for fluorescence quenching and protection against nuclease cleavage. The aptamer-target complex is released from the Nano-Q leading to fluorescence recovery and availability for cleavage by DNase I or cryonase, which releases the target that can then be recycled for detaching another F-aptamer from the Nano-Q and used for cyclic fluorescence intensity amplification and quantification of very low target concentrations.[105,106] In addition, based on the same principle, Exo I, which can specifically digest ssDNA from 3' to 5', has been applied for

target recycling in fluorescent aptasensors.[107] However, certain aptamers (*e.g.* ATP, ochratoxin A) inhibit the Exo I digestion upon binding to the target,[108,109] which are not applicable to the fluorescent strategy using nucleases-assisted target recycling. The different responses of these aptamer-target complexes to Exo I digestion may be due to the differences in binding mechanism and conformational changes of aptamers towards targets, which must be carefully considered in this Exo I-assisted design strategy.

Recycling of cDNA is usually performed via ribonuclease H (RNase H) and exonuclease III (Exo III). RNase H can selectively hydrolyze RNA in a double-stranded DNA/RNA hybrid.[110] As shown in **Figure 3D**, this approach requires an aptamer, primary cDNA (represented by cDNA1 in the diagram), and an extra RNA labeled with F-Q at 3' termini and 5' termini (F-RNA-Q) for signal readout. In the absence of the target, the aptamer partially hybridizes with cDNA to form the aptamer-cDNA duplex, and F-RNA-Q remains a single strand resisting the digestion by RNase H, resulting in low fluorescence due to the proximity of F-Q. In the presence of the target, the aptamer-cDNA duplex liberates cDNA, which can then hybridize with F-RNA-Q. The resulting cDNA-RNA duplex is digested by RNase H, which recycles cDNA and digests F-RNA-Q, such that F is released from Q accompanied with strong fluorescence. This cycle is repeated with the same cDNA and the extra F-RNA-Q and results in many free fluorophores. Similarly, Exo III, which can stepwise hydrolyze dsDNA from its flush or concave 3' hydroxyl termini but is inactive on ssDNA or dsDNA with protruding 3' termini (overhangs of a few nucleotides),[111] is suitable to construct the aptasensors via cDNA recycling signal amplification by addition of extra F-DNA probes and Nano-Q after termination of cycling.[112]

3.1.3 Exponential amplification reaction (EXPAR)

EXPAR, first reported by Galas' group in 2003, is an isothermal and rapid (<30 min) amplification technology with high amplification efficiency (>10^6-fold) to synthesize short oligonucleotides (8-16 bases) by combining the amplification template, endonuclease, and polymerase.[113] EXPAR has been applied for the sensing of various targets (*e.g.*, microRNA, DNA, kinases, small molecules) using fluorescence methods.[114-117] EXPAR can be classified into one-template (X'-X'), two-

template (X'-Y' and Y'-Y'), and extended Y'-X'-X' template systems.[118] The EXPAR systems (X'-Y'/Y'-Y' and Y'-X'-X') are mainly used in fluorescent biosensors to detect nucleic acid targets.[115] In the one-template (X'-X') EXPAR aptasensor shown in **Figure 3E**, the EXPAR template contains a trigger binding sequence (X'), a recognition sequence for a particular endonuclease, and a DNA-polymerase extension sequence (X') to generate a signal reporter strand (X).[116,119] The cDNA released from the structure-switching aptamer upon target binding is usually selected as the trigger DNA (X) that hybridizes with X' in the template and initiating the EXPAR process to produce additional X (on the second X' sequence in the template) that are then cleaved by the endonuclease for producing more X for amplified signal outputs. Once sufficient X reporter strands are produced, various fluorescence readout strategies can be applied (**Figure 3F**): *i)* X can be used as a template for DNA-AgNC synthesis;[116] *ii)* When EXPAR is adapted to produce an excess of dsDNA from the X'-X' template, a label-free method using dsDNA specific dyes (*e.g.*, SYBR Green) can be used;[114] *iii)* X can be designed to fold into a G4 that is able to activate G4-specific dyes.[117] It is worth mentioning that high background signals generated by non-specific amplification is a serious issue in EXPAR-based assays, which may be caused by the interaction between the template and the interfering DNA sequences in the matrix and the non-specific binding among different templates.[118] Different measures, such as the introduction of DNA strands that can lock the template, the blocking of 3'-end of the template with phosphate, and the incorporation of materials with adsorption capacity (*e.g.*, GO, single-strand binding proteins), can substantially suppress non-specific amplification.[115,120,121]

3.1.4 Pros and cons

RCA fluorescent aptasensors amplify the target-aptamer recognition event into a long ssDNA product to realize signal output with a broad range of formats, providing the advantages of flexible design, constant temperature, and high sensitivity. However, the RCA process requires a multi-step procedure and a relatively long reaction time. There is a lack of theoretical guidance for the sequence design of specific circular templates, which increases the complexity of the method. Nuclease-assisted recycling amplified fluorescent aptasensors have low sequence design

requirements and provide a universally applicable detection strategy. They are a good choice for multiple detection with simplicity and rapidity by using multi-color fluorescent probes. The most prominent feature of EXPAR fluorescent aptasensors is that they can produce high-efficiency amplification within 30 minutes, enabling rapid and sensitive detection. The endonuclease in EXPAR system endows the method with high sensitivity and specificity. However, a specific recognition site in the template is required to activate the function of endonuclease and multiple steps are necessary to perform the amplification reaction, which limit the applicability and simplicity of the method. Significant non-specific amplification can impair the analysis performance and it is recommended to introduce background reduction measures in EXPAR, which does not compromise the performance of the quantification step. In general, enzyme-assisted amplified fluorescent aptasensors are limited by multi-step procedures and rather harsh experimental conditions.

3.2 Enzyme-free DNA amplification strategies

3.2.1 Hybridization chain reaction (HCR)

HCR, first proposed by R. M. Dirks and N. A. Pierce in 2004, is an isothermal and enzyme-free signal amplification technology based on DNA strand displacement reactions.[122] The linear HCR can be extended to non-linear amplification, *e.g.*, by branched HCR or dendritic HCR.[123] In the HCR process, an initiator DNA strand causes a pair of complementary DNA hairpins (H1 and H2) to alternately open up and hybridize in a chain reaction, resulting in the formation of long dsDNA concatemers.[124] The key to efficient HCR lies in the judicious design of the two hairpins, which must be carefully constructed by modulating the lengths and GC contents of loops, stems, and toeholds.[122,125] HCR-based biosensors have been designed with different signal transduction methods, including colorimetry, fluorometry, electrochemistry, surface plasmon resonance, or electrochemiluminescence.[124] HCR-based aptasensors can be developed using both the aptamer or the cDNA as initiator DNA. When the aptamer is designed as hairpin DNA containing the HCR initiator sequence, the target-aptamer binding can open the hairpin and expose the initiator DNA,

which then triggers HCR of H1 and H2 (**Figure 4A(a)**).[126] Another approach is the target-dependent release of cDNA from an aptamer-cDNA duplex, such that the cDNA serves as DNA initiator for HCR (**Figure 4A(b)**).[127]

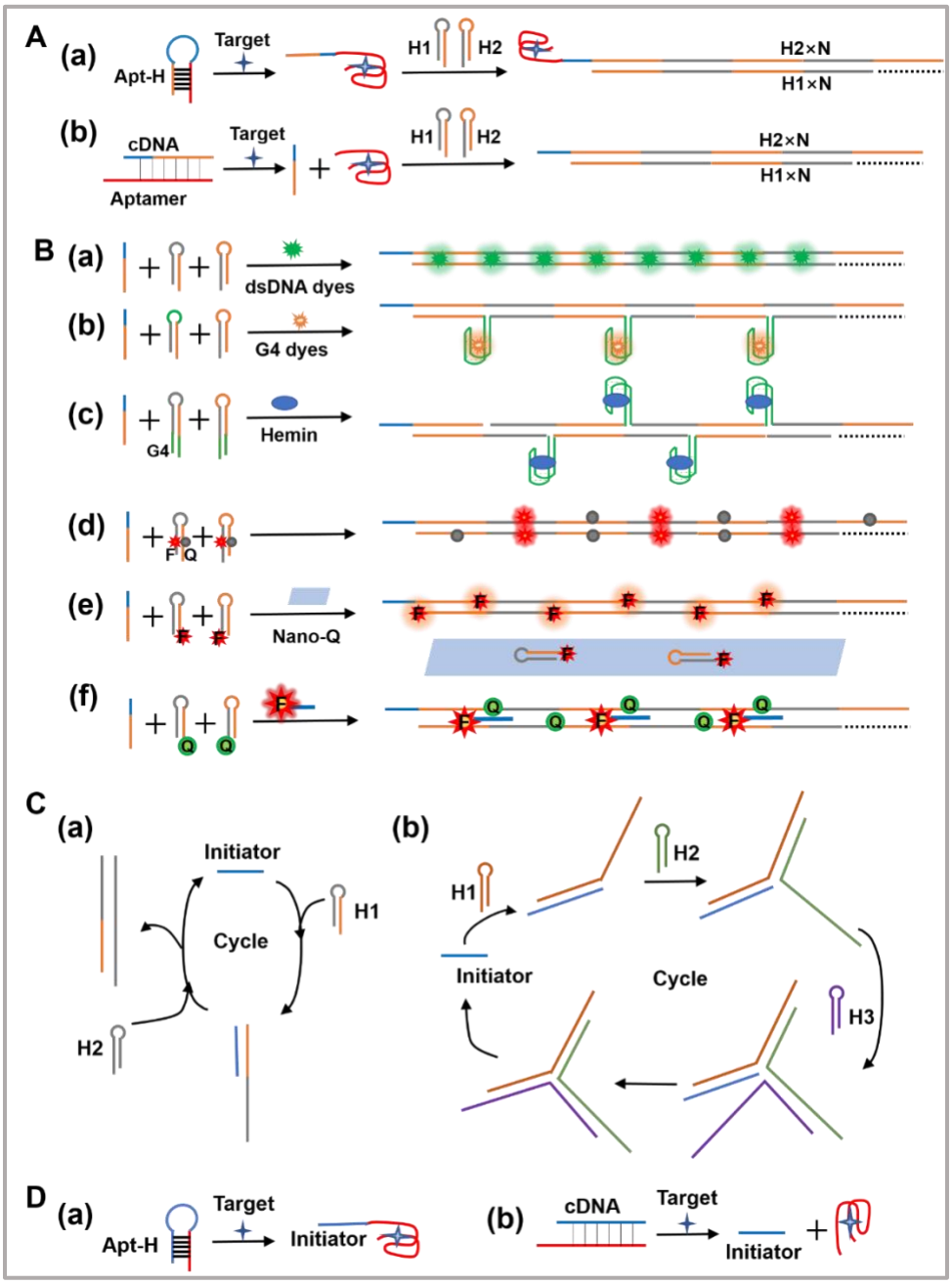

Figure 4. Enzyme-free DNA amplification techniques. **A:** Principle of HCR-based aptasensors: (a) The DNA initiator (orange sequence) is contained in a DNA aptamer hairpin that opens upon target binding. The exposed DNA initiator sequence then opens H1 (orange sequence), which then opens H2 (gray sequence), which again opens H1 (orange sequence) and so forth (chain reaction) to produce a long dsDNA

concatemer; (b) Similarly, a released cDNA (upon target-aptamer binding) can be the DNA initiator for HCR. **B:** Approaches of exploiting the HCR product for amplified fluorescence signal generation: (a) Direct activation of dsDNA-specific dyes; (b) HCR product forms G4 structures and activates G4-specific dyes; (c) HCR product forms G4 structures and combines with hemin to G4 DNAzyme, which can activate the generation of fluorescent products; (d) F-Q labeled on hairpins (H1 and H2) are separated from each other within the HCR product; (e) F-DNA hairpins get adsorbed and quenched by Nano-Q but HCR unfolds the hairpins and the HCR product is not adsorbed, such that fluorescence is recovered; (f) Triplex DNA formed by HCR product and F-DNA results in fluorescence quenching. **C:** Principle of CHA: (a) The DNA initiator sequence opens H1 (orange sequence), which then opens H2 (gray sequence) to form a H1-H2 dsDNA and release the DNA initiator for an additional cycle; (b) The DNA initiator sequence opens H1 (orange sequence), which then opens H2 (green sequence) and H3 (purple sequence) successively to form a H1-H2-H3 junction and release the DNA initiator for the next cycle. **D:** The DNA initiator (blue sequence) of CHA is contained in a DNA aptamer hairpin that opens upon target binding (a), or in cDNA released from an aptamer-cDNA duplex upon target-aptamer binding (b).

Signal transduction in HCR-based fluorescence aptasensors can be performed label-free, via dsDNA specific dyes that may emit strong fluorescence in response to the long dsDNA structure in the HCR products (**Figure 4B(a)**),[128] via G4-specific dyes insert into the G4 structure generated in the HCR products by incorporating G4 sequence into one of the hairpins (**Figure 4B(b)**),[129] or via G4/hemin DNAzymes that catalyze the reaction between substrate and H_2O_2 to generated fluorescent products using G4 structures formed in the HCR products by linking split G4 sequences to the ends of both hairpins (**Figure 4B(c)**)[130]. HCR aptasensors can also be carried out via functionalized hairpins, in which H1 and H2 are F-Q labeled (low fluorescence) and the HCR product displaces F away from Q, thereby leading to fluorescence recovery (**Figure 4B(d)**),[119] or Nano-Q adsorbs and quenches the free F-H1 and F-H2 hairpins but not the F-containing HCR product (**Figure 4B(e)**),[126] or Q and F are labeled to the hairpins and an additional DNA probe, respectively, and a triplex DNA structure formed by the HCR product and the additional F-DNA probe brings F and Q in close proximity, such that the fluorescence of F is quenched (**Figure 4B(f)**).[131,132]

3.2.2 Catalytic hairpin assembly (CHA)

CHA, initially employed by Turberfield and co-workers as fuel for autonomous DNA devices, is

triggered by a catalyst to form stable DNA duplexes from two complementary DNA hairpins.[133] Later, Yin *et al.* and Li *et al.* proposed several types of self-assembly pathways, in which an ssDNA initiator catalyzes the hybridization of hairpins through a succession of toehold-mediated strand displacement reactions.[134,135] Here, two common CHA approaches using two hairpins or three hairpins are introduced. For the CHA approach using two hairpins, the initiator sequence opens H1, which then hybridizes to H2 (to form a H1-H2 dsDNA) and releases the initiator DNA for another cycle of H1-H2 duplex formation to produce many H1-H2 CHA products (**Figure 4C(a)**).[134,135] In the three-hairpin CHA approach, an initiator sequence mediates the self-assembly of the haripins and the recycling of initiator to form a three-arm branched junction structure (**Figure 4C(b)**).[135] CHA has been widely applied to construct aptasensors using multiple signal transduction strategies.[136] Similar to HCR, both aptamer (**Figure 4D(a)**) and cDNA (**Figure 4D(b)**) can be used as CHA initiators in CHA-based aptasensors.[137,138] Because the CHA product is also dsDNA (although shorter than HCR products), quantifying target-dependent CHA aptasensors is very similar to HCR, and includes the following fluorescent signal formats: *i)* Employing fluorescent probes in response to the dsDNA CHA products, such as dsDNA-specific CuNP synthesis;[138] *ii)* Employing F-Q labeled hairpins in the CHA process;[137] *iii)* Employing fluorophore-functionalized hairpins, in which Nano-Q adsorb and quench the free F-hairpins but not the F-containing CHA products;[139] *iv)* CHA product combines with an additional F-Q duplex reporter to separate F from Q.[140] Recently, employing FRET donor and the acceptor functionalized hairpins, Xu *et al.* reported a CHA-based biosensor for the quantification of microRNA that has the potential to overcome the environmental susceptibility of HCR.[141] This FRET CHA strategy can also be adapted to develop fluorescent CHA aptasensors for the quantification of non-nucleic acid targets.

3.2.3 Pros and cons

Enzyme-free amplified fluorescent aptasensors have smoother experimental conditions, and provide the advantages of simple operation, constant temperature, favorable practicability, visual analysis, and high sensitivity. Most HCR fluorescent aptasensors mentioned above employ

traditional linear HCR, which is simple in sequence design and in establishment of strategies for multiple detection. However, typical HCR adopts a linear growth mechanism via cascade chain reaction, resulting in limited signal amplification efficiency and sensitivity. Non-linear HCR is an effective measure to obtain high sensitivity but it is less used in fluorescent aptasensors due to the requirement of more complex sequence design than for linear HCR. CHA fluorescent aptasensors are carried out by a modular circuit of primers, which produces higher signal amplification and sensitivity. It is simple in sequence design and can be used for multiplexed detection by adjusting the hairpin sequences and F-Q labeling according to the primer. However, the strategies of CHA fluorescent aptasensors are mainly based on labeled F or F-Q, thus bearing a considerable cost. The label-free CHA strategy using DNA-CuNPs is cost-effective but DNA-CuNPs is easier to synthesize on poly-T or A/T dsDNA templates, which limits sequence design and applicability of the method. Both HCR and CHA adopt the process of initiator-triggered strand displacement reaction that rely on free energy-driven assembly of DNA hairpins. Hence, in the construction of HCR or CHA-based aptasensors, it is crucial to carefully consider thermodynamics and kinetics, and rationally design sequences of DNA hairpins to ensure the link between target recognition and amplification reaction for good performance, that is, the target-aptamer binding induces the release of primers to trigger effective amplification process, and no background leakage occurs without the presence of target. Although there are some design principles for HCR and CHA, specific theoretical guidance including the optimization of hairpin sequences and thermodynamic evaluation in HCR or CHA-based aptasensors remain to be explored to provide the theoretical basis for a universal application of these strategies.

3.3 Cascade signal amplification

Cascade signal amplification assays that sequentially combine two or more amplification approaches can potentially provide even more efficient signal amplification and thus, lower limits of detection. The principle of cascade signal amplification is that the products of the previous reaction trigger the following reaction, thereby connecting multiple signal amplification modules.

For example, RCA can be combined with CHA[142] or HCR.[143] RCA can also be used as the second reaction when the RCA primers are produced by a previous amplification via polymerization/nicking reaction catalyzed by DNA polymerase and endonuclease,[144] or nuclease digestion-aided recycling amplification.[145] Other examples include the cascade amplification reactions using enzyme-assisted strand displacement amplification to trigger the process of CHA,[146] or employing the product of EXPAR to trigger HCR.[119,147]

Cascade-amplified fluorescent aptasensors convert the aptamer-target recognition event into cascade reaction products for readout, thereby obtaining ultra-high sensitivity and satisfactory analysis performance due to the integration of the unique properties of each amplification technique. However, the cascade reaction leads to cumbersome operation, prolonged reaction time, more DNA reactants, and more complex requirements for sequence design, undermining the convenience and rapidity of the method. Cascade amplification strategies rely on the combination of enzyme-required and enzyme-free techniques, which does not only make the experimental conditions more stringent, but also weakens the outstanding advantages of enzyme-free formats in HCR or CHA. To avoid non-specific background leakage and obtain effective amplification, the mutual fit between the different amplification technologies or the coupling of structure-switching aptamer with amplification technologies is critical. However, complexities of sequence design and experimental details are often not sufficiently discussed, thus compromising the reproducibility and versatility of these methods. More efforts are needed to develop cascade amplification fluorescent aptasensors with simple operation, short time, facile design of DNA sequence, enzyme-free formats, and good stability.

4 Application of fluorescent aptasensor for the detection of food chemical contaminants

Many of the fluorescent aptasensor design strategies presented above have been applied to develop assays for different food chemical contaminants. In this section, we discuss representative examples and, taken into account the very large amount of literature concerning fluorescent

aptasensors, mainly focus on recent studies (publications from 2019 to 2021). An overview of the different applications can also be found in **Table 1** at the end of this section.

4.1 Detection of toxins

Toxins listed as food contaminants mainly include marine toxins and agricultural toxins. The marine toxins (*e.g.*, palytoxin, saxitoxin) can cause human poisoning through biological vectors, such as marine shellfish or fish. Agricultural toxins, mainly mycotoxins (*e.g.*, aflatoxin, ochratoxin A), can be produced in most agricultural products and pose a threat to human health through the food chain. In recent years, a variety of aptasensors has been developed for toxins to ensure food safety.[148,149] Here, we focus on the application of fluorescent aptasensors in the detection of common toxins by discussing representative examples (spanning a broad range of materials, sensitivities, and modes of application) of the most common types of fluorescent aptasensors.

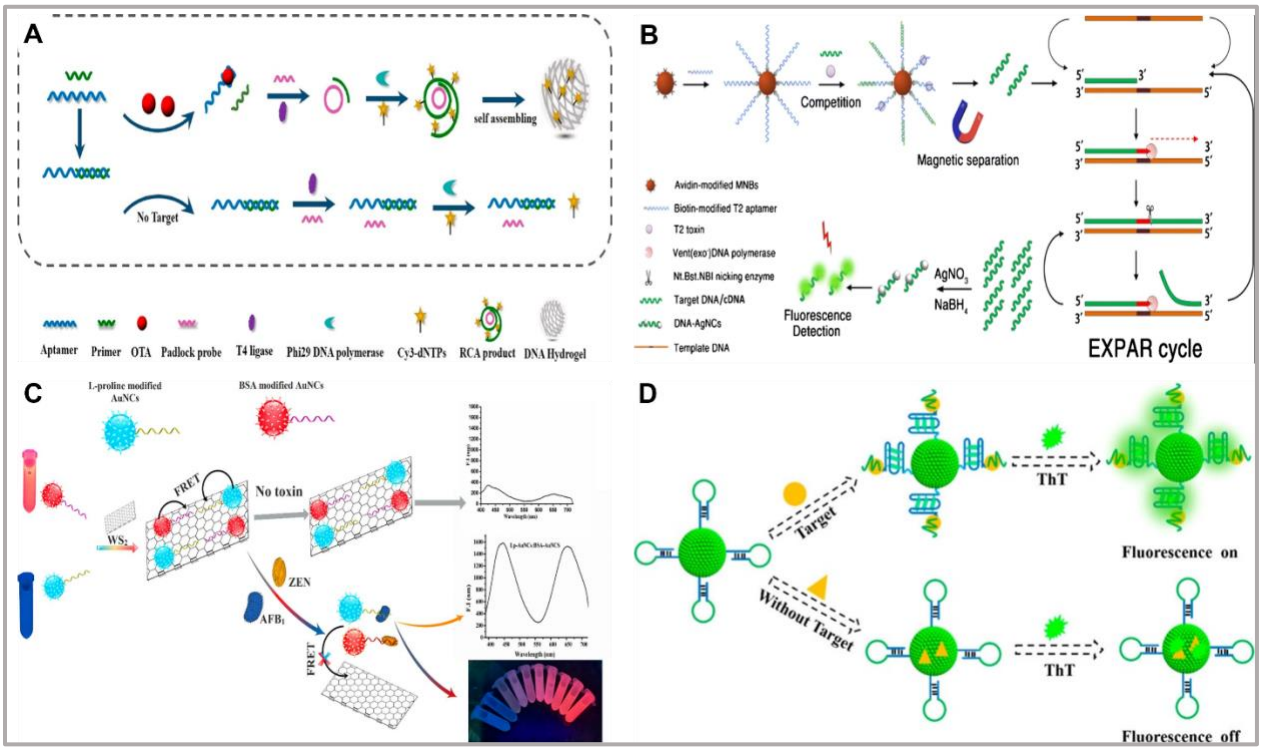

Figure 5. Recent examples of fluorescent aptasensors for toxins. **A:** Upon OTA-aptamer binding, the primer is released from aptamer-primer complex and combines with a padlock probe to form a circular template via T4 ligase. When incorporated with Cy3-dNTPs and Phi29 DNA polymerase, the RCA reaction is initiated to form a fluorescent DNA hydrogel for signal readout. The RCA process and the formation of fluorescent DNA hydrogel do not occur without OTA. Reproduced from Hao, L.; Wang, W.; Shen, X.; Wang, S.; Li, Q.;

An, F.; Wu, S. J. Agric. Food Chem. 2020, 68, 369-375 (ref 98). Copyright 2020 American Chemical Society. **B:** Biotin-modified T-2 mycotoxin (T2) aptamers are anchored on avidin-modified MBs and combine with cDNA to form MB-aptamer-cDNA assemblies. Upon T2-aptamer interaction, remaining cDNA is magnetically separated and induces the EXPAR cycle to amplify cDNA, which serves as template for the synthesis of fluorescent DNA-AgNCs. Reprinted by permission from Springer Nature: MICROCHIMICA ACTA. Competitive fluorometric assay for the food toxin T-2 by using DNA-modified silver nanoclusters, aptamer-modified magnetic beads, and exponential isothermal amplification. Zhang, M.; Wang, Y.; Yuan, S.; Sun, X.; Huo, B.; Bai, J.; Peng, Y.; Ning, B.; Liu, B.; Gao, Z. Microchimica Acta 2019, 186 (4), 219 (ref # 116). Copyright 2019. **C:** Blue-emitting AuNCs (L-proline-AuNCs) functionalized with AFB1 aptamer and red-emitting AuNCs (BSA-AuNCs) modified with ZEN aptamer are adsorbed on the surface of WS_2, leading to fluorescence quenching via FRET. The AFB1-aptamer binding and ZEN-aptamer binding induce the surface detachment and fluorescence recovery, which can be analyzed with a single excitation wavelength. Reproduced from Khan, I. M.; Niazi, S.; Yu, Y.; Mohsin, A.; Mushtaq, B. S.; Iqbal, M. W.; Rehman, A.; Akhtar, W.; Wang, Z. Anal. Chem. 2019, 91, 14085-14092 (ref 86). Copyright 2019 American Chemical Society. **D:** G4-containing aptamer chimeras are immobilized on PhC barcodes. The mycotoxin-aptamers interaction leads to G4-ThT combination and fluorescence enhancement. Reproduced from Zhang, D.; Cai, L.; Bian, F.; Kong, T.; Zhao, Y. Anal. Chem. 2020, 92, 2891-2895 (ref 27). Copyright 2020 American Chemical Society.

4.1.1 Aflatoxin (AFT)

Based on dual-strand structure switches composed of a fluorophore-labeled aptamer and a quencher labeled cDNA, fluorescent aptasensors have been developed for AFT with different fluorophore/quencher pairs, such as FAM/TAMRA for aflatoxin M1 (AFM1)[30] or FAM/BHQ1 for aflatoxin B1 (AFB1).[31] Using a dual-terminal labeling with FAM/BHQ1, the sensitivity could be improved around 50-fold compared to the single-terminal functionalization strategy.[31] Using the change in fluorescence intensity between an aptamer/ThT G4 complex and an aptamer/AFB1 complex, Li *et al.* developed a simple label-free turn-off fluorescence aptasensor for detecting AFB1 in 20 min with an LOD of 1 ng mL^{-1} in plant-derived food.[26] Another label-free aptasensor was designed, in which the aptamers were used as molecular recognition probes and Rh6G was loaded into the MSNs as signal probes, with an LOD of 0.13 ng mL^{-1} for quantifying AFB1.[44] Through the synergetic utilization of a 9,10-distyrylanthracene derivative (DSAI) as AIE probe, Deng *et al*. developed a turn-off fluorescence aptasensor based on an intrinsic aptamer conformation response FRET probe for one-pot mix-and-read detection of AFB1 with an LOD of

0.29 ng mL^{-1}.[50] Upon target binding, the conformation-switching aptamer brought the terminal TAMRA dye in closer proximity to DSAI, which resulted in significantly enhanced FRET from DSAI to TAMRA. Based on a quaternized tetra-phenylethenesal derivate (TPE-Z) and GO, a simple and label-free fluorescent aptasensor for AFB1 was developed.[49] In the absence of AFB1, a TPE-Z/aptamer complex with strong fluorescence was formed, which was quenched after the addition of GO. Upon target binding, the formation of AFB1/aptamer complex induced the release of TPE-Z/aptamer from the surface of GO, resulting in fluorescence recovery. The assay was performed by simply mixing TPE-Z, AFB1 aptamer, GO, and the AFB1 samples with a detection limit of 0.25 ng mL^{-1}.

Relying on the DNA functionalization and fluorescence quenching of NMs, different nano-aptasensors were developed for AFB1. Thanks to the finding that humic acid can readily adsorb ssDNA aptamers and act as quencher of the blue fluorescence of aptamer-modified CDs, Guo *et al*. described an aptamer-based fluorescence assay for AFB1 with an LOD of 70 pg mL^{-1}.[150] Taking advantage of ET and aptamer-cDNA hybridization, Lu *et al.* developed a target-driven switch-on fluorescence aptasensor for trace AFB1 determination by employing ET between aptamer-modified CdZnTe QD donors and cDNA-conjugated AuNP acceptors, and the LOD was determined as 20 pg mL^{-1}.[56] In their work, the coating of CdZnTe QDs on SiO_2 carrier can effectively avoid the self-agglomeration of the ultra-small particle labels.

4.1.2 Ochratoxin A (OTA)

Various dye-based fluorescent aptasensors have been designed for OTA detection. Incorporating the selective quenching effects of GO and OTA-induced detachable dsDNA structures with periodical units (coined nanoladders) containing ROX-labeled ssDNA and aptamer ssDNA sequences, Xu *et al.* developed a highly sensitive fluorescence turn-off aptasensor for the detection of OTA.[151] In the dsDNA nanoladders, the fluorescence intensity of ROX remained strong due to the very weak adsorption to GO. OTA-aptamer binding detached the nanoladders and released the ROX-DNA, which was then adsorbed and quenched by GO. Sensitivity improvements were accomplished by simply adding two mismatched bases to replace the sturdy nanoladders with frail

nanoladders, enabling the detection of OTA with an LOD of 0.1 nM (~40 pg mL^{-1}). Based on the G4-selective dye ThT, a ratiometric FRET aptasensor was proposed for robust and ultrafast detection of OTA.[152] In this work, FRET could occur between ThT and terminal-labeled FAM, which was turned off in the presence of OTA due to the disassembly of the G4 structure and the detachment of ThT from the aptamer, thus allowing quantification of OTA with an LOD of 0.38 ng mL^{-1} and a very rapid detection time of 30 s. The FRET aptasensor allowed for a 77% enhancement of signal to background ratio compared to the ThT-based fluorescent aptasensor without FRET and provided robust measurements at different probe concentrations. AIE dyes can avoid the concentration or aggregation-induced quenching of conventional dyes and serve as powerful probes for developing label-free aptasensors. A turn-on fluorescent aptasensor was proposed to detect OTA by using DSAI AIE dyes and Exo I.[52] The high affinity of the positively charged DSAI to the negatively charged aptamers resulted in AIE, which lighted up DSAI with strong fluorescence in the presence of OTA because the OTA-aptamer complex resisted Exo I digestion. In the absence of OTA, the aptamer was digested with the addition Exo I, leading to the dispersion of DSAI and low fluorescence. The adoption of AIE dyes led to an enhancement of the signal-to-background ratio of more than 104% compared to conventional nucleic acid dyes, thus favoring the sensitive detection of OTA with an LOD of 0.4 ng mL^{-1}. Furthermore, only one aptamer sequence was involved in the assay, avoiding complex aptamer probe structure design.

Detection of OTA could also be demonstrated by using a single fluorescent nanoprobe. Taking advantage of structure-switching aptamers and the ability of terminal deoxynucleotidyl transferase (TdT) and 2'-deoxythymidine 5'-triphosphate (dTTP) to generate long polythymine as template for CuNPs, a separation-required fluorescence enhancement method was presented for the determination of OTA.[73] The interaction of OTA with its aptamer caused structural changes, which influenced the synthesis and fluorescence of DNA-templated CuNPs, leading to a 2.0 nM (~0.8 ng mL^{-1}) LOD for OTA. FRET aptasensors for OTA can be designed based on functionalized nanomaterials and DNA adsorption. Bi *et al.* developed a new fluorescence aptasensor for OTA analysis with graphitic carbon nitride QDs (g-CNQDs) as donor and cobalt oxyhydroxide (CoOOH)

nanosheets as quencher.[153] The method exhibited good specificity for OTA, an LOD of 0.5 nM (~0.2 ng ml^{-1}), and favorable results to quantify OTA in barley and corn flour.

Fluorescent aptasensors based on DNA amplification techniques, such as nuclease-aided recycling amplification,[110,112] HCR,[129] and RCA[98] were also applied for the sensitive detection of OTA. For example, in a structure-switching aptamer approach, RNase H was applied to cleave the RNA in cDNA/RNA hybrid and release the cDNA, leading to cDNA recycling signal amplification.[110] In a structure-switching aptasensors that utilized the adsorption affinity of dye-labeled ssDNA with GO, cDNA hybridized with a specifically designed hairpin DNA and Exo III was applied to digest dsDNA for cDNA release to generate a cyclic hybridization–hydrolysis process for signal amplification.[112] Qian *et al.* reported a simple, sensitive, and label-free fluorescent aptasensor for OTA detection through NMM binding with G4 structures generated in HCR products.[129] The study combined computer simulation and biological experiments. The strategy could detect OTA with an LOD of 4.9 pM (~2 pg mL^{-1}) and satisfactory results for wheat flour and red wine samples. Combining RCA and structure-switching aptamers, a sensitive fluorescent DNA hydrogel aptasensor based on the self-assembly of dye-labeled RCA products was developed for OTA with an LOD of 0.01 ng mL^{-1} (**Figure 5A**).[98] In this strategy, the aptamer first hybridized with a primer, which was released upon OTA-aptamer binding. The released primer hybridized with a padlock probe to form a circular template and initiate the RCA reaction by adding ligase, polymerase, and dNTPs. The fluorescent DNA hydrogel was obtained by adding cyanine (Cy3) dye-dUTP together with dNTPs, and the fluorescence intensity of the DNA hydrogel was positively correlated with OTA concentration.

4.1.3 T-2 mycotoxin (T-2)

Taking advantage of the excellent spectral properties of UCNPs with the good adsorption and quenching abilities of MOFs, Zhao *et al.* developed an aptasensor for the sensitive detection of T-2 with an LOD of 0.087 ng mL^{-1}, which enabled the sensitive detection of trace amounts of T-2 in contaminated food samples, such as beer and corn flour, exhibiting benefits of lower background, excellent selectivity, low cost, and satisfactory recoveries.[154] Making use of structure-switching

aptamers, magnetic separation, EXPAR, and DNA-AgNCs, Gao *et al.* described a DNA-amplified assay for T-2 (**Figure 5B**).[116] In this method, the interaction of T-2 with the aptamer induced the release of cDNA, which was collected by magnetic separation to trigger EXPAR and obtain C-base-rich ssDNA. The C-base-rich ssDNA served as the template to form fluorescent AgNCs, enabling the determination of T-2 with an LOD as low as 30 fg mL^{-1}.

4.1.4 Microcystin-LR (MC-LR)

Using structure-switching aptamers, fluorescent aptasensors were developed for the detection of MC-LR. Zhang *et al.* proposed a simple fluorescent method to detect MC-LR based on dsDNA-templated CuNCs.[81] The method can monitor MC-LR in a wide concentration range of 0.01-1000 μg L^{-1} with an LOD of 4.8 ng L^{-1} and it does not require labeled fluorescent probes or complicated experimental techniques. Utilizing the differential affinity of the Cy3-cDNA and Cy3-cDNA/aptamer duplex with gold nanostars (GNSs), Li *et al.* developed a fluorescence−SERS dual-modal aptasensor for the detection of MC-LR.[155] The preferential binding of MC-LR toward the aptamer leads to simultaneous but opposite signal changes of fluorescence (off) and SERS (on). The dual-modality quantitative detection endows the method with higher precision compared to single mode of fluorescence or SERS.

4.1.5 Other toxins and multiplexed detection

The above-mentioned fluorescent aptasensor approaches can also be used to quantify other toxins. For example, Gu *et al.* developed a highly sensitive and rapid FRET aptamer assay for saxitoxin (STX) detection using DNase I-assisted target recycling signal amplification, graphene quantum dots (GQDs) as donors, and magnetic reduced graphene oxide (MRGO) as acceptors and magnetic separators.[156] Owing to the DNase I-catalyzed target recycling, the fluorescent aptamer assay with DNase I possessed a broader detection range (0.1–100 $ng \cdot mL^{-1}$) and a lower LOD (0.035 $ng \cdot mL^{-1}$) than that of the assay without DNase I.

Multiple mycotoxins may coexist and contaminate food and feeds, implying the enhancement of toxicity and an increased health risks. Therefore, it is necessary to explore simultaneous detection methods to accurately assess the degree of mycotoxins contamination and reduce the

analysis time and cost. Commonly used approaches rely on the interaction between aptamer-modified multicolored fluorescence probes and NMs with fluorescence quenching capability. For example, employing multicolor-emissive Ln^{3+} (Dy^{3+}, Tb^{3+}, Eu^{3+})-doped fluorescent NMs functionalized with aptamers as bioprobes and tungsten disulfide (WS_2) nanosheets as fluorescence quencher, a turn-on time-resolved fluorometric aptasensor was described for the simultaneous detection of zearalenone (ZEN), T-2, and AFB1 without mutual interference.[88] Without washing and separation steps, the simultaneous recognition of the three mycotoxins can be performed in a single solution using one excitation wavelength and different gate times with high signal-to-noise ratio. Using aptamer-functionalized dual-color AuNCs as energy donor and WS_2 nanosheet as energy acceptor, Wang *et al.* reported an aptamer induced FRET biosensor for simultaneous recognition of AFB1 and ZEN with a single excitation wavelength (**Figure 5C**).[86] Semiquantitative determination of AFB1 and ZEN was realized through photo visualization. By using the versatility of structure-switching aptamers, Xiong *et al*. developed a dual-DNA-tweezer nanomachine for one-step simultaneous detection of AFB1 and OTA.[90] The two DNA tweezers were assembled at both terminals of the DNA nanomachine, sharing two long arm sequences. The F-Q labeled dual DNA tweezers are locked closely by the aptamers and exhibit low fluorescence signal. Mycotoxin-aptamer binding can open the DNA tweezers, leading to turn-on fluorescence signals. The method displayed favorable sensitivity, specificity, and accuracy for simultaneous detection of AFB1 and OTA. A novel label-free aptasensor for multiplexed quantification of mycotoxins was proposed by immobilizing a molecular beacon G4-aptamer chimera on photonic crystal (PhC) barcodes (**Figure 5D**).[27] Target-aptamer binding induced the exposure of the G4 and ThT-G4 combination for producing high fluorescence. The multiplexed detection of mycotoxins was realized by adjusting the structural color of the PhC barcode with the advantages of rapid detection (30 min), high sensitivity (LOD = 0.70 pg mL^{-1}), and favorable applicability in real samples (recovery from *circa* 80 to 120%).

4.1.6 Pros and cons

Fluorescent aptasensors have been widely applied in toxin detection, spanning various strategies

and using a variety of fluorescent materials for signal readout and various DNA amplification techniques to improve the sensitivity. Multiplexed detection of toxins has been realized through approaches such as single excitation multicolor NPs, photonic barcodes, and structure-switching aptamer. In the laboratory, these methods achieve improved sensitivity (LODs range from fg mL^{-1} to ng mL^{-1}) and satisfactory results in food samples. However, there are only few reports on portable, commercial, and officially approved fluorescent aptasensors for toxins. In addition, most of the assays investigate the analytical performance for toxins, but often lack the fundamental characterization of the aptasensors, including the affinity of toxins and aptamers, the relationship between the configuration changes of aptamers upon aptamer-toxins binding and the nanosurface-adsorption, and the competitive binding ability of aptamers to toxins versus cDNA with different sequences.

4.2 Detection of Veterinary drug residues

Veterinary drugs play an important role in preventing and treating animal diseases and improving production efficiency and the quality of animal products. However, the misuse or abuse of veterinary drugs inevitably leads to the residue of harmful substances in animal-derived food, causing direct harm to human health, such as toxic effects, the risk of cancer and birth defects, and the intestinal microflora imbalance. Veterinary drugs that are more likely to cause excessive residues in animal-derived food mainly include antibiotics (*e.g.*, kanamycin, chloramphenicol, tetracycline), sulfonamides (*e.g.*, sulfadimethoxine), and hormone drugs (*e.g.*, clenbuterol hydrochloride). Aptasensors have been described to better monitor veterinary drug residues due to the advantages of rapid response, high specificity, and simple fabrication.[157,158]

4.2.1 Kanamycin (KAN)

Sun *et al.* designed a dual-strand structure switch, which was composed of FAM-labeled aptamers and Dabcyl quencher-labeled cDNA, for the quantification of KAN within 30 min, yielding an LOD of 13.5 nM (~6.5 ng mL^{-1}).[159] Because such relatively simple and quick assays exhibit unsatisfactory sensitivity for KAN, DNA signal amplification techniques have been applied to

improve the analytical sensitivity of structure switching KAN aptasensors. For example, Zhang *et al.* described a zero background and enzyme-free dual amplification strategy combining target recycling and HCR.[128] In the assay, double Y-shaped DNA probes including capture and signal amplification probes were respectively immobilized on gold bars and on magnetic bars, and the hairpins of HCR were separated in different arms of the Y-shaped DNA probe to avoid non-specific background amplification of HCR. Upon addition of KAN, target recycling and HCR between the two bars were triggered simultaneously to form many long dsDNA that activated SYBR Green fluorescence and resulted in an LOD of 0.45 pg mL^{-1} for KAN. Based on the adsorption of aptamers on the surface of AuNPs to resist salt-induced aggregation, Ye *et al.* designed a simple method for the determination of KAN via ET between DNA-AgNCs and AuNPs with an LOD of 1.0 nM (~0.49 ng mL^{-1}).[160] Because DNA-AgNCs were used as the fluorescence probes, the aptasensor did not require NM functionalization.

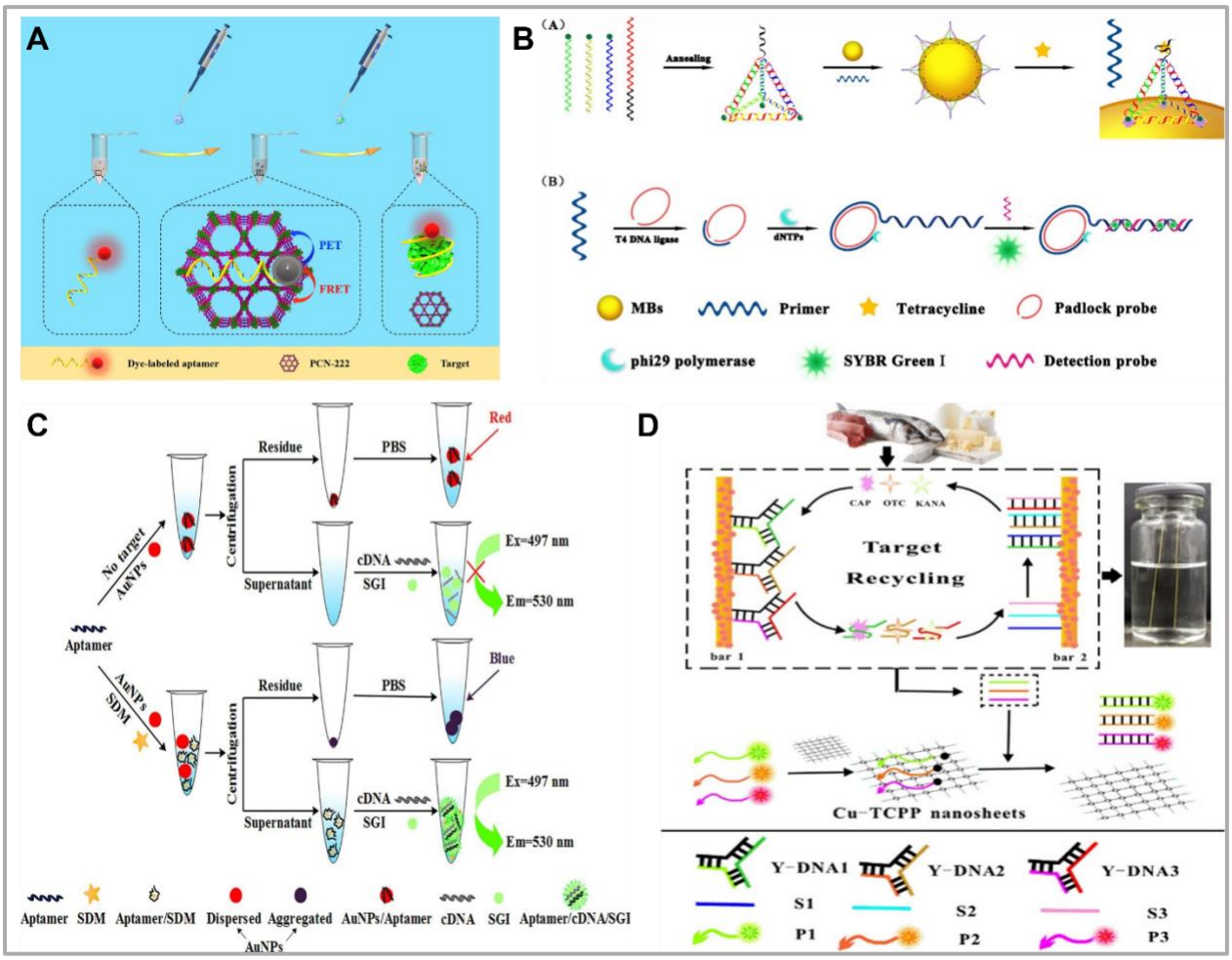

Figure 6. Recent examples of fluorescent aptasensors for veterinary drug residues. **A:** PCN-222 adsorbs the dye (FAM)-labeled aptamer and leads to fluorescence quenching. Target (CAP)-aptamer binding results in surface detachment and fluorescence recovery. Reprinted from Biosens. Bioelectron., Vol. 149, Liu, S.; Bai, J.; Huo, Y.; Ning, B.; Peng, Y.; Li, S.; Han, D.; Kang, W.; Gao, Z. A zirconium-porphyrin MOF-based ratiometric fluorescent biosensor for rapid and ultrasensitive detection of chloramphenicol, 111801 (ref 163). Copyright 2020, with permission from Elsevier. **B:** A DNA tetrahedron, which is prepared with one aptamer and three biotin-modified DNA strands through hybridization, is functionalized on a MBs and interacts with primers to form an assembly (primer-apt-tet-MBs). TET-aptamer binding induces primer release, which combines with a padlock probe to form a circular template via T4 DNA ligase and initiates the RCA process with the help of dNTPs and phi29 polymerase. Detection probes hybridize to the RCP to generate dsDNA for fluorescence detection with SYBR Green I. Reproduced from Zhang, Z.; Wang, S.; Ma, J.; Zhou, T.; Wang, F.; Wang, X.; Zhang, G. ACS Biomater. Sci. Eng. 2020, 6, 3114-3121 (ref 100). Copyright 2021 American Chemical Society. **C:** In the absence of SDM, aptamers adsorb to the surface of AuNPs, protecting AuNPs from PBS-induced aggregation and remaining at red color in the residue. The supernatant is non-fluorescent with the addition of cDNA and SYBR Green I. In the presence of SDM, aptamer-target complexes fail to protect the AuNPs, leading to AuNPs aggregation in the residue and high fluorescence of SYBR Green I in the supernatant due to the formation of aptamer-cDNA duplexes. Reprinted from Food

Chem., Vol. 309, Chen, X.; Lin, Z.; Hong, C.; Yao, Q.; Huang, Z. A dichromatic label-free aptasensor for sulfadimethoxine detection in fish and water based on AuNPs color and fluorescent dyeing of double-stranded DNA with SYBR Green I, 125712 (ref 168). Copyright 2020, with permission from Elsevier. **D:** Three aptamer-containing Y-DNA probes (Y-DNA1 for CAP, Y-DNA2 for OTC, and Y-DNA3 for KAN) are assembled on stirring bar 1, and three corresponding specific cDNAs are immobilized on stirring bar 2. Three fluorophore (FAM, ROX, and Cy5)-labeled ssDNA probes (P1, P2 and P3) are adsorbed by Cu-TCPP nanosheets. Target-aptamer binding induces the release of aptamer to combine with cDNA on bar 2, and the disintegration of ssDNA on bar 1 to hybridize with fluorophore-labeled ssDNA probes, which results in target recycling and fluorescence intensity recoveries. Reproduced from Yang, Q.; Hong, J.; Wu, Y.; Cao, Y.; Wu, D.; Hu, F.; Gan, N. ACS Appl. Mater. Interfaces 2019, 11, 41506-41515 (ref 83). Copyright 2019 American Chemical Society.

4.2.2 Chloramphenicol (CAP)

Based on the versatility of structure-switching aptamers, several fluorescent aptasensors have been developed for the determination of CAP. Tu *et al.* designed a simple turn-off fluorescent strategy for CAP based on the formation of THMS between dual-labeled STP and a label-free aptamer, and the LOD was 1.2 nM (~0.39 ng mL^{-1}).[35] Zhang *et al.* proposed a mix-and-read fluorescence turn-on assay for CAP based on the formation of dual THMS probes between dual-labeled loop probes and label-free stem probes.[37] The dual THMS assay can significantly reduce the background and increase the signal-to-noise ratio by 195%, achieving sensitive detection of CAP with a detection limit of 0.18 nM and reliable applicability in fish and milk. Sun and co-workers proposed a three-DNA-strand structure switch for the rapid sensing of CAP, which was composed of aptamer, FAM-labeled cDNA, and BHQ1-labeled cDNA.[32] The length and position of FAM-labeled cDNA, and BHQ1-labeled cDNA were optimized in the assay. FAM fluorescence quenched by BHQ1 was recovered in the presence of CAP, achieving the monitoring of CAP with an LOD of 0.70 ng mL^{-1}. A similar three-DNA structure switch approach was previously proposed by Sharma *et al.*.[161] In a modified fluorescence turn-off approach, to avoid the issue of dynamic quenching due to the presence of fluorophore and quencher in the same solution, the aptamer was immobilized through maleimide chemistry on microplates and dehybridized reporter oligonucleotides were eliminated from the reaction mixture. Thus, background signals could be eliminated without applying any external force (*e.g.*, magnetic) to separate the two DNA strands. Combining structure-switching

with a double stirring bar-assisted dual enzyme-free signal amplification and using two Y-shaped DNA probes, an LOD of 16 pM (~5.2 pg mL^{-1}) CAP in spiked milk and fish samples could be realized with an assay time of only 60 min.[162] By the ingenious design of Y-shaped DNA probes on the bars, CAP-aptamer binding triggered simultaneous target recycling and CHA, resulting in the formation of G4, which was detected with the G4-specific dye ThT.

Relying on the strong adsorption and fluorescence quenching ability of MOF, two dye-based fluorescent sensing strategies were explored for CAP.[163,164] Lu *et al.* successfully prepared the bimetallic organic framework nanomaterial Cu/UiO-66 by coordinate bonding of MOF UiO-66 with Cu^{2+} and established a fluorescence method for the quantitative detection of CAP using phosphate and ROX double-labeled aptamers and Cu/UiO-66.[164] The method displayed low fluorescence background, good reproducibility, and high sensitivity with LOD of 0.09 nM (30 pg mL^{-1}). Liu *et al.* developed a ratiometric fluorescent aptasensor based on FAM-labeled aptamers and zirconium-porphyrin MOF (PCN-222) (**Figure 6A**).[163] The adsorption of PCN-222 toward the FAM-labeled aptamer originates from hydrogen bonding, π-π stacking, electrostatic, and coordination interactions. The H2TCPP ligand of PCN-222 exhibited stable fluorescence emission at 675 nm as reference signal that remained unchanged with CAP concentration. Thus, a ratiometric assay could be established combined with the strong fluorescence quenching of PCN-222 toward FAM, which allowed CAP quantification within 26 min (1 min for quenching and 25 min for target incubation) with an LOD of 80 fg mL^{-1}.

Structure-switching fluorescent aptasensors using HCR for signal amplification were applied in the detection of CAP to improve the sensitivity. Ma *et al.* designed a separation-based dual amplification strategy to detect CAP with Exo I-assisted target recycling and HCR amplification.[127] The binding thermodynamics, structure switching, and binding domain of CAP-aptamer binding were explored by isothermal titration calorimetry, circular dichroism, and molecular docking. In the absence of CAP, the aptamer-binding domain is blocked by the HCR initiator. The binding of CAP and aptamer induces the exposure of initiator, which activates the Exo I-assisted CAP cyclic process, and triggers the HCR to form long DNA concatemers composed

of fluorescent FAM groups. This dual amplification strategy allowed for the detection of CAP within a broad linear concentration range from 0.001 to 100 nM and with an LOD of 0.3 pM (~0.1 pg mL^{-1}). Li *et al*. developed a separation-free FRET sensing platform for CAP using HCR, triplex DNA, and FAM-TAMRA donor-acceptor pairs.[131] CAP-aptamer binding induced the release of trigger DNA and the subsequent HCR process to form the triplex DNA, leading to the FRET pairs in close proximity and a significant donor fluorescence decrease. The quantitative detection of CAP can be completed within 30 min with an LOD of 1.2 pg mL^{-1}.

4.2.3 Tetracycline (TET)

Based on the G4 structure of the TET aptamer, Dai *et al.* developed a label-free aptasensor for TET with ThT as fluorescent probe.[165] Owing to the aptamer-TET interaction and concomitant disassembly of the G4 structure, the fluorescence intensity gradually decreased with increasing TET concentration, resulting in an LOD of 1 nM (~0.4 ng mL^{-1}). Relying on the interaction between NM quencher and aptamer-functionalized fluorescent nanoprobes, turn-on fluorescence aptasensors were constructed to detect TET. Ma *et al.* developed an aptamer-based fluorometric TET assay using molybdenum(IV) disulfide (MoS_2) nanosheets as an efficient quencher and aptamer-modified VS_2 QDs as fluorescent probes.[166] The fluorescent nanoprobe aptasensor could detect TET with an LOD of 0.06 ng mL^{-1}. Similarly, based on aptamer-modified nitrogen-doped graphene QDs (N-GQDs-aptamer) as signal output and CoOOH nanoflakes as fluorescence quencher, Zhang *et al.* designed a FRET aptasensor to monitor TET with an LOD of 0.95 ng mL^{-1} and achieved acceptable results in animal-derived food.[167]

Structure-switching fluorescent aptasensors have also been in the focus of TET assay developments. He *et al.* designed a turn-on fluorometric assay for TET based on THMS formed by label-free aptamer and bis-pyrene-labeled STP.[36] TET-aptamer binding caused the formation of pyrene excimers, whose fluorescence could be further enhanced by γ-cyclodextrin to quantify TET within a linear concentration range of 5 to 100 nM and with an LOD of 1.6 nM (~0.7 ng mL^{-1}). By assembling aptamer-pendant DNA tetrahedron nanostructure-functionalized MBs (Apt-tet MBs) and ROX labeled cDNA (ROX-cDNA), Hong *et al.* developed a fluorescent method for TET

detection.[82] TET-aptamer binding can induce the separation of ROX-cDNA from the assembly, resulting in fluorescence enhancement. This tetrahedron functionalization strategy could reduce surface-effects and increase the reaction rate to yield decreased reaction time and reduced false positives, facilitating the quantification of TET with an LOD of 6 pg mL^{-1}. This approach was further optimized by combining Apt-tet MBs with an RCA reaction, which was used for TET detection in fish and honey samples (**Figure 6B**).[100] The cDNA primer released by the TET-aptamer interaction can trigger the RCA process and the generation of long tandem ssDNA, which can hybridize with detection probes for fluorescence signal readout with SYBR Green I, accomplishing TET detection with an LOD of 0.72 pg mL^{-1}.

4.2.4 Other veterinary drug residues and multiplexed detection

In addition to antibiotics residues, some other veterinary drug residues, such as sulfadimethoxine (SDM), may have negative effects on human health. Although structure-switching aptasensors present a rather generic approach for various targets, some aptamers have a higher affinity to the cDNA compared to the target. Chen *et al.* exploited this "inverse" affinity by using a dichromatic label-free aptasensor for SDM detection based on AuNPs absorption (color) and fluorescence of SYBR Green I-stained dsDNA (**Figure 6C**).[168] In the absence of SDM, the aptamers attach to the AuNPs and after centrifugation the redispersed residue (aptamer-AuNPs) shows a red color, whereas the supernatant is non-fluorescent after addition of cDNA and SYBR Green I. In the presence of SDM, the aptamer-SDM complexes detach from the AuNPs, leading to AuNPs aggregation and a switch to blue color in the redispersed residue, and enhanced fluorescence of SYBR Green I in the supernatant due to the formation of aptamer-cDNA duplexes. Background signals are significantly reduced because the excess aptamers that remain on the AuNPs are removed with the centrifugation step before the addition of cDNA.

Multiplexed fluorescent aptasensors for veterinary drug residues have also been developed. Youn *et al.* designed a separation-free aptasensor for the triplexed detection of SDM, KAN, and ampicillin utilizing the adsorption and quenching ability of GO to three aptamers labeled with Cy3, FAM, and Cy5, respectively.[169] The assay also applied DNase I-assisted cyclic enzymatic signal

amplification for an approximately 2.1-fold signal increase and could simultaneously detect SDM, KAN, and ampicillin with LODs of 2.0 ng mL^{-1}, 2.7 ng mL^{-1}, and 2.3 ng mL^{-1}, respectively. Yang *et al.* proposed a 2D-MOF-based fluorescent aptasensor for triplexed analysis of CAP, OTC, and KAN using a double stirring bar-assisted target replacement approach (**Figure 6D**).[83] In their method, the fluorescent dyes FAM, ROX, and Cy5 were used with 2D-MOFs as universal quenchers. In the absence of targets, three specific Y-shaped DNA probes containing the three (CAP, OTC, and KAN) aptamers were assembled on one and the three specific cDNAs on another stirring bar. Target-aptamer binding disintegrated the Y-DNA and subsequently the targets were displaced from the aptamers on bar 1 due to hybridization of the aptamers to the cDNAs on bar 2, thus recycling the targets for additional cycles of Y-DNA-aptamer-target displacement. At the same time, the fluorophore-labeled ssDNA probes could specifically hybridize to the disintegrated ssDNA (from the Y-DNAs of bar 1) to form dsDNAs, which were released from the MOFs and resulted in target specific fluorescence intensity recovery of FAM, ROX, and Cy5, respectively. The multicolor fluorescence could avoid interferences from different probes and the sample matrix.

4.2.5 Pros and cons

Fluorescent aptasensor for veterinary drugs residues focuses on G4 displacement, structural switching, nanosurface-adsorption, and multiplexed detection. By integrating new functional DNA molecules (such as tetrahedral DNA nanostructures), the structure-switching aptasensors were demonstrated to shorten the detection time and improve the accuracy in complex food samples. Exploiting the "inverse" affinity of aptamer and cDNA could ingeniously avoid the problem of insufficient aptamer affinity, which provides a new avenue for implementing more aptamers into assays for different targets. The combination of structure-switching aptasensors and DNA amplification technology (HCR, CHA, RCA) has achieved great enhancement in sensitivity (LODs as low as pg mL^{-1}). The basic researches on CAP aptamers, including binding thermodynamics, binding domain, and the length and position of cDNA in structure switches, provide theoretical guides for the design of aptamer-based assays. However, the most widely used fluorescent probes remain organic dyes, which may cause problems concerning long-term stability

and photobleaching.

4.3 Detection of pesticide residues

Pesticide residues could directly or indirectly cause serious environmental and food pollution. Common pesticide residues in food include organophosphorus pesticides (*e.g.*, isocarbophos, chlorpyrifos, diazinon), neonicotinoid pesticides (*e.g.*, acetamiprid), carbamate pesticides (*e.g.*, carbendazim), heterocyclic pesticides (*e.g.*, fipronil), and pyrethroid pesticides.

4.3.1 Organophosphorus pesticides (OPs)

Residues of OPs can have low or highly toxic effects on humans, which can irreversibly inhibit the enzyme acetylcholinesterase and bring about the accumulation of the acetylcholine neurotransmitter in nerves, leading to serious threat to the nervous system and vital organs.[170] Thus, the analysis of OPs residues is highly significant to estimate poisoning by OPs and assure health protection. Using aptamer-modified L-cysteine capped CdS QDs (apt-CdS QDs) adsorbed and quenched by GO, Arvand *et al.* developed an aptasensor for the selective detection of diazinon.[57] The fluorescence of apt-CdS QDs was quenched by GO but restored upon the diazinon-aptamer binding, achieving the diazinon detection with an LOD of 0.13 nM (~40 pg mL^{-1}).

4.3.2 Acetamiprid

Acetamiprid is a high-efficiency and broad-spectrum neonicotinoid insecticide widely applied to control different insects on crops, fruits, leafy vegetables, and tea trees.[171] Although with lower toxic effects for humans and mammals in comparison to organophosphorus pesticides and other traditional insecticides, acetamiprid can cause potential harm to human health, such as effects on embryo development and genetic toxicity.[172] Since He *et al.* reported the isolation and identification of a DNA aptamer for acetamiprid, numerous optical and electrochemical aptasensors have been developed for the quantitative determination of acetamiprid.[173,174] Currently, two main acetamiprid aptamers are used in aptasensors: one is a 49-nt sequence (5'-TGTAATTTGTCTGCAGCGGTTCTTGATCGCTGACACCATATTATGAAGA-3')[173] and the other is 20-nt sequence (5'-CTGACACCATATTATGAAGA-3')[175] DNA.

Relying on the influence of AuNPs in different aggregation states on the fluorescence of CDs via IFE, Qin *et al.* reported a label-free IFE aptasensor.[176] The established method did not require modification of NMs or aptamer and offered high selectivity and sensitivity towards acetamiprid with satisfactory results in real samples. Utilizing the phenomena that ssDNA-modified and dsDNA-modified AuNPs show different stability against salt induction, Yang *et al.* demonstrated an aptamer-based aggregation assay that involved the principle of target-triggered structure-switching of aptamers and IFE between DNA-modified UCNPs and dsDNA-modified AuNPs.[65] In this assay, DNA and high salt concentrations are applied to tune the ratio of monodisperse and aggregated AuNPs. Compared with the modification-free IFE aptasensors for acetamiprid, the rationally designed DNA-functionalized AuNPs nanoprobes in this colorimetric and fluorescent assay showed superior selectivity to potential interfering substances, including thiols and cations. To reduce the background interference of the sample matrix, separation of molecular recognition and signal output was conducted through discarding of the sample matrix before salt induction.

Li *et al.* developed a label-free THMS-based fluorescent method for acetamiprid using ssDNA grafted by two G-rich split DNA sequences at its two ends as STP (**Figure 7A**).[38] D-penicillamine and histidine-functionalized graphene quantum dots (DPA-GQD-His) and OPD were employed as signal probes. The acetamiprid-aptamer binding can induce the triplex-to-G4 molecular switch and the subsequent formation of G4/hemin DNAzyme, which can catalyze the oxidation of OPD to the yellow fluorescent product DAP. The ET between DPA-GQD-His and DAP results in increased fluorescence of the oxidation product and reduced fluorescence of the DPA-GQD-His, achieving the acetamiprid detection with an LOD of 0.38 fM (~0.09 fg mL^{-1}). The obvious signal amplification was realized through the catalytic activity of G4/hemin DNAzyme, which was further enhanced by histidine in DPA-GQD-His. Fluorophore conjugation of the THMS-based aptamers is not required, thereby avoiding possible interference with the affinity of the aptamer. More importantly, these strategies are generic by virtue of replacing the corresponding aptamer sequence without changing the triple-helix structure. Using AT-rich dsDNA-templated CuNPs as fluorescent probes, a label-free and enzyme-free aptasensor was established for

detecting acetamiprid with an LOD of 2.37 nM (~0.53 ng mL^{-1}).[177] The AT-rich dsDNA was formed through acetamiprid-induced hybridization of two elaborately designed hairpin DNAs, generating significantly enhanced fluorescence of CuNPs with increasing acetamiprid concentration.

4.3.3 Others pesticides

Fluorescent aptasensors have also been developed for a few other pesticides. For example, utilizing the strategy of salt-induced AuNP-aggregation to modulate the fluorescence emission of Rhodamine B, Su *et al.* proposed a label-free and non-functionalized fluorescent aptasensor for the detection of carbendazim.[178] By designing a simple structure-switching aptamer, the sensing of fipronil in liquid eggs was performed by FRET between FAM-labeled aptamer and partially complementary TAMRA-labeled cDNA.[179] Utilizing the aptamer adsorption onto MnO_2 nanosheets, Ouyang *et al.* constructed a turn-on fluorescence assay for the monitoring of carbendazim through ET between aptamer-modified UCNPs and MnO_2 nanosheets.[180] Similarly, Zhang *et al.* built a fluorescent platform for the detection of fipronil exploiting the interaction between FAM-labeled aptamer and the oxidized SWCNHs.[181] The oxidized SWCNHs were shown to have the advantages of good stability, good dispersion, and satisfactory applicability.

4.3.4 Pros and cons

Although fluorescent aptasensors have been applied in the detection of pesticides, some aptamers (*e.g.*, for OPs) are broad-spectrum binders with limited specificity, and thus, only a few pesticides can be specifically recognized. This limitation is probably caused by the difficulty in screening and evaluating aptamers with high affinity and specificity towards pesticides. At present, the principle of fluorescent aptasensors for pesticide is mainly based on the adsorption of aptamers on the surface of NMs and desorption upon aptamer-pesticide binding. These aptamer-based fluorescence strategies exhibit limited sensitivity without the assistance of DNA amplification. Because of the weaker aptamer affinity, competitive binding of aptamers with pesticides and cDNA is less adopted, which makes it a challenge to apply DNA amplification in pesticide aptasensors.

4.4 Detection of heavy metal ions

4.4.1 Lead ions (Pb^{2+})

Pb^{2+} is a typical toxic heavy metal environmental pollutant that has been reported to be harmful to human health with adverse effects on the hemopoietic system, the nervous system, and the kidneys.[182] A variety of optical and electrochemical aptasensors for Pb^{2+} detection have been developed.[183] Typical Pb^{2+} aptamers that can form G4 structures upon Pb^{2+} binding (for the detection with G4-specific dyes) and have been frequently used in fluorescent aptasensors are T30695 (5'-GGGTGGGTGGGTGGGT-3')[184] and AGRO100 (5'-GGTGGTGGTGGTTGT GGTGGTGGTGG-3').[185] Recently, Wu *et al.* constructed a simple and convenient Pb^{2+}-induced G4 polymorphism-based ratiometric aptasensor by introducing a DNA-intercalating dye (4',6-diamidino-2-phenylindole, DAPI) as the internal fluorescence reference (**Figure 7B**).[182] In the absence of Pb^{2+}, the aptamers formed stable parallel G4 structures with K^+, which allowed for the binding of NMM and DAPI, resulting in high fluorescence emission of both signal reporters. Pb^{2+} competed with K^+ to form compact antiparallel G4 structures that can bind DAPI but not NMM, giving rise to reduced NMM fluorescence but unchanged DAPI fluorescence. The ratiometric fluorescence detection using NMM and DAPI with single-wavelength excitation can lead to significant improvements of accuracy and reproducibility of such assays. Utilizing the adsorption and quenching capacity of GO to fluorophore-functionalized aptamers, Khoshbin *et al.* developed a simple paper-based aptasensor for the sensitive detection of Pb^{2+} within about 10 min.[184] Pb^{2+} induced the release of FAM-T30695 from the GO surface and FAM fluorescence was recovered. The aptasensing array exhibited a high sensitivity to Pb^{2+} with an LOD 0.5 pM (~0.1 pg mL^{-1}) and could be applied to determine Pb^{2+} in tap water, lake water, milk, and human blood serum with satisfactory results.

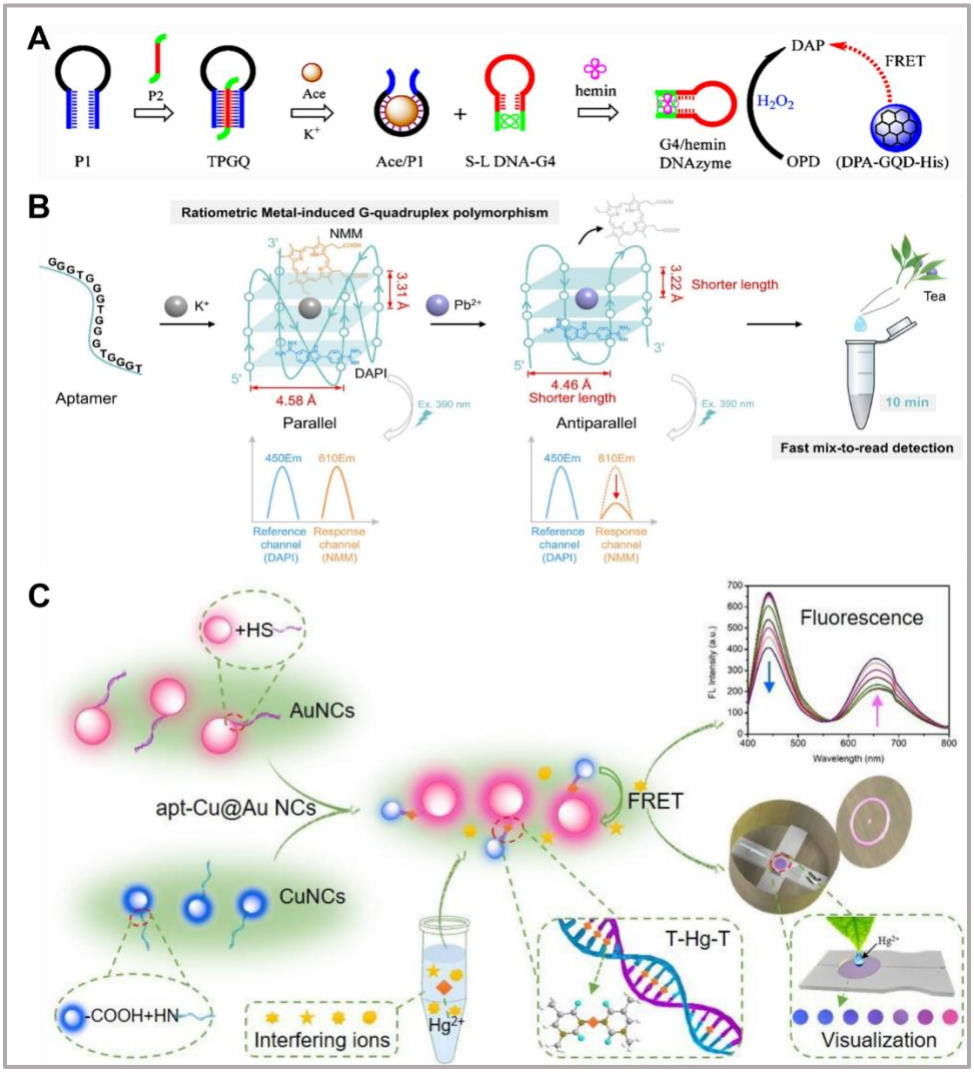

Figure 7. Recent examples of fluorescent aptasensors for pesticides and heavy metal ions. **A:** Aptamer-containing P1 hybridizes with G-rich-sequences-containing P2 to form TPGQ. The acetamiprid (Ace)-aptamer interaction induces the disassembly of TPGQ, the release of P2 and the formation of G4/hemin DNAzyme, which catalyzes the oxidation of OPD to fluorescent DAP in the presence of H_2O_2. The ET from DPA-GQD-His to DAP results in increased DAP fluorescence and reduced DPA-GQD-His fluorescence. Reprinted by permission from Springer Nature: MICROCHIMICA ACTA. Dual amplification in a fluorometric acetamiprid assay by using an aptamer, G-quadruplex/hemin DNAzyme, and graphene quantum dots functionalized with D-penicillamine and histidine. Li, N.; Li, R.; Sun, X.; Yang, Y.; Li, Z. Microchimica Acta 2020, 187, 158 (ref # 38). Copyright 2019. **B:** Parallel G4 structures formed by K^+-aptamer binding show high fluorescence signals of NMM and DAPI. Pb^{2+}-aptamer binding incudes the formation of antiparallel G4 structures with unchanged DAPI but decreased NMM fluorescence intensity. Reprinted from Food Chem., Vol. 343, Wu, Y.; Shi, Y.; Deng, S.; Wu, C.; Deng, R.; He, G.; Zhou, M.; Zhong, K.; Gao, H. Metal-induced G-quadruplex polymorphism for ratiometric and label-free detection of lead

pollution in tea, 128425 (ref 182). Copyright 2021, with permission from Elsevier. **C:** The Hg^{2+}–responsive formation of T–Hg^{2+}–T structures bring the aptamerT1-modified CuNCs and aptamerT2-modified AuNCs in close proximity, causing fluorescence quenching of CuNCs and fluorescence enhancement of AuNCs due to ET, which can be visualized via color changes of fluorescence. Reprinted from Food Chem., Vol. 344, Shi Y.; Li, W.; Feng, X.; Lin, L.; Nie, P.; Shi, J.; Zou, X.; He, Y. Sensing of mercury ions in Porphyra by Copper @ Gold nanoclusters based ratiometric fluorescent aptasensor, 128694 (ref 187). Copyright 2021, with permission from Elsevier.

4.4.2 Mercury ions (Hg^{2+})

Hg^{2+} is a highly toxic metal environmental pollutant with a negative impact on human health even at low concentrations due to the accumulation in the body through the food chain.[186] To ensure an efficient trace determination of Hg^{2+}, a variety of fluorescent aptasensors have been designed primarily depending on the T-Hg^{2+}-T base mismatch whose binding force exceeds that of the natural A-T pair. Utilizing DNA-immobilized NMs, Shi *et al.* implemented ssDNA-aptamer-modified CuNCs and AuNCs into a ratiometric assay for Hg^{2+} determination in Porphyra (**Figure 7C**).[187] Without Hg^{2+}, DNA-CuNCs and DNA-AuNCs were well dispersed in solution but combined due to the formation of T–Hg^{2+}–T structures in the presence of Hg^{2+}, which caused ET between CuNCs and AuNCs and concomitant quenching of CuNCs and sensitization of AuNCs fluorescence that could be visualized as a color change and provided an LOD of 4.9 nM (~1 ng mL^{-1}) Hg^{2+}. The ratiometric fluorescence visualization device based on smart phone readout on a microfluidic chip was designed to realize visual detection of Hg^{2+} ions with good portability, usefulness, and affordability.

Several non-immobilized fluorescent Hg^{2+} nano-aptasensors have been designed using QD probes[188,189] or DNA templated AgNCs (DNA-AgNCs).[190] Exploiting aptamer-programmed self-assembly of functionalized CdTe QDs, Guo *et al*. proposed a fluorescent nano-aptasensor, in which two pieces of T-rich aptamer sequences were attached to CdTe QDs.[188] The extent of QD self-assembly depended on the specific binding of T-rich aptamers with Hg^{2+}, resulting in a significant fluorescence decrease and red-shift because of ET between the assembled QDs. Based on this principle, the detection of Hg^{2+} was carried out with an LOD of 3.3 nM (~0.67 ng mL^{-1}). Another

label-free fluorescent nano-aptasensor was based on DNA-templated ZnO QDs as the probe and was further developed into an electronic detection device for rapid Hg^{2+} detection.[189] The binding of Hg^{2+} with poly T aptamers leads to the formation of hairpin-like T-Hg^{2+}-T duplex structures, which acts as template to form ZnO fluorescent QDs, displaying significantly enhanced fluorescence emission with increasing Hg^{2+} concentration. In the absence of Hg^{2+}, the ZnO QDs cannot be synthesized due to the lack of duplex template. Different from the common sensing method of synthesis and then functionalization, Hg^{2+} detection was simultaneously accomplished during the synthesis of QDs with an LOD of 0.5 nM (~0.1 ng mL^{-1}). Recently, by skillfully combining T-Hg^{2+}-T nanoladders as signal amplification and DNA-AgNCs as signal identification, Wang *et al.* constructed a label-free and enzyme-free turn-on biosensor for Hg^{2+} ions.[190] DNA-AgNCs was successfully synthesized using the DNA template with sequence of $C_6G_5C_6$ that extended at the 5'-end of the DNA probe. In the presence of Hg^{2+}, the formation of T-Hg^{2+}-T nanoladders resulted in the fluorescence enhancement of DNA-AgNCs. GO was applied as energy acceptor to quench the fluorescence of the free DNA-AgNCs that did not involve in the assembly of T-Hg^{2+}-T nanoladders, thereby reducing the background fluorescence of DNA-AgNCs. The amplified method realized the detection of Hg^{2+} with an LOD of 7.4 pM (~1.5 pg mL^{-1}).

4.4.3 Cadmium ions (Cd^{2+})

Cd^{2+} may accumulate in human organs and cause significant harm to human health including renal dysfunction, itai-itai disease, and osteoporosis.[191] Aptasensors have been established for the monitoring of Cd^{2+} levels by using various signal elements, including AuNPs,[192] glucometers,[193] smart phones,[194] and fluorescent probes.[195]

Label-free fluorescence aptasensor based on conformational switching from aptamer-cDNA to aptamer-Cd^{2+} was established using dsDNA-specific dyes (*e.g.*, SYBR Green) as the signal reporters with an LOD of 0.34 ng mL^{-1}.[195] In the absence of Cd^{2+}, dsDNA-specific dyes can bind to the small groove of dsDNA composed of aptamer and cDNA, generating high fluorescence intensity. Specific binding of aptamers to Cd^{2+} induced conformation switching of aptamer from dsDNA to a stem-loop structure, along with a dramatic decrease of fluorescence intensity. Another

label-free fluorescence aptasensor for Cd^{2+} implemented DNA-circuit-based signal amplification via hairpin probe-mediated toehold binding and branch migration.[196] The Cd^{2+}-aptamer complex was used as initiator for DNA self-assembly of two hairpin probes, generating numerous free G-rich sequences. After incubation with K^+ and NMM, an active G4-K^+-NMM complex could be formed, which yielded a high fluorescence signal. In the absence of Cd^{2+}, the DNA circuit was restricted, such that only a weak fluorescence signal could be detected. The enzyme-free DNA circuit with G4-based turn-on fluorescence displayed high sensitivity for Cd^{2+} with an LOD of 5 pM (~0.56 pg mL^{-1}).

4.4.4 Other metal ions and multiplexed detection

Although Pb^{2+}, Hg^{2+}, and Cd^{2+} represent the most important toxic heavy metal ions in food and for which aptamers have been developed, also other metal ions can cause harm to human health when present at high concentrations. For example, silver ions (Ag^+) can be harmful when its content in drinking water exceeds 0.9 μM.[197] Fluorescent biosensors for Ag^+ detection mainly rely on the specific binding of Ag^+ to cytosine (C) bases and the formation of stable C-Ag^+-C structures.[198] A triplexed fluorescent aptasensor for the simultaneous detection of Hg^{2+}, Pb^{2+}, and Ag^+ was designed by Lu *et al.* using three different aptamers labeled with distinct dyes (FAM-PHg, TAMRA-PPb, and Cy5-PAg) and GO as fluorescence quencher.[199] The different targets released the adsorbed aptamers from the GO and the recovered fluorescence intensities of the distinct dyes could be used to selectively quantify Hg^{2+}, Pb^{2+}, and Ag^+ from the same sample via synchronous scanning fluorescence spectroscopy. Utilizing FAM-labeled aptamers and GO, Khoshibin *et al.* established a paper-based aptasensor for the simultaneous monitoring of Hg^{2+} and Ag^+.[200] The assay exploited a portable single-wavelength fluorescence microscope to perform the simultaneous detection, which provided the method with the merits of low cost, short time (10 min), and high sensitivity (LODs of 1.3 pM (~0.36 pg mL^{-1}) Hg^{2+} and 1 pM (~0.24 pg mL^{-1}) Ag^+).

4.4.5 Pros and cons

Fluorescent aptasensors using dye displacement, nanosurface-adsorption, and DNA hybridization have been used for the detection of heavy metal ions with the advantages of simple operation, rapid

detection, and high sensitivity. Among them, the ratiometric fluorescent aptasensor based on G4 displacement exhibits enhanced anti-interference ability. Using the changes of the fluorescence color in response to metal ions, visualized analysis was carried out with portability and practicability through smart phones and microfluidic chips. For the Hg^{2+} aptasensors that depend on the T-Hg^{2+}-T interaction, the DNA sequence (ploy-T or sequence containing bases T, C and G) can be flexibly designed according to the corresponding strategies, but the interference of Ag^{+} (*e.g.*, C-Ag^{+}-C) should be considered and avoided to ensure the specificity for Hg^{2+} detection. For the Pb^{2+} aptasensors that rely on the Pb^{2+}-induced formation of antiparallel G4 structures, the specificity could be influenced by Na^{+} or K^{+}, which can induce the formation of parallel G4 structures. To avoid this problem, Pb^{2+}-responsive RNA cleavage DNAzyme can be an ideal candidate for selective quantification of Pb^{2+} because it shows superior specificity to Pb^{2+} and appealing flexibility in combination with signal amplification technologies.[201] Fluorescent strategies for Pb^{2+} or Hg^{2+} that rely on the Pb^{2+}-induced formation of antiparallel G4 structures or the interaction of T-Hg^{2+}-T cannot be applied to the detection of other targets by simply replacing the corresponding aptamers.

4.5 Other food chemical contaminants

4.5.1 Bisphenol A (BPA)

Bisphenol A (BPA) is mainly used for the production of polycarbonate plastics and epoxy resins, which are widely applied in the manufacturing of food contact materials, such as water pipes, plastic (milk) bottles, and food and drink (milk powder) packaging/cans.[202] It has been reported that BPA can interfere with the basic physiological processes and cause various disorders, including metabolic disease, thyroid function, neurological effect, and cancer.[203,204] In many countries, BPA is restricted to use in plastic infant feeding bottles.[205] As a promising tool to monitor BPA, aptasensors have been developed for BPA detection with significant progress.[206]

Using BPA-aptamer binding-induced release of Cy3-labeled aptamers from black phosphorus and fluorescence recovery of Cy3, Qian *et al.* fabricated an optical aptasensor for BPA using

hollow core anti-resonant fibers (HARF) (**Figure 8A**).[207] Cy3-aptamer functionalized black phosphorus was modified on the inner surface of HARF, which endowed the assay with high selectivity and two orders of magnitude sensitivity enhancement with an LOD of 1.7 pM (~0.39 pg mL^{-1}). Xu *et al*. implemented a FRET aptasensor for BPA, in which BPA-aptamer binding can induce the disassembly of aptamer modified UCNPs and cDNA modified PCN-224 MOFs.[208] Owing to the superior colloidal stability of PCN-224 MOFs under high concentration of NaCl, the assay was demonstrated to monitor BPA in high-salt (340 mM) food samples with satisfactory results.

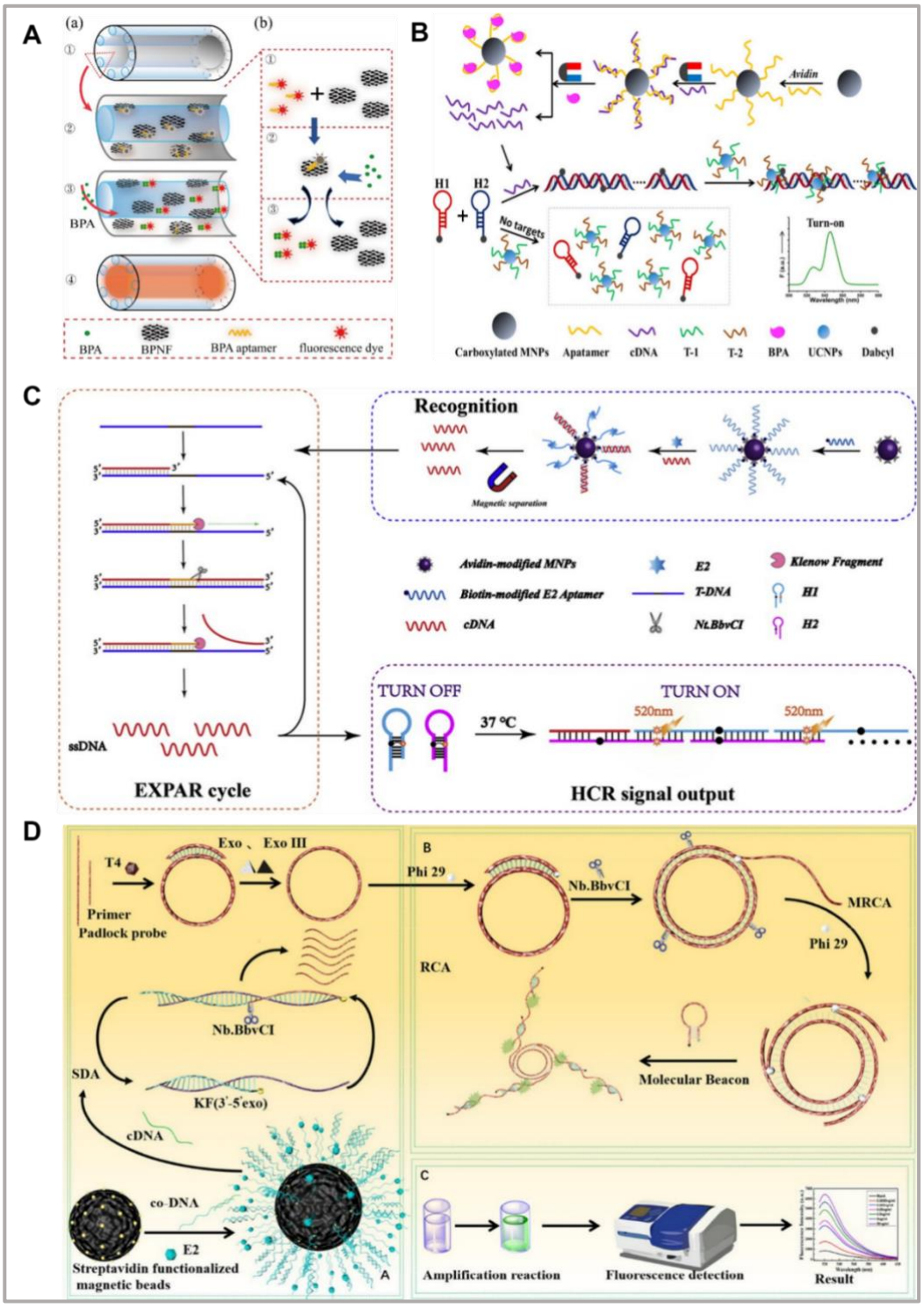

Figure 8. Recent examples of fluorescent aptasensors for others chemical food contaminants. **A:** Black phosphorus nanoflakes (BPNF), modified on the inner surface of HARF, can adsorb Cy3-aptamer and lead to fluorescence quenching. BPA-aptamer binding induces the release of Cy3-aptamer from BPNF and concomitant fluorescence recovery. Reprinted from Biosens. Bioelectron., Vol. 149, Qiao, P.; Wang, X.; Gao, S.; Yin, X.; Wang, Y.; Wang, P. Integration of black phosphorus and hollow-core anti-resonant fiber enables

two-order magnitude enhancement of sensitivity for bisphenol A detection, 111821 (ref 207). Copyright 2020, with permission from Elsevier. **B:** Duplexes of cDNA and aptamer-modified carboxylated MNPs are removed by magnetic separation in the absence of BPA or disassembled in the presence of BPA. The released cDNA triggers HCR of two Dabcyl-labeled hairpins (H1 and H2) to form dsDNA products, which can combine with UCNPs-modified DNA to form triplex structure, leading to UCNP luminescence quenching and Dabcyl fluorescence sensitization via ET. Reproduced from Wang, Y.; Zhao, X.; Huo, B.; Ren, S.; Bai, J.; Peng, Y.; Li, S.; Han, D.; Wang, J.; Han, T.; Gao, Z. ACS Appl. Bio Mater. 2021, 4, 763-769 (ref 132). Copyright 2021 American Chemical Society. **C:** 17 β-estradiol (E2)-aptamer binding on avidin-modified MNPs releases cDNA, which, after magnetic separation, induces EXPAR. The EXPAR ssDNA products trigger HCR of two FAM-BHQ1 labeled hairpins (H1 and H2), resulting in fluorescence recovery due to the separation of FAM from BHQ1 within the HCR products. Reprinted from Anal. Chim. Acta, Vol. 1116, Wang, Y.; Zhao, X.; Zhang, M.; Sun, X.; Bai, J.; Peng, Y.; Li, S.; Han, D.; Ren, S.; Wang, J.; Han, T.; Gao, Y.; Ning, B.; Gao, Z. A fluorescent amplification strategy for high-sensitive detection of 17 β-estradiol based on EXPAR and HCR, pp. 1-8 (ref 119). Copyright 2020, with permission from Elsevier. **D:** The same principle of E2-aptamer dependent cDNA release can induce an SDA reaction to produce many ssDNA primers (with the aid of Nb.BbvCI and KF polymerase) to initiate RCA and MRCA, whose products unfold dye-quencher-modified molecular beacons, resulting in fluorescence recovery. Reproduced from Wang, W.; Peng, Y.; Wu, J.; Zhang, M.; Li, Q.; Zhao, Z.; Liu, M.; Wang, J.; Cao, G.; Bai, J.; Gao, Z. Anal. Chem. 2021, 93, 4488-4496 (ref 216). Copyright 2021 American Chemical Society.

With the aim to reach extremely low LODs, BPA aptasensors have also implemented various DNA amplification strategies. Combining structure-switching aptamer, magnetic separation, and HCR amplification, Wang *et al.* developed a FRET aptasensor for BPA detection (**Figure 8B**).[132] BPA-aptamer binding induced the release of cDNA to trigger HCR that produces Dabcyl-modified dsDNA, which can interact with UCNPs-functionalized ssDNA to form triplex structure, resulting in effective FRET from UCNPs to Dabcyl. The BPA-dependent amplified UCNP-to-Dabcyl FRET resulted in an LOD of 0.057 ng mL^{-1}.

4.5.2 17β-Estradiol (ES)

ES is a typical environmental endocrine disruptor that can have harmful effects on the environment and interfere with the normal endocrine function organism.[209] Since the first report of a ES-specific aptamer in 2007,[210] a variety of aptasensors have been developed for monitoring ES, including chemiluminescent,[211] electrochemical,[212-214] and fluorescent[119] signal transduction. Sha *et al.* designed a DNA-functionalized FRET ratiometric nano-aptasensor through the DNA hybridization

between a MIL-53-NH_2 modified aptamer (MIL-53-apt) and $Ru(bpy)_3^{2+}$-doped silica NPs modified with cDNA ($RuSiO_2$-cDNA).[215] FRET occured between MIL-53-apt and $RuSiO_2$-cDNA in the absence of ES and was turned off upon ES-target binding, resulting in reduced fluorescence of MIL-53 and increased fluorescence of $RuSiO_2$. The ratiometric dual wavelength quantification of ES provided high accuracy and avoided false positives, yielding an LOD of 0.3 nM (~82 pg mL^{-1}). A combination of structure-switching aptamers and cascaded EXPAR-HCR amplification was designed for detecting very low concentrations of ES (**Figure 8C**).[119] The structure switch was composed of cDNA and aptamer immobilized on MBs. ES-aptamer binding released the cDNA as a trigger sequence to activate EXPAR, which produced a large amount of short ssDNA to initiate HCR, thereby fabricating long dsDNA strands and restoring the initially quenched FAM fluorescence in H1 and H2 hairpins containing FAM-BHQ1 FRET pairs. The incorporation of cascade amplification enabled an LOD of 0.37 pg mL^{-1} ES. Taking advantages of structure-switching aptamers, magnetic separation, strand displacement amplification (SDA), RCA, and multi-primed RCA (MRCA), Wang *et al.* designed a fluorescent sensing platform for ES detection (**Figure 8D**).[216] ES-aptamer binding initiated the cascaded amplification reaction of SDA-RCA-MRCA to generate a long ssDNA, which can recognize and unfold the molecular beacons to restore fluorescence for quantifying ES with an LOD of 63 fM (~17 fg mL^{-1}).

4.5.3 Pros and cons

By integrating HARF, the nanosurface-adsorption fluorescent aptasensor for BPA detection achieved two orders of magnitude enhancement of the sensitivity. Based on structure-switching aptamer and single or cascade DNA amplification technology, the fluorescent aptasensors realize highly sensitive detection of BPA and ES (LODs down to pM or even fM). However, fluorescent labeling of nucleic acids are required in these strategies which increases the cost. Also, the enzyme-based cascade amplification methods require strict control of reaction conditions to ensure enzyme activity, which make it a challenge to achieve robust and reproducible detection under complex conditions. Moreover, almost no principle for the design of primer sequence is provided as the theoretical guide.

Table 1: Overview of fluorescent aptasensors for the determination of common food chemical contaminants.

Design strategy	Targets	Assay temp. (°C)	Analysis time (min)	Buffers	LODs	Sample types	Ref.
Dye displacement aptasensors	AFB1	37	20	HEPES	0.2 ng mL^{-1}	11 kinds of plant-derived food	26
	OTA	RT	< 1	Tris-HCl	0.38 ng mL^{-1}	Coffee and oat	152
	TET	25	6	water	1 nM	Honey and milk	165
	Pb^{2+}	RT	10	Tris-HCl	58.59 nM	Water and tea	182
Structure-switching aptasensors	Acetamiprid	RT, 37	200	PBS	0.38 fM	Tea	38
	Fipronil	RT	60	1×selection buffer	53.8 ppb	Liquid eggs	179
	AFB1	RT	36	Acetate and PBS	0.91 ng mL^{-1}	Peanut oil and broad bean paste	31
	KAN	RT	30	Tris-HCl	13.52 nM	Milk	159
	CAP	RT; 37; RT	40; 45; 30	PBS	1.2 nM; 0.70 ng mL^{-1}; 0.039 pg mL^{-1}	Honey; milk; honey	35,32,161
	TET	RT	50	PBS	1.6 nM	Milk	36
	SDM	RT	21	PBS	3.41 ng mL^{-1}	Water and fish	168
Nanosurface-adsorption aptasensors	OTA	37	155	Tris-HCl	4.59 nM	Wine	151
	CAP	RT	40; 26	Tris-HCl	0.09 nM; 0.08 pg mL^{-1}	Fish; Milk and shrimp	164,163
	fipronil	RT	30	Tris-HCl	3 nM	Honey, water and corn	181
	Pb^{2+}	RT	10	Tris–HCl	0.5 pM	Milk	184

Dye-doped mesoporous silica nanoparticle aptasensors	AFB1	37	180	PBS	0.13 ng mL^{-1}	Oil, corn, peanut, oat meal, rice	44
Aggregation induced emission (AIE) aptasensors	AFB1	RT; RT	90; < 1	Tris-HCl; Tris-HCl	0.25 ng mL^{-1}; 0.29 ng mL^{-1}	Milk, corn, rice; bean paste, peanut oil, corn	49,50
	OTA	RT, 37	45	—	0.4 ng mL^{-1}	Coffee and wine	52
Aptasensors based on fluorescent nanomaterials and FRET	AFB1	37	55	Tris–HCl	20 pg mL^{-1}	Peanuts	56
	T-2	37	50	Tris-HCl	0.087 ng mL^{-1}	Beer and corn flour	154
	TET	25	40	PBS	0.95 ng mL^{-1}	Milk, honey, fish, chicken muscle, and unfertilized eggs	167
	Diazinon	RT	55	PBS	0.13 nM	Water, cucumber and apple	57
	BPA	RT	120	water	0.02 nM	Drink	208
	ES	37	180	TE	0.2 nM	Serum	215
Aptasensors based on fluorescent nanomaterials and IFE	Acetamiprid	37; 37	75; 70	HEPES; —	1.5 nM; 0.36 nM	Water; Tea	176, 65
Aptasensors based on DNA-templated fluorescent metal nanoclusters	Acetamiprid	RT	90	MOPS	2.37 nM	Apple, ginger	177
	OTA	37, RT	190	Tris–HCl, Tris–HAc	2.0 nM	Red wine	73
	MC-LR	—	130	MOPS	4.8 ng L^{-1}	Water	81
Aptasensors using a single	TET	37	30	PBS	6 pg mL^{-1}	Honey and water	82

fluorescent probe	Hg^{2+}	RT; RT	60; 20	Borate; PBS	3.3 nM; 0.5 nM	Water; Water	188,189
Aptasensors using multiple fluorescent probes	OTA, AFB1	25	30	—	0.1 ppb, 0.035 ppb	Corn, olive oil, peanut; peanut oil, sesame and soybean oil	90
	ZEN, T-2, AFB1	RT, 37	60	PBS	0.51 pg mL^{-1}, 0.33 pg mL^{-1}, 0.40 pg mL^{-1}	Maize	88
	AFB1, ZEN	37	60	—	0.34 pg mL^{-1}, 0.53 pg mL^{-1}	Maize	86
	CAP, OTC, KAN	RT	30	PBS	1.5 pM, 2.4 pM, 0.9 pM,	Milk	83
	Hg^{2+}, Pb^{2+}, Ag^{+}	35	12	Tris-HNO_3	0.2, 0.5, 2 nM	Soil	199
	SDM, KAN, ampicillin	RT, 37	75	Tris-HCl	1.997 ng mL^{-1}, 2.664 ng mL^{-1}, 2.337 ng mL^{-1}	Milk	169
RCA-based aptasensors	OTA	37, 4	900	—	0.01 ng mL^{-1}	Beer	98
	TET	37, 25, 65	340	Tris-HCl	0.724 pg mL^{-1}	Fish and honey	100
Nuclease-assisted recycling amplification based aptasensors	OTA	RT; 37	90; 200	Tris–HCl; PBS	0.08 ng mL^{-1}; 0.96 nM	Red wine; Red wine	110,112
	STX	37	50	Tris	0.035 ng·mL^{-1}	Clams	156
EXPAR-based aptasensors	T-2	37, 0, 4	213	PBS	30 fg/mL	Oats and corn	116
HCR-based aptasensors	OTA	37	85	Tris−HCl	4.9 pM	Wheat flour and red wine	129
	CAP	37; 37	150; 30	Tris-HCl; PBS	0.3 pM; 1.2 pg mL^{-1}	Water and milk; Milk	127,131
	BPA	37, 25	420	PBS	0.057 ng mL^{-1}	Milk and water	132
	KAN	RT	65	PBS	0.45 pg mL^{-1}	Milk	128
CHA-based aptasensors	CAP	RT, 37	420	Tris-HCl	16 pM	Milk	162

Cascade signal amplification based aptasensors	ES	37	203	PBS	63.09 fM	Water and milk	216
	ES	37	240	nuclease buffer	0.37 pg mL^{-1}	Milk and water	119

5 Conclusions and outlook

In this review we presented different design strategies of fluorescent aptasensors and their application in the quantification of food chemical contaminants with a focus on the recent literature (mainly 2019 to 2021). Many different concepts and applications of fluorescent aptasensors for food analysis have been developed and we apologize to all colleagues, whose studies we have not discussed within our certainly limited selection. We still hope that our overview provided a general guideline and inspiration for the design and optimization of fluorescent aptasensing platforms to further improve existing concepts and design completely new approaches for simpler, faster, more sensitive, more selective, more multiplexed, more reproducible, more precise, and more accurate analysis of food contaminants.

The design of aptasensors offers an extremely large versatility that can be both advantageous and disadvantageous because of the many combination possibilities from a very large choice of materials and concepts. From the DNA point of view, aptamers can be rather simple ss or dsDNAs that are displaced via aptamer-target binding, structure-switching DNAs that are transformed via aptamer-target interactions, or split DNAs that are combined via aptamer-target interactions. For all of those aptamers, the target-binding affinity and selectivity are extremely important and a careful aptamer selection is paramount for efficient aptasensors. Additionally, DNA provides the possibility of signal amplification with numerous enzyme-based and enzyme-free strategies that can even be combined in a parallel or sequential manner. These concepts are usually exploited for accomplishing the detection of extremely low target concentrations but also often come with the disadvantages of more complicated (more materials, more steps, longer time) experimental protocols and usually require a much more careful design and control of the different steps to assure a reliable sensing performance. In particular, enzymes can be very sensitive to the

environmental and experimental conditions (*e.g.*, temperature, ion concentration, pH, *etc.*) that are essential to maintain the activity of the enzyme. Moreover, the generation of background signals (*e.g.*, due to non-specific amplification) must be avoided. From the fluorescence point of view, the commonly used materials are fluorescent or quenching dyes and NMs that can be organic or inorganic, absorb and fluoresce at a broad spectral range from the UV to the NIR, and require conjugation to DNA or simply intercalate non-specifically with ss or dsDNA (label-free approach). Most often, the interaction between two or more fluorescent and/or quenching materials is used to avoid separation steps. In those cases, different ET (*e.g.*, FRET or IFE) or aggregation (*e.g.*, AIE) mechanisms can be exploited for fluorescence turn-on or turn-off intensity sensing (but also wavelength, lifetime, or polarization changes can be used for sensing). The dimension and stability of the fluorescent/quenching materials are also very important. Aptasensors using fluorescent dyes as signal probes usually possess the advantages of simple operation and no need of complex functionalization, whereas photobleaching and low photostability may limit their application in the determination of targets in complex food matrices. Aptasensors utilizing fluorescent nanoprobes own the superiorities of good photostability and strong anti-interference ability, which can positively contribute to a detection with high sensitivity and reproducibility. However, the reproducibility of production is usually much higher for molecular materials and NMs may suffer from significant batch-to-batch differences concerning size, shape, and photophysical properties. Also, covalent and controlled coupling of fluorescent nanoprobes with nucleic acids, such that both the DNA and the nanoprobe retain their respective properties, performances, and functionalities, can be much more difficult compared to dye-DNA fluorescence bioconjugation. Thus, despite or because of the large versatility in the aptasensor design it is of paramount importance to carefully combine, control, and verify all steps of the initial development and the final experimental protocol.

Over the recent years, a growing number of fluorescent aptasensors have been applied in the field of food safety to provide an effective tool for monitoring food contaminants. Based on the above-mentioned design strategies, we have discussed the application of fluorescent aptasensors

in the quantification of various food chemical contaminants, such as toxins, pesticide residues, veterinary drug residues, heavy metals, BPA, and ES (**Table 1**). The many different targets and sensing approaches confirm the versatility of fluorescent aptasensors and the broad range of sensitivities and detection limits that can be realized for those different targets. Although we have tried to mention LODs for the most applications and LODs are also often used in the literature to compare different approaches, LOD values should always be considered with great care (and often with suspicion). It has become very popular to use the LOD as an important performance parameter to justify the impact of a bioassay and although the LOD (usually defined as the concentration corresponding to the signal value on the assay calibration curve that is three standard deviations above the signal value of the blank) and sensitivity (slope of the assay calibration curve) are important analytical performance parameters, they strongly depend on the environment, the experimental conditions, and the determination of the blank (zero concentration) signal and its standard deviation. Small changes in sample and assay components and conditions, temperature, time, experimental procedures and setups, and the analysis of the experimental results can lead to large differences. Therefore, a very careful and detailed description (by authors) and evaluation (by readers) of the materials and methods is extremely important to understand and appreciate the analytical value of a fluorescent aptasensor.

With the technological and scientific progress, fluorescent aptasensors have been advanced into simple, portable, rapid, and effective tools to meet the requirements of on-site trace detection of food contaminants even directly in different types of food samples. Although aptamers have been used in various fluorescent sensing platforms, including homogeneous detection methods in solution to portable detection devices, such as microfluidic chips, electronic detection devices, and smartphone-based readers, there are still several technical problems that require improvements or need to be overcome: *i)* There are many types of food contaminants, but specific and sensitive aptamers exist only for a part of them. Hence, aptamers specific to other food pollutants need to be selected and optimized to enlarge the target portfolio. *ii)* The target affinity of aptamers can be easily affected by the sample components (*e.g.*, buffer), temperature, pH, and its self-folding.

Therefore, both precisely controlled and optimized experimental conditions and stable and efficient aptamers with high target affinities are of utmost importance. *iii)* Because food samples are characterized by a large variety and complex matrix components, aptasensors with strong anti-interference capacity are necessary. Furthermore, to improve the applicability of fluorescent aptasensors, it is essential to study effective measures for reducing or eliminating matrix effects. *iv)* Most aptasensor studies focus on the implementation into an analytical application for specific targets with a mere description of the experimental phenomena. However, to better understand, control, and optimize the experimental conditions, it is also necessary to carry out in-depth exploration and verification of the underlying fluorescence and ET mechanisms, conformational changes, target-aptamer affinities, and binding kinetics. *v)* Most multiplexed fluorescent aptasensors cannot operate with a single excitation wavelength, resulting in more cumbersome operation. Hence, implementation of multicolor fluorescent nanomaterials (*e.g.*, QDs), advanced multiplexing concepts exploiting multiple fluorescence properties (*e.g.*, color, lifetime, intensity, polarization), parallel detection of many small-volume samples (*e.g.*, micro or nanoarrays), or other multiplexing concepts (*e.g.*, DNA circuits) are required to advance efficient multi-target analysis. *vi)* A small number of portable devices have been reported for the determination of food chemical contaminants and the recent progress in smartphone-based fluorescence analysis has a strong potential to translate fluorescent aptasensors into commercial applications and decentralized and democratized sensing.

List of Abbreviations

A	Acceptor
AFB1	aflatoxin B1
AFM1	aflatoxin M1
AgNCs	Silver nanoclusters
AIE	Aggregation-induced emission
AFT	Aflatoxin

AuNPs	Gold nanoparticles
AuNRs	Gold nanorods
BHQ	Black hole quencher
BPA	Bisphenol A
CAP	Chloramphenicol
CDs	Carbon dots
CHA	Catalytic hairpin assembly
CNMs	Carbon nanomaterials
CoOOH	Cobalt oxyhydroxide
D	Donor
DAPI	4’,6-diamidino-2-phenylindole
DNA	Deoxyribonucleic acid
DNase I	Deoxyribonuclease I
dNTPs	Deoxyribonucleotide triphosphates
DPA-GQD-His	D-penicillamine and histidine-functionalized graphene quantum dot
DSA	9,10-distyrylanthracene
DSAI	9,10-distyrylanthracene derivative
dTTP	2’-deoxythymidine 5’-triphosphate
EDC	1-ethyl-3-(3-dimethyllaminopropyl) carbodiimide hydrochloride
ELISAs	enzyme linked immunosorbent assays
ES	17β-Estradiol
ET	Energy transfer
Exo I	Exonuclease I
EXPAR	Exponential amplification reaction
F	Fluorophore
FAM	Carboxyfluorescein
FRET	Förster resonance energy transfer
G4	G-quadruplex
g-CNQDs	graphitic carbon nitride QDs
GO	Graphene oxide
GQDs	Graphene quantum dots
GNSs	Gold nanostars
HARF	Hollow core anti-resonant fiber
HCR	Hybridization chain reaction

HRCA	Hyperbranched rolling circle amplification
IFE	Inner filter effect
KAN	Kanamycin
LRCA	Linear rolling circle amplification
LOD	Limit of detection
MBs	Magnetic beads
MC-LR	Microcystin-LR
MNCs	Metal nanoclusters
MNMs	Metal nanomaterials
MOFs	Metal organic frameworks
MRCA	Multi-primed RCA
MRGO	Magnetic reduced graphene oxide
MSNs	Mesoporous silica nanoparticles
MWCNTs	Multi-walled carbon nanotubes
MXenes	Transition-metal carbides and carbonitrides
Nano-Q	Nanomaterial-based fluorescence quencher
NHS	N-hydroxysuccinimide
NMs	Nanomaterials
NMM	N-methylmorpholine
NSET	Nanosurface energy transfer
OPs	Organophosphorus pesticides
OTA	Ochratoxin A
OTC	Oxytetracycline
PhC	Photonic crystal
Q	Quencher
QDs	Quantum dots
RCA	Rolling circle amplification
RCP	Rolling circle amplification product
ROX	Carboxy-X-rhodamine
RNA	Ribonucleic acid
RNase H	ribonuclease H
$RuSiO_2$	$Ru(bpy)_3^{2+}$-doped silica nanoparticles
SDA	Strand displacement amplification
SDM	Sulfadimethoxine
SELEX	Systematic evolution of ligands by exponential enrichment

SERS	Surface-enhanced Raman spectroscopy
SFP	Single fluorescent probes
SSAs	Structure-switching aptamers
STP	Signal transduction probe
STX	Saxitoxin
SWCNHs	Single-walled carbon nanohorns
SWCNTs	Single-walled carbon nanotubes
T-2	T-2 mycotoxin
TAMRA	Carboxytetramethylrhodamine
TdT	Terminal deoxynucleotidyl transferase
TET	Tetracycline
THMS	Triple-helix DNA molecular switch
ThT	Thioflavin T
TMDNSs	Transition-metal chalcogenides and oxides nanosheets
TO	Thiazole orange
TPE	1,2-diphenyl-1,2-di(p-tolyl)ethene
UCNPs	Upconversion NPs
ZEN	Zearalenone

Notes

The authors report no conflicts of interest.

Biographies

Ying Li is currently PhD student in Food Science and Engineering at Jilin University, Changchun, China. Her research focuses on biosensors and their application in food safety.

Ruifang Su is currently PhD student in Chemistry at the University of Rouen Normandie. Her research focuses on probing nanosurface-environment interactions by FRET from lanthanide complexes to quantum dots.

Hongxia Li is currently Associate Professor of food quality and safety at Jilin University,

Changchun, China. Her research interests cover biosensors and their application in food safety.

Jiajia Guo is currently Associate Professor at Shenzhen Institutes of Advanced Technology, Chinese Academy of Sciences. She holds a PhD in Nanotechnology (2019) from the University of Paris Saclay (France). From 2019 to 2021, she worked as a postdoc at the Massachusetts Institute of Technology (MIT, USA). Her research interests are confocal/TIRF microscopy-based smFRET and interaction, structure, and dynamics of cancer-related proteins, DNA, and RNA.

Niko Hildebrandt is currently Guest Professor in the Department of Chemistry at Seoul National University (South Korea). He holds a PhD in Physical Chemistry (2007) from the University of Potsdam (Germany). He has been research group leader at various institutes in Germany (Fraunhofer IAP) and France (IEF, C2N, I2BC, COBRA) and Full Professor at Université Paris-Saclay (France) since 2010. Niko's main research interests are time-resolved luminescence spectroscopy and microscopy and the application of luminescent, nano, and bio materials for multiplexed FRET biosensing and bioimaging.

Chunyan Sun is currently Professor of food quality and safety at Jilin University, Changchun, China. She received her PhD degree in Analytical Chemistry at Changchun Institute of Applied Chemistry, Chinese Academy of Sciences (2006). Her research interests cover biosensors and their application in food safety.

Acknowledgements

This work has been supported by the Korean National Research Foundation, Seoul National University, Université Paris-Saclay, University of Copenhagen, Université de Rouen Normandie, INSA Rouen Normandie, Centre National de la Recherche Scientifique (CNRS), European Regional Development Fund (ERDF), Labex SynOrg (ANR-11-LABX-0029), Carnot Insitut I2C, XL-Chem graduate school for research (ANR-18-EURE-0020 XL CHEM), Region Normandie, National Natural Science Foundation of China (No. 31571919), Science and Technology Development Program of Jilin Province (No. 20200201218JC), and "Thirteenth Five-Year" Science and Technology Project of Education Department of Jilin Province (No. JJKH20201010KJ).

References

(1) Kunzelmann, M.; Winter, M.; Åberg, M.; Hellenäs, K.-E.; Rosén, J. *Analytical and Bioanalytical Chemistry* **2018,** *410* (22), 5593-5602.

(2) Mukherjee, S.; Bhattacharyya, S.; Ghosh, K.; Pal, S.; Halder, A.; Naseri, M.; Mohammadniaei, M.; Sarkar, S.; Ghosh, A.; Sun, Y.; Bhattacharyya, N. *Trends in Food Science & Technology* **2021,** *109*, 674-689.

(3) Cui, X.; Jin, M.; Du, P.; Chen, G.; Zhang, C.; Zhang, Y.; Shao, Y.; Wang, J. *Food and Agricultural Immunology* **2018,** *29* (1), 638-652.

(4) Feng, C.; Dai, S.; Wang, L. *Biosensors and Bioelectronics* **2014,** *59*, 64-74.

(5) Alhadrami, H. A. *Biotechnology and Applied Biochemistry* **2018,** *65* (3), 497-508.

(6) Ellington, A. D.; Szostak, J. W. *Nature* **1990,** *346*, 30.

(7) Bock, L.; Griffin, L.; Latham, J.; Vermaas, E.; Toole, J. *Nature* **1992,** *355*, 6.

(8) Song, S.; Wang, L.; Li, J.; Zhao, J.; Fan, C. *TrAC Trends in Analytical Chemistry* **2008,** *27* (2), 108-117.

(9) Munzar, J. D.; Ng, A.; Juncker, D. *Chemical Society Reviews* **2019,** *48* (5), 1390-1419.

(10) Safarpour, H.; Dehghani, S.; Nosrati, R.; Zebardast, N.; Alibolandi, M.; Mokhtarzadeh, A.; Ramezani, M. *Biosensors and Bioelectronics* **2020,** *148*, 111833.

(11) Wang, T.; Chen, C.; Larcher, L. M.; Barrero, R. A.; Veedu, R. N. *Biotechnology Advances* **2019,** *37* (1), 28-50.

(12) Yang, Y.; Yin, S.; Li, Y.; Lu, D.; Zhang, J.; Sun, C. *TrAC Trends in Analytical Chemistry* **2017,** *95*, 1-22.

(13) Zhou, W.; Jimmy Huang, P.-J.; Ding, J.; Liu, J. *Analyst* **2014,** *139* (11), 2627-2640.

(14) Acquah, C.; Danquah, M. K.; Yon, J. L. S.; Sidhu, A.; Ongkudon, C. M. *Analytica Chimica Acta* **2015,** *888*, 10-18.

(15) Zhao, W.; Xu, J.; Chen, H. *Chemical Reviews* **2014,** *114* (15), 7421-7441.

(16) Sharma, A.; Khan, R.; Catanante, G.; Sherazi, T. A.; Bhand, S.; Hayat, A.; Marty, J. L. *Toxins* **2018,** *10* (5), 197.

(17) Kurup, C. P.; Tlili, C.; Zakaria, S. N. A.; Ahmed, M. U. *Biointerface Research in Applied Chemistry* **2021**.

(18) Pehlivan, Z. S.; Torabfam, M.; Kurt, H.; Ow-Yang, C.; Hildebrandt, N.; Yüce, M. *Microchimica Acta* **2019,** *186* (8), 563.

(19) Ghorbani, F.; Abbaszadeh, H.; Dolatabadi, J. E. N.; Aghebati-Maleki, L.; Yousefi, M. *Biosensors and Bioelectronics* **2019,** *142*, 111484.

(20) Schmitz, F. R. W.; Valério, A.; de Oliveira, D.; Hotza, D. *Applied Microbiology and Biotechnology* **2020,** *104* (16), 6929-6939.

(21) Xiang, W.; Lv, Q.; Shi, H.; Xie, B.; Gao, L. *Talanta* **2020,** *214*, 120716.

(22) Yousefi, M.; Dehghani, S.; Nosrati, R.; Zare, H.; Evazalipour, M.; Mosafer, J.; Tehrani, B. S.; Pasdar, A.; Mokhtarzadeh, A.; Ramezani, M. *Biosensors and Bioelectronics* **2019,** *130*, 1-19.

(23) Zhang, K.; Li, H.; Wang, W.; Cao, J.; Gan, N.; Han, H. *ACS Sensors* **2020,** *5* (12), 3721-3738.

(24) Zhao, X.; Dai, X.; Zhao, S.; Cui, X.; Gong, T.; Song, Z.; Meng, H.; Zhang, X.; Yu, B. *Spectrochimica Acta Part A: Molecular and Biomolecular Spectroscopy* **2021,** *247*, 119038.

(25) Zhu, C.; Li, L.; Wang, Z.; Irfan, M.; Qu, F. *Biosensors and Bioelectronics* **2020,** *160*, 112213.

(26) Li, Y.; Wang, J.; Zhang, B.; He, Y.; Wang, J.; Wang, S. *Microchimica Acta* **2019,** *186* (4), 214.

(27) Zhang, D.; Cai, L.; Bian, F.; Kong, T.; Zhao, Y. *Analytical Chemistry* **2020,** *92* (4), 2891-2895.

(28) Chen, J.; Meng, H.; An, Y.; Geng, X.; Zhao, K.; Qu, L.; Li, Z. *Talanta* **2020,** *209*, 120510.

(29) Tian, F.; Zhou, J.; Fu, R.; Cui, Y.; Zhao, Q.; Jiao, B.; He, Y. *Food Chemistry* **2020,** *320*, 126607.

(30) Qiao, Q.; Guo, X.; Wen, F.; Chen, L.; Xu, Q.; Zheng, N.; Cheng, J.; Xue, X.; Wang, J. *Frontiers in Chemistry* **2021,** *9* (139).
(31) Xia, X.; Wang, Y.; Yang, H.; Dong, Y.; Zhang, K.; Lu, Y.; Deng, R.; He, Q. *Food Chemistry* **2019,** *283*, 32-38.
(32) Ma, X.; Li, H.; Qiao, S.; Huang, C.; Liu, Q.; Shen, X.; Geng, Y.; Xu, W.; Sun, C. *Food Chemistry* **2020,** *302*, 125359.
(33) Zhao, Y.; Li, X.; Yang, Y.; Si, S.; Deng, C.; Wu, H. *Biosensors and Bioelectronics* **2020,** *149*, 111840.
(34) Jalalian, S. H.; Taghdisi, S. M.; Danesh, N. M.; Bakhtiari, H.; Lavaee, P.; Ramezani, M.; Abnous, K. *Analytical Methods* **2015,** *7* (6), 2523-2528.
(35) Tu, C.; Dai, Y.; Zhang, Y.; Wang, W.; Wu, L. *Spectrochimica Acta Part A: Molecular and Biomolecular Spectroscopy* **2020,** *224*, 117415.
(36) He, H.; Xie, C.; Yao, L.; Ning, G.; Wang, Y. *Journal of Fluorescence* **2021,** *31* (1), 63-71.
(37) Zhang, Y.; Du, X.; Deng, S.; Li, C.; He, Q.; He, G.; Zhou, M.; Wang, H.; Deng, R. *Journal of Agricultural and Food Chemistry* **2020,** *68* (35), 9524-9529.
(38) Li, N.; Li, R.; Sun, X.; Yang, Y.; Li, Z. *Microchimica Acta* **2020,** *187* (3), 158.
(39) Gao, H.; Zhao, J.; Huang, Y.; Cheng, X.; Wang, S.; Han, Y.; Xiao, Y.; Lou, X. *Analytical Chemistry* **2019,** *91* (22), 14514-14521.
(40) Cui, H.; Fu, X.; Yang, L.; Xing, S.; Wang, X. *Talanta* **2021,** *228*, 122219.
(41) Lv, M.; Zhou, W.; Tavakoli, H.; Bautista, C.; Xia, J.; Wang, Z.; Li, X. *Biosensors and Bioelectronics* **2021,** *176*, 112947.
(42) Sun, Y.; Qi, T.; Jin, Y.; Liang, L.; Zhao, J. *RSC Advances* **2021,** *11* (17), 10054-10060.
(43) Kholafazad Kordasht, H.; Pazhuhi, M.; Pashazadeh-Panahi, P.; Hasanzadeh, M.; Shadjou, N. *TrAC Trends in Analytical Chemistry* **2020,** *124*, 115778.
(44) Tan, H.; Ma, L.; Guo, T.; Zhou, H.; Chen, L.; Zhang, Y.; Dai, H.; Yu, Y. *Analytica Chimica Acta* **2019,** *1068*, 87-95.
(45) Chen, Z.; Sun, M.; Luo, F.; Xu, K.; Lin, Z.; Zhang, L. *Talanta* **2018,** *178*, 563-568.
(46) Luo, J.; Xie, Z.; Lam, J. W. Y.; Cheng, L.; Chen, H.; Qiu, C.; Kwok, H. S.; Zhan, X.; Liu, Y.; Zhu, D.; Tang, B. Z. *Chemical Communications* **2001**, 10.1039/B105159H (18), 1740-1741.
(47) Würthner, F. *Angewandte Chemie International Edition* **2020,** *132* (34), 14296-14301.
(48) Zhu, C.; Pang, S.; Xu, J.; Jia, L.; Xu, F.; Mei, J.; Qin, A.; Sun, J.; Ji, J.; Tang, B. *Analyst* **2011,** *136* (16), 3343-3348.
(49) Jia, Y.; Wu, F.; Liu, P.; Zhou, G.; Yu, B.; Lou, X.; Xia, F. *Talanta* **2019,** *198*, 71-77.
(50) Zhao, Z.; Yang, H.; Deng, S.; Dong, Y.; Yan, B.; Zhang, K.; Deng, R.; He, Q. *Dyes and Pigments* **2019,** *171*, 107767.
(51) Guo, Y.; Zhao, C.; Liu, Y.; Nie, H.; Guo, X.; Song, X.; Xu, K.; Li, J.; Wang, J. *Analyst* **2020,** *145* (11), 3857-3863.
(52) Zhu, Y.; Xia, X.; Deng, S.; Yan, B.; Dong, Y.; Zhang, K.; Deng, R.; He, Q. *Dyes and Pigments* **2019,** *170*, 107572.
(53) Hildebrandt, N.; Medintz, I. L. Wiley-VCH Verlag GmbH: 2014.
(54) Wang, J.; Li, B.; Lu, Q.; Li, X.; Weng, C.; Yan, X.; Hong, J.; Zhou, X. *Microchimica Acta* **2019,** *186* (6), 356.
(55) Chen, C.; Hildebrandt, N. *TrAC Trends in Analytical Chemistry* **2020,** *123*, 115748.
(56) Lu, X.; Wang, C.; Qian, J.; Ren, C.; An, K.; Wang, K. *Analytica Chimica Acta* **2019,** *1047*, 163-171.
(57) Arvand, M.; Mirroshandel, A. A. *Food Chemistry* **2019,** *280*, 115-122.
(58) Xu, S.; Nie, Y.; Jiang, L.; Wang, J.; Xu, G.; Wang, W.; Luo, X. *Analytical Chemistry* **2018,** *90* (6), 4039-4045.

(59) Shen, Y.; Wu, T.; Zhang, Y.; Ling, N.; Zheng, L.; Zhang, S.-L.; Sun, Y.; Wang, X.; Ye, Y. *Analytical Chemistry* **2020,** *92* (19), 13396-13404.
(60) Lakowicz, J. R., Protein fluorescence. In *Principles of fluorescence spectroscopy*, Springer: 1983, pp 341-381.
(61) Chen, X.; Lin, Z.; Hong, C.; Zhong, H.; Yao, Q.; Huang, Z. *Applied Spectroscopy* **2019,** *73* (3), 294-303.
(62) Song, Y.; Xu, G.; Wei, F.; Cen, Y.; Sohail, M.; Shi, M.; Xu, X.; Ma, Y.; Ma, Y.; Hu, Q. *Microchimica Acta* **2018,** *185* (2), 139.
(63) Wang, W.; Wang, Y.; Pan, H.; Cheddah, S.; Yan, C. *Microchimica Acta* **2019,** *186* (8), 544.
(64) Qu, F.; Ding, Y.; Lv, X.; Xia, L.; You, J.; Han, W. *Analytical and Bioanalytical Chemistry* **2019,** *411* (17), 3979-3988.
(65) Yang, L.; Sun, H.; Wang, X.; Yao, W.; Zhang, W.; Jiang, L. *Microchimica Acta* **2019,** *186* (5), 308.
(66) Shao, N.; Zhang, Y.; Cheung, S.; Yang, R.; Chan, W.; Mo, T.; Li, K.; Liu, F. *Analytical Chemistry* **2005,** *77* (22), 7294-7303.
(67) Zhang, X.; Servos, M. R.; Liu, J. *Langmuir* **2012,** *28* (8), 3896-3902.
(68) Sun, C.; Zhao, S.; Qu, F.; Han, W.; You, J. *Microchimica Acta* **2020,** *187* (1), 34.
(69) Chen, Y.; Phipps, M. L.; Werner, J. H.; Chakraborty, S.; Martinez, J. S. *Accounts of Chemical Research* **2018,** *51* (11), 2756-2763.
(70) Liu, M.; Tang, F.; Yang, Z.; Xu, J.; Yang, X. *Journal of Analytical Methods in Chemistry* **2019,** *2019*, 1095148.
(71) Ou, G.; Zhao, J.; Chen, P.; Xiong, C.; Dong, F.; Li, B.; Feng, X. *Analytical and Bioanalytical Chemistry* **2018,** *410* (10), 2485-2498.
(72) Guo, Y.; Pan, X.; Zhang, W.; Hu, Z.; Wong, K.-W.; He, Z.; Li, H.-W. *Biosensors and Bioelectronics* **2020,** *150*, 111926.
(73) He, Y.; Tian, F.; Zhou, J.; Jiao, B. *Microchimica Acta* **2019,** *186* (3), 199.
(74) Petty, J. T.; Zheng, J.; Hud, N. V.; Dickson, R. M. *Journal of the American Chemical Society* **2004,** *126* (16), 5207-5212.
(75) Zhang, M.; Gao, G.; Ding, Y.; Deng, C.; Xiang, J.; Wu, H. *Talanta* **2019,** *199*, 238-243.
(76) Zhang, X.; Khan, I. M.; Ji, H.; Wang, Z.; Tian, H.; Cao, W.; Mi, W. *Polymers* **2020,** *12* (1), 152.
(77) Li, J.; Zhong, X.; Zhang, H.; Le, X. C.; Zhu, J.-J. *Analytical Chemistry* **2012,** *84* (12), 5170-5174.
(78) Yeh, H.-C.; Sharma, J.; Shih, I.-M.; Vu, D. M.; Martinez, J. S.; Werner, J. H. *Journal of the American Chemical Society* **2012,** *134* (28), 11550-11558.
(79) Rotaru, A.; Dutta, S.; Jentzsch, E.; Gothelf, K.; Mokhir, A. *Angewandte Chemie International Edition* **2010,** *49* (33), 5665-5667.
(80) Qing, Z.; He, X.; He, D.; Wang, K.; Xu, F.; Qing, T.; Yang, X. *Angewandte Chemie International Edition* **2013,** *52* (37), 9719-9722.
(81) Zhang, Y.; Lai, Y.; Teng, X.; Pu, S.; Yang, Z.; Pang, P.; Wang, H.; Yang, C.; Yang, W.; Barrow, C. J. *Analytical Methods* **2020,** *12* (13), 1752-1758.
(82) Hong, C.; Zhang, X.; Dai, C.; Wu, C.; Huang, Z. *Analytica Chimica Acta* **2020,** *1120*, 50-58.
(83) Yang, Q.; Hong, J.; Wu, Y.; Cao, Y.; Wu, D.; Hu, F.; Gan, N. *ACS Applied Materials & Interfaces* **2019,** *11* (44), 41506-41515.
(84) Sun, Y.; Fan, J.; Cui, L.; Ke, W.; Zheng, F.; Zhao, Y. *Microchimica Acta* **2019,** *186* (3), 152.
(85) Cui, F.; Sun, J.; de Dieu Habimana, J.; Yang, X.; Ji, J.; Zhang, Y.; Lei, H.; Li, Z.; Zheng, J.; Fan, M.; Sun, X. *Analytical Chemistry* **2019,** *91* (22), 14681-14690.

(86) Khan, I. M.; Niazi, S.; Yu, Y.; Mohsin, A.; Mushtaq, B. S.; Iqbal, M. W.; Rehman, A.; Akhtar, W.; Wang, Z. *Analytical Chemistry* **2019,** *91* (21), 14085-14092.
(87) Jiang, Y.; Tang, Y.; Miao, P. *Nanoscale* **2019,** *11* (17), 8119-8123.
(88) Niazi, S.; Khan, I. M.; Yu, Y.; Pasha, I.; Shoaib, M.; Mohsin, A.; Mushtaq, B. S.; Akhtar, W.; Wang, Z. *Microchimica Acta* **2019,** *186* (8), 575.
(89) Xu, X.; Ji, J.; Chen, P.; Wu, J.; Jin, Y.; Zhang, L.; Du, S. *Analytica Chimica Acta* **2020,** *1125*, 41-49.
(90) Xiong, Z.; Wang, Q.; Xie, Y.; Li, N.; Yun, W.; Yang, L. *Food Chemistry* **2021,** *338*, 128122.
(91) Seo, H. B.; Gu, M. B. *Journal of Biological Engineering* **2017,** *11* (1), 11.
(92) Stojanovic, M. N.; de Prada, P.; Landry, D. W. *Journal of the American Chemical Society* **2000,** *122* (46), 11547-11548.
(93) Debiais, M.; Lelievre, A.; Smietana, M.; Müller, S. *Nucleic Acids Research* **2020,** *48* (7), 3400-3422.
(94) You, J.; You, Z.; Xu, X.; Ji, J.; Lu, T.; Xia, Y.; Wang, L.; Zhang, L.; Du, S. *Microchimica Acta* **2019,** *186* (1), 43.
(95) Ma, Y.; Geng, F.; Wang, Y.; Xu, M.; Shao, C.; Qu, P.; Zhang, Y.; Ye, B. *Biosensors and Bioelectronics* **2019,** *134*, 36-41.
(96) Ali, M. M.; Li, F.; Zhang, Z.; Zhang, K.; Kang, D.-K.; Ankrum, J. A.; Le, X. C.; Zhao, W. *Chemical Society Reviews* **2014,** *43* (10), 3324-3341.
(97) Gu, L.; Yan, W.; Liu, L.; Wang, S.; Zhang, X.; Lyu, M. *Pharmaceuticals* **2018,** *11* (2), 35.
(98) Hao, L.; Wang, W.; Shen, X.; Wang, S.; Li, Q.; An, F.; Wu, S. *Journal of Agricultural and Food Chemistry* **2020,** *68* (1), 369-375.
(99) Zhang, Z.; Wang, S.; Ma, J.; Zhou, T.; Wang, F.; Wang, X.; Zhang, G. *ACS Biomaterials Science & Engineering* **2020,** *6* (5), 3114-3121.
(100) Hong, C.; Zhang, X.; Ye, S.; Yang, H.; Huang, Z.; Yang, D.; Cai, R.; Tan, W. *ACS Applied Materials & Interfaces* **2021,** *13* (17), 19695-19700.
(101) Huang, R.; He, L.; Li, S.; Liu, H.; Jin, L.; Chen, Z.; Zhao, Y.; Li, Z.; Deng, Y.; He, N. *Nanoscale* **2020,** *12* (4), 2445-2451.
(102) Wang, J.; Wang, Y.; Liu, S.; Wang, H.; Zhang, X.; Song, X.; Huang, J. *Analytica Chimica Acta* **2019,** *1060*, 79-87.
(103) Niazi, S.; Khan, I. M.; Yu, Y.; Pasha, I.; Lv, Y.; Mohsin, A.; Mushtaq, B. S.; Wang, Z. *Sensors and Actuators B: Chemical* **2020,** *315*, 128049.
(104) Yan, M.; Bai, W.; Zhu, C.; Huang, Y.; Yan, J.; Chen, A. *Biosensors and Bioelectronics* **2016,** *77*, 613-623.
(105) Lou, Y.; Peng, Y.; Luo, X.; Yang, Z.; Wang, R.; Sun, D.; Li, L.; Tan, Y.; Huang, J.; Cui, L. *Microchimica Acta* **2019,** *186* (8), 494.
(106) Xie, W.; He, S.; Fang, S.; Liang, L.; Shi, B.; Wang, D. *Analytica Chimica Acta* **2021,** *1173*, 338698.
(107) Shen, Y.; Shen, X.; Ge, J.; Qu, L.; Li, Z. *New Journal of Chemistry* **2021,** *45* (25), 11347-11351.
(108) Fan, Y.; Mou, Z.; Wang, M.; Li, J.; Zhang, J.; Dang, F.; Zhang, Z. *Analytical Chemistry* **2018,** *90* (22), 13708-13713.
(109) Yu, X.; Lin, Y.; Wang, X.; Xu, L.; Wang, Z.; Fu, F. *Microchimica Acta* **2018,** *185* (5), 259.
(110) Wu, K.; Ma, C.; Zhao, H.; Chen, M.; Deng, Z. *Food Chemistry* **2019,** *277*, 273-278.
(111) Zuo, X.; Xia, F.; Xiao, Y.; Plaxco, K. W. *Journal of the American Chemical Society* **2010,** *132* (6), 1816-1818.
(112) Liu, M.; Li, X.; Li, B.; Du, J.; Yang, Z. *Microchimica Acta* **2020,** *187* (1), 46.
(113) Van Ness, J.; Van Ness, L. K.; Galas, D. J. *Proceedings of the National Academy of Sciences* **2003,** *100* (8),

4504-4509.
(114) Chen, H.; Wang, Z.; Chen, X.; Lou, K.; Sheng, A.; Chen, T.; Chen, G.; Zhang, J. *Analyst* **2019,** *144* (6), 1955-1959.
(115) Wu, H.; Wu, J.; Liu, Y.; Wang, H.; Zou, P. *Microchimica Acta* **2019,** *186* (11), 715.
(116) Zhang, M.; Wang, Y.; Yuan, S.; Sun, X.; Huo, B.; Bai, J.; Peng, Y.; Ning, B.; Liu, B.; Gao, Z. *Microchimica Acta* **2019,** *186* (4), 219.
(117) Zhang, Y.; Cui, Y.; Li, X.; Du, Y.; Tang, A.; Kong, D. *Chemical Communications* **2019,** *55* (53), 7611-7614.
(118) Reid, M. S.; Le, X. C.; Zhang, H. *Angewandte Chemie International Edition* **2018,** *57* (37), 11856-11866.
(119) Wang, Y.; Zhao, X.; Zhang, M.; Sun, X.; Bai, J.; Peng, Y.; Li, S.; Han, D.; Ren, S.; Wang, J.; Han, T.; Gao, Y.; Ning, B.; Gao, Z. *Analytica Chimica Acta* **2020,** *1116*, 1-8.
(120) Reid, M. S.; Paliwoda, R. E.; Zhang, H.; Le, X. C. *Analytical Chemistry* **2018,** *90* (18), 11033-11039.
(121) Wang, J.; Zou, B.; Rui, J.; Song, Q.; Kajiyama, T.; Kambara, H.; Zhou, G. *Microchimica Acta* **2015,** *182* (5), 1095-1101.
(122) Dirks, R. M.; Pierce, N. A. *Proceedings of the National Academy of Sciences* **2004**, *101* (43), 15275-15278.
(123) Zeng, Z.; Zhou, R.; Sun, R.; Zhang, X.; Cheng, Z.; Chen, C.; Zhu, Q. *Biosensors and Bioelectronics* **2021,** *173*, 112814.
(124) Zhang, C.; Chen, J.; Sun, R.; Huang, Z.; Luo, Z.; Zhou, C.; Wu, M.; Duan, Y.; Li, Y. *ACS Sensors* **2020,** *5* (10), 2977-3000.
(125) Ang, Y. S.; Yung, L.-Y. L. *Chemical Communications* **2016,** *52* (22), 4219-4222.
(126) Yang, D.; Zhang, X.; Kou, X.; Shao, X.; Miao, P. *Particle & Particle Systems Characterization* **2020,** *37* (4), 1900488.
(127) Ma, P.; Sun, Y.; Khan, I. M.; Gu, Q.; Yue, L.; Wang, Z. *Microchimica Acta* **2020,** *187* (9), 505.
(128) Zhang, K.; Cao, J.; Wu, Y.; Hu, F.; Li, T.; Wang, Y.; Gan, N. *Microchimica Acta* **2019,** *186* (2), 120.
(129) Qian, M.; Hu, W.; Wang, L.; Wang, Y.; Dong, Y. *Toxins* **2020,** *12* (6), 376.
(130) Bai, Y.; Zhang, H.; Zhao, L.; Wang, Y.; Chen, X.; Zhai, H.; Tian, M.; Zhao, R.; Wang, T.; Xu, H.; Feng, F. *Talanta* **2021,** *221*, 121451.
(131) Li, Y.; Wang, L.; Zhao, L.; Li, M.; Wen, Y. *Food Chemistry* **2021,** *357*, 129769.
(132) Wang, Y.; Zhao, X.; Huo, B.; Ren, S.; Bai, J.; Peng, Y.; Li, S.; Han, D.; Wang, J.; Han, T.; Gao, Z. *ACS Applied Bio Materials* **2021,** *4* (1), 763-769.
(133) Green, S. J.; Lubrich, D.; Turberfield, A. J. *Biophysical Journal* **2006,** *91* (8), 2966-2975.
(134) Li, B.; Ellington, A. D.; Chen, X. *Nucleic Acids Research* **2011,** *39* (16), e110-e110.
(135) Yin, P.; Choi, H. M. T.; Calvert, C. R.; Pierce, N. A. *Nature* **2008,** *451* (7176), 318-322.
(136) Liu, J.; Zhang, Y.; Xie, H.; Zhao, L.; Zheng, L.; Ye, H. *Small* **2019,** *15* (42), 1902989.
(137) Wang, S.; Li, X.; Jiang, B.; Yuan, R.; Xiang, Y. *Sensors and Actuators B: Chemical* **2019,** *298*, 126929.
(138) Ye, T.; Peng, Y.; Yuan, M.; Cao, H.; Yu, J.; Li, Y.; Xu, F. *Microchimica Acta* **2019,** *186* (12), 760.
(139) He, J. H.; Cheng, Y. Y.; Zhang, Q. Q.; Liu, H.; Huang, C. Z. *Talanta* **2020,** *219*, 121276.
(140) Li, S.; Liu, X.; Liu, S.; Guo, M.; Liu, C.; Pei, M. *Analytica Chimica Acta* **2021,** *1141*, 21-27.
(141) Xu, J.; Guo, J.; Golob-Schwarzl, N.; Haybaeck, J.; Qiu, X.; Hildebrandt, N. *ACS Sensors* **2020,** *5* (6), 1768-1776.
(142) Wang, J.; Wang, Y.; Liu, S.; Wang, H.; Zhang, X.; Song, X.; Yu, J.; Huang, J. *Analyst* **2019,** *144* (10), 3389-3397.

(143) Hu, X.; Zhang, H.; Zhou, Y.; Liang, W.; Yuan, R.; Chen, S. *Microchimica Acta* **2019,** *186* (8), 582.
(144) Li, D.; Zhang, T.; Yang, F.; Yuan, R.; Xiang, Y. *Analytical Chemistry* **2020,** *92* (2), 2074-2079.
(145) Fan, T.; Mao, Y.; Liu, F.; Zhang, W.; Lin, J.-S.; Yin, J.; Tan, Y.; Huang, X.; Jiang, Y. *Talanta* **2019,** *200*, 480-486.
(146) Zhang, M.; Wang, Y.; Wu, P.; Wang, W.; Cheng, Y.; Huang, L.; Bai, J.; Peng, Y.; Ning, B.; Gao, Z.; Liu, B. *Analytica Chimica Acta* **2020,** *1119*, 18-24.
(147) Shao, X.; Feng, Y.; Zhu, L.; Zhang, Y.; Luo, Y.; Mei, X.; Yuan, C.; Xu, W. *Sensors and Actuators B: Chemical* **2020,** *303*, 126988.
(148) Ye, W.; Liu, T.; Zhang, W.; Zhu, M.; Liu, Z.; Kong, Y.; Liu, S. *Toxins* **2020,** *12* (1), 1.
(149) Zhang, N.; Liu, B.; Cui, X.; Li, Y.; Tang, J.; Wang, H.; Zhang, D.; Li, Z. *Talanta* **2021,** *223*, 121729.
(150) Guo, M.; Hou, Q.; Waterhouse, G. I. N.; Hou, J.; Ai, S.; Li, X. *Talanta* **2019,** *205*.
(151) Shao, X.; Zhu, L.; Feng, Y.; Zhang, Y.; Luo, Y.; Huang, K.; Xu, W. *Analytica Chimica Acta* **2019,** *1087*, 113-120.
(152) Zeng, H.; Zhu, Y.; Ma, L.; Xia, X.; Li, Y.; Ren, Y.; Zhao, W.; Yang, H.; Deng, R. *Dyes and Pigments* **2019,** *164*, 35-42.
(153) Bi, X.; Luo, L.; Li, L.; Liu, X.; Chen, B.; You, T. *Talanta* **2020,** *218*, 121159.
(154) Zhao, X.; Wang, Y.; Li, J.; Huo, B.; Huang, H.; Bai, J.; Peng, Y.; Li, S.; Han, D.; Ren, S.; Wang, J.; Gao, Z. *Analytica Chimica Acta* **2021,** *1160*, 338450.
(155) Li, M.; Lin, H.; Paidi, S. K.; Mesyngier, N.; Preheim, S.; Barman, I. *ACS Sensors* **2020,** *5* (5), 1419-1426.
(156) Gu, H.; Hao, L.; Ye, H.; Ma, P.; Wang, Z. *Microchimica Acta* **2021,** *188* (4), 118.
(157) Luan, Y.; Wang, N.; Li, C.; Guo, X.; Lu, A. *Antibiotics* **2020,** *9* (11), 787.
(158) Tao, X.; Peng, Y.; Liu, J. *Journal of Food Drug Analysis* **2020,** *28* (4), 575-594.
(159) Ma, X.; Qiao, S.; Sun, H.; Su, R.; Sun, C.; Zhang, M. *Frontiers in Chemistry* **2019,** *7*, 29.
(160) Ye, T.; Peng, Y.; Yuan, M.; Cao, H.; Yu, J.; Li, Y.; Xu, F. *Microchimica Acta* **2018,** *186* (1), 40.
(161) Sharma, R.; Akshath, U. S.; Bhatt, P.; Raghavarao, K. *Sensors and Actuators B: Chemical* **2019,** *290*, 110-117.
(162) Hong, F.; Lin, X.; Wu, Y.; Dong, Y.; Cao, Y.; Hu, F.; Gan, N. *Microchimica Acta* **2019,** *186* (3), 150.
(163) Liu, S.; Bai, J.; Huo, Y.; Ning, B.; Peng, Y.; Li, S.; Han, D.; Kang, W.; Gao, Z. *Biosensors and Bioelectronics* **2020,** *149*, 111801.
(164) Lu, Z.; Jiang, Y.; Wang, P.; Xiong, W.; Qi, B.; Zhang, Y.; Xiang, D.; Zhai, K. *Analytical and Bioanalytical Chemistry* **2020,** *412* (22), 5273-5281.
(165) Dai, Y.; Zhang, Y.; Liao, W.; Wang, W.; Wu, L. *Spectrochimica Acta Part A: Molecular and Biomolecular Spectroscopy* **2020,** *238*, 118406.
(166) Ma, X.; Du, C.; Zhang, J.; Shang, M.; Song, W. *Microchimica Acta* **2019,** *186* (12), 837.
(167) Zhang, L.; Wang, J.; Deng, J.; Wang, S. *Analytical and Bioanalytical Chemistry* **2020,** *412* (6), 1343-1351.
(168) Chen, X.; Lin, Z.; Hong, C.; Yao, Q.; Huang, Z. *Food Chemistry* **2020,** *309*, 125712.
(169) Youn, H.; Lee, K.; Her, J.; Jeon, J.; Mok, J.; So, J.-i.; Shin, S.; Ban, C. *Scientific Reports* **2019,** *9* (1), 7659.
(170) Selvolini, G.; Băjan, I.; Hosu, O.; Cristea, C.; Săndulescu, R.; Marrazza, G. *Sensors* **2018,** *18* (7), 2035.
(171) Saberi, Z.; Rezaei, B.; Ensafi, A. A. *Microchimica Acta* **2019,** *186*, 273.
(172) Jiao, Z.; Zhang, H.; Jiao, S.; Guo, Z.; Zhu, D.; Zhao, X. *Food Analytical Methods* **2019,** *12* (3), 668-676.
(173) He, J.; Liu, Y.; Fan, M.; Liu, X. *Journal of Agricultural and Food Chemistry* **2011,** *59* (5), 1582-1586.
(174) Verdian, A. *Talanta* **2018,** *176*, 456-464.
(175) Shi, H.; Zhao, G.; Liu, M.; Fan, L.; Cao, T. *Journal of Hazardous Materials* **2013,** *260*, 754-761.

(176) Qin, X.; Lu, Y.; Bian, M.; Xiao, Z.; Zhang, Y.; Yuan, Y. *Analytica Chimica Acta* **2019,** *1091*, 119-126.
(177) Fan, K.; Kang, W.; Qu, S.; Li, L.; Qu, B.; Lu, L. *Talanta* **2019,** *197*, 645-652.
(178) Su, L.; Wang, S.; Wang, L.; Yan, Z.; Yi, H.; Zhang, D.; Shen, G.; Ma, Y. *Spectrochimica Acta Part A: Molecular and Biomolecular Spectroscopy* **2020,** *225*, 117511.
(179) Kim, T.-Y.; Lim, J. W.; Lim, M.-C.; Song, N.-E.; Woo, M.-A. *Biotechnology and Bioprocess Engineering* **2020,** *25* (2), 246-254.
(180) Ouyang, Q.; Wang, L.; Ahmad, W.; Rong, Y.; Li, H.; Hu, Y.; Chen, Q. *Food Chemistry* **2021,** *349*, 129157.
(181) Zhang, J.; Feng, T.; Zhang, J.; Liang, N.; Zhao, L. *Analytical Methods* **2021,** *13* (29), 3282-3291.
(182) Wu, Y.; Shi, Y.; Deng, S.; Wu, C.; Deng, R.; He, G.; Zhou, M.; Zhong, K.; Gao, H. *Food Chemistry* **2021,** *343*, 128425.
(183) Dolati, S.; Ramezani, M.; Abnous, K.; Taghdisi, S. M. *Sensors and Actuators B: Chemical* **2017,** *246*, 864-878.
(184) Khoshbin, Z.; Housaindokht, M. R.; Izadyar, M.; Verdian, A.; Bozorgmehr, M. R. *Analytica Chimica Acta* **2019,** *1071*, 70-77.
(185) Xu, L.; Shen, X.; Hong, S.; Wang, J.; Zhang, Y.; Wang, H.; Zhang, J.; Pei, R. *Chemical Communications* **2015,** *51* (38), 8165-8168.
(186) Li, X.; Du, Z.; Lin, S.; Tian, J.; Tian, H.; Xu, W. *Food Chemistry* **2020,** *316*, 126303.
(187) Shi Y.; Li, W.; Feng, X.; Lin, L.; Nie, P.; Shi, J.; Zou, X.; He, Y. *Food Chemistry* **2021,** *344*, 128694.
(188) Guo, H.; Li, J.; Li, Y.; Wu, D.; Ma, H.; Wei, Q.; Du, B. *Analytica Chimica Acta* **2019,** *1048*, 161-167.
(189) Kiruba Daniel, S. C. G.; Kumar, A.; Sivasakthi, K.; Thakur, C. S. *Sensors and Actuators B: Chemical* **2019,** *290*, 73-78.
(190) Wang, J.; Du, C.; Yu, P.; Zhang, Q.; Li, H.; Sun, C. *Sensors and Actuators B: Chemical* **2021,** *348*, 130707.
(191) Li, S.; Ma, X.; Pang, C.; Tian, H.; Xu, Z.; Yang, Y.; Lv, D.; Ge, H. *Microchimica Acta* **2019,** *186* (12), 823.
(192) Xu, L.; Liang, J.; Wang, Y.; Ren, S.; Wu, J.; Zhou, H.; Gao, Z. *Molecules* **2019,** *24* (15), 2745.
(193) Zeng, L.; Gong, J.; Rong, P.; Liu, C.; Chen, J. *Talanta* **2019,** *198*, 412-416.
(194) Gan, Y.; Liang, T.; Hu, Q.; Zhong, L.; Wang, X.; Wan, H.; Wang, P. *Talanta* **2020,** *208*, 120231.
(195) Zhou, B.; Yang, X.; Wang, Y.; Yi, J.; Zeng, Z.; Zhang, H.; Chen, Y.; Hu, X.; Suo, Q. *Microchemical Journal* **2019,** *144*, 377-382.
(196) Pan, J.; Zeng, L.; Chen, J. *Chemical Communications* **2019,** *55* (79), 11932-11935.
(197) Wei, Z.; lan, Y.; Zhang, C.; Jia, J.; Niu, W.; Wei, Y.; Fu, S.; Yun, K. *Spectrochimica Acta Part A: Molecular and Biomolecular Spectroscopy* **2021,** *260*, 119927.
(198) Ono, A.; Cao, S.; Togashi, H.; Tashiro, M.; Fujimoto, T.; Machinami, T.; Oda, S.; Miyake, Y.; Okamoto, I.; Tanaka, Y. *Chemical Communications* **2008**, 10.1039/B808686A (39), 4825-4827.
(199) Lu, Z.; Wang, P.; Xiong, W.; Qi, B.; Shi, R.; Xiang, D.; Zhai, K. *Environmental Technology* **2020,** *317*, 1-27.
(200) Khoshbin, Z.; Housaindokht, M. R.; Verdian, A. *Analytical Biochemistry* **2020,** *597*, 113689.
(201) Yang, Y.; Li, W.; Liu, J. *Analytica Chimica Acta* **2021,** *1147*, 124-143.
(202) Zhu, Y.; Gu, X.; Jiang, F.; Jia, R.; Jin, M.; Chen, M.; Zhang, G. *Food and Agricultural Immunology* **2018,** *29* (1), 1106-1115.
(203) Allsop, T. D. P.; Neal, R.; Wang, C.; Nagel, D. A.; Hine, A. V.; Culverhouse, P.; Ania Castañón, J. D.; Webb, D. J.; Scarano, S.; Minunni, M. *Biosensors and Bioelectronics* **2019,** *135*, 102-110.
(204) Guo, Z.; Tang, J.; Li, M.; Liu, Y.; Yang, H.; Kong, J. *Analytical and Bioanalytical Chemistry* **2019,** *411* (29), 7807-7815.

(205) Jia, M.; Sha, J.; Li, Z.; Wang, W.; Zhang, H. *Food Chemistry* **2020,** *317*, 126459.
(206) Rajabnejad, S.-H.; Badibostan, H.; Verdian, A.; Karimi, G. R.; Fooladi, E.; Feizy, J. *Microchemical Journal* **2020,** *155,* 104722.
(207) Qiao, P.; Wang, X.; Gao, S.; Yin, X.; Wang, Y.; Wang, P. *Biosensors and Bioelectronics* **2020,** *149*, 111821.
(208) Xu, Z.; Zhang, L.; Long, L.; Zhu, S.; Chen, M.; Ding, L.; Cheng, Y. *Frontiers in Bioengineering and Biotechnology* **2020,** *8*, 1478.
(209) Ni, X.; Xia, B.; Wang, L.; Ye, J.; Du, G.; Feng, H.; Zhou, X.; Zhang, T.; Wang, W. *Analytical Biochemistry* **2017,** *523*, 17-23.
(210) Kim, Y. S.; Jung, H. S.; Matsuura, T.; Lee, H. Y.; Kawai, T.; Gu, M. B. *Biosensors and Bioelectronics* **2007,** *22* (11), 2525-2531.
(211) Yang, R.; Liu, J.; Song, D.; Zhu, A.; Xu, W.; Wang, H.; Long, F. *Microchimica Acta* **2019,** *186* (11), 726.
(212) Liu, X.; Deng, K.; Wang, H.; Li, C.; Zhang, S.; Huang, H. *Microchimica Acta* **2019,** *186* (6), 347.
(213) Ming, T.; Wang, Y.; Luo, J.; Liu, J.; Sun, S.; Xing, Y.; Xiao, G.; Jin, H.; Cai, X. *ACS Sensors* **2019,** *4* (12), 3186-3194.
(214) Yao, X.; Gao, J.; Yan, K.; Chen, Y.; Zhang, J. *Analytical Chemistry* **2020,** *92* (12), 8026-8030.
(215) Sha, H.; Yan, B. *Journal of Colloid and Interface Science* **2021,** *583*, 50-57.
(216) Wang, W.; Peng, Y.; Wu, J.; Zhang, M.; Li, Q.; Zhao, Z.; Liu, M.; Wang, J.; Cao, G.; Bai, J.; Gao, Z. *Analytical Chemistry* **2021,** *93* (10), 4488-4496.

For Table of Contents Only